August 1974

# THE NATIONAL SHIPBUILDING RESEARCH PROGRAM

## NDT: LOW-COST ALTERNATIVES TO FILM RADIOGRAPHY

U.S. Department of Commerce
Maritime Administration

in cooperation with
Todd Shipyards Corporation

# Report Documentation Page

*Form Approved*
*OMB No. 0704-0188*



| 1. REPORT DATE | 2. REPORT TYPE | 3. DATES COVERED |
|---|---|---|
| **AUG 1974** | **N/A** | **-** |

| 4. TITLE AND SUBTITLE | 5a. CONTRACT NUMBER |
|---|---|
| **The National Shipbuilding Research Program** | 5b. GRANT NUMBER |
| | 5c. PROGRAM ELEMENT NUMBER |
| 6. AUTHOR(S) | 5d. PROJECT NUMBER |
| | 5e. TASK NUMBER |
| | 5f. WORK UNIT NUMBER |
| 7. PERFORMING ORGANIZATION NAME(S) AND ADDRESS(ES)<br>**Naval Surface Warfare Center CD Code 2230 - Design Integration Tools Building 192 Room 128-9500 MacArthur Blvd Bethesda, MD 20817-5700** | 8. PERFORMING ORGANIZATION REPORT NUMBER |
| 9. SPONSORING/MONITORING AGENCY NAME(S) AND ADDRESS(ES) | 10. SPONSOR/MONITOR'S ACRONYM(S) |
| | 11. SPONSOR/MONITOR'S REPORT NUMBER(S) |

12. DISTRIBUTION/AVAILABILITY STATEMENT
**Approved for public release, distribution unlimited**

13. SUPPLEMENTARY NOTES

14. ABSTRACT

15. SUBJECT TERMS

| 16. SECURITY CLASSIFICATION OF: | | | 17. LIMITATION OF ABSTRACT | 18. NUMBER OF PAGES | 19a. NAME OF RESPONSIBLE PERSON |
|---|---|---|---|---|---|
| a. REPORT | b. ABSTRACT | c. THIS PAGE | | | |
| **unclassified** | **unclassified** | **unclassified** | **SAR** | **154** | |

**Standard Form 298 (Rev. 8-98)**
Prescribed by ANSI Std Z39-18

INTERM REPORT
NOT FOR PUBLIC DISTRIBUTION

# FOREWORD

This report is the end product of one of the many research projects being performed under the National Shipbuilding Research Program. The program is a cooperative, cost-shared effort between the Maritime Administrations Office of Advanced Ship Development and the shipbuilding indus - try. The objective, as conceived by the Ship Production Committee of the Society of Naval Architects and Marine Engineers, emphasizes productivity.

The research effort described herein is one of the nine General Category projects being managed and cost-shared by Todd Shipyards Corporation. It was performed in re-sponse to the task statement titled "Nondestructive Testing[11]. The work was assigned, by sub-contract, to the McDonnell Douglas Astronautics Company (MDAC) after evaluation of several proposals.

Mr. D. A. Tiede of the MDAC Materials and Processes Department was the Project Manager. Mr. J. Jortner was responsible for the analysis of acceptance criteria, Mr. G. E. Bockrath assisted in the fracture analysis, and Mr. S. N. Rosenwasser assisted in the preparation of the MDAC draft of the report.

Mr. L. D. Chirillo, Todd Shipyards Corporation, Seattle Division, was the Program Manager. Mr. C. S. Jonson, Special Project Engineer, Los Angeles Division, provided technical direction. Mr. W. J. Lester, Welding Engineer, Los Angeles Division, provided the nondestructive testing specimens. Mr. R. F. Heady, Seattle Division, coordinated the final editing effort.

## EXECUTIVE SUMMARY


This report describes explorations of:

- nondestructive testing (NDT) techniques for welds in ship hulls and in pipe
- test criteria

It is primarily intended for NDT and welding specialists.

Lower- cost alternatives to film radiography (RT) were experimentally evaluated. Conventional ultrasonic testing (UT), UT using a liquid-filled wheel, ultrasonic delta scan, acoustic holography, and acoustic emission techniques were applied to test panels and pipes containing purposely introduced weld defects. A comparison of the inspection results with both laboratory x-ray inspection and visual examination of the actual defects confirmed that the UT techniques were the only suitable alternatives to RT for hull welds. A suitable alternative to RT for pipe inspection was not found.

The cost comparison between shipyard applied RT and UT indicated that the estimated savings from using UT on a medium size tanker hull can be as much as $19,000. The rationale leading to this estimate and others was not concurred with by all shipbuilders who reviewed the initial draft. Their comments on costs and on other aspects of the report are incorporated as footnotes.

The American Bureau of Shipping (ABS) hull weld inspection requirements were evaluated in the context of current shipyard inspection practice, failure histories, ductile rupture and brittle fracture probability, and a simplified fatigue crack-growth analysis. The recommendations derived from the results of this evaluation include:

- The common practice of customers requiring more inspection than specified in the already- conservative ABS requirements should be discontinued. Savings up to an estimated $28,000 for a medium size tanker hull could be realized immediately. Pas sages of this report and the discussion of ship failures in Appendix A should convince customers of the adequacy of the ABS minimum.

- **UT requirements should be revised to reduce check-point lengths from 50" to 22". This report confirms that UT sensitivity is not significantly different from that for the idealized RT against which it was compared. Even allowing for the differences in UT and RT criteria, a UT check-point length of 22" would yield the same order of reject rate as for the RT check-point length of 18".**

- **UT employing a transducer housed in a liquid-filled wheel should be further investigated. It demonstrated a potential for improved coupling and faster inspection rates.**

**The researcher also recommended that further study be undertaken which would specifically utilize the capability of UT to measure height and depth, in addition to length of a defect. However, a reviewer's analysis based on the crack-growth theory described in this report indicated that the addition of height and depth criteria would probably not lead to a decrease in required repair. One reason is that shipyard UT may not measure height and depth with the accuracy necessary to make a judgment of a flaw's fatigue life. If UT were sufficiently accurate, addition of height and depth ctriteria might result in more rejected weld. Further high-cycle/low-stress experimental work would be necessary to confirm this tentative conclusion. But for now, the existing UT accept- reject criteria appear adequate and reasonable.**

**The possible reduction of pipe-weld inspection and repair cost by relaxing the current Coast Guard Requirements could not be justified.**

**As one shipbuilder stated, this report is "a comprehensive analysis of the current problems and cost related to NDT of weldments in ship hulls; the final recommendations represent substantial cost savings and continued reliability".**

## CONTENTS

## FIGURES

## TABLES

## Section 1

## INTRODUCTION AND SUMMARY

### 1.1 OBJECTIVE

The objective of the work reported herein was to determine ways to reduce the cost of nondestructive inspection of ship welds. The present study, as well as others sponsored by the United States Maritime Administration (MARAD), is intended to assist the U. S. shipyards in becoming more competitive with foreign shipyards.

### 1.2 APPROACH

The approach employed in this program was to examine the possibilities of lowering weld inspection costs by:

A. Decreasing the amount of inspection.
B. Adjusting the current defect-acceptance criteria in order to eliminate repair of insignificant flaws.
C. Replacing radiography with suitable lower-cost alternatives.

The current requirements for nondestructive inspection of hull and pipe welds were analyzed for cost-saving potential. The requirements were reviewed in terms of how they are being applied as determined from interviews with shipyard inspection personnel. The results of typical hull-weld inspections were assessed by review of two sets of hull radiographs. The effect of weld flaws on ship reliability and the most probable failure modes were determined by a historical survey of fracture and cracking in ships. The current defect-acceptance criteria were evaluated with the aid of calculations that predict approximate fatigue-crack growth.

Conventional ultrasonic shear-wave inspection using a wedge, ultrasonic shear-wave inspection using a liquid-filled wheel, ultrasonic delta scan, acoustic holography, and acoustic emission techniques were experimentally evaluated using panels and pipes containing purposely introduced weld defects. Magnetic-particle and eddy-current techniques were not evaluated because they are limited to surface and shallow sub- surface flaws. The inspection results were compared first to those of X-ray, as a baseline reference, and second to the actual defects revealed by the fracture of selected panel specimens. The results of the analysis of inspection requirements and the evaluation of alternative inspection techniques were used to recommend changes to the current requirements.

## 1.3 SUMMARY

The requirements for radiographic inspection of hull welds specify a sample size of approximately 1. 5 per cent of the weld within the midship 0.6 length. The provisional requirements for ultrasonic inspection specify inspection of approximately three times the weld length specified by the radiographic requirements. Shipyards often inspect more than the minimum required by either requirement, usually at the request of the purchaser.

The rejection rate varies from shipyard to shipyard but probably is somewhere between 10 and 20 per cent on the average. This rate of rejection and the small sample size suggest that many rejectable defects exist in the un-inspected weld.

A review of structural failure modes in ship hulls and the participation of weld defects in failures indicates that ductile rupture and brittle fracture are unlikely. The most likely failure mode is fatigue growth of defects to full penetration and subsequent slow growth to a size (approximately 8 to 12 in. ) that may result in brittle fracture under extreme conditions. Fatigue cracks in modern ships occur primarily in the hull skeleton and not in hull plating. The low incidence of catastrophic ship failures implies that the current inspection requirements are conservative.

An analysis of the fatigue growth of defects indicated that the high-cycle/ low-stress amplitudes are responsible for most of the growth. While there is little supporting experimental data, the analysis suggested several implications relevant to the current inspection requirements. A fatigue crack in simple tension will penetrate the thickness before it extends significantly in length. The initial crack height and its depth below the surface will significantly influence the time to penetration. With a knowledge of these two parameters, many defects currently being repaired might be left uncorrected.

From the standpoint of fatigue growth leading to eventual brittle fracture, radiographic acceptance criteria appear conservative for the majority of hull welds. The ultrasonic acceptance criteria are less conservative due to the larger initially acceptable defect sizes. Both criteria could be nonconservative in regions of high stress concentration, as the fatigue growth in these areas might be increased by factors of 10 or more. Thus, the importance of screening design details to eliminate high stress concentrations is reemphasized. NDT cannot be substituted for proper design.

Of the techniques evaluated against the X-ray yardstick, ultrasonic shear-wave provided the best sensitivity. Delta scan, acoustic holography, and acoustic emission were not found practicable for shipyard weld inspection.

The liquid - filled wheel was more sensitive than wedge shear - wave inspection due to improved coupling. The sensitivity of the wedge shear-wave technique could be improved by a change in the calibration procedure to allow for changes in coupling. Each shear-wave technique pro - vides information on the height of the defect and its depth below the surface. Both readings could be important in reducing the amount of repair required. The data obtained in this program revealed that ultrasonic defect-length indications are, on the average, about the same = those from radiographs.

The cost of wedge shear-wave inspection was estimated to be up to about one- fifth that of radiography.[1] Savings attainable under the current re - quirements (including the cost of repair) were estimated to vary from $6,400 to $19,000 for a 786-ft-long tanker, considering minimum required and typical amounts of inspection, respectively. If the checkpoint length were reduced to that employed for radiography, the savings would increase to between $10, 000 and $30, 000 for the ranges of inspection considered.

Based on the results of the program, the following recommendations are made concerning the current hull-weld criteria:

A. The minimum amount of inspection currently required is conservative and should not be exceeded if the weld process is demonstrated to be in control.

B. The provisional ultrasonic requirements should be modified to reduce the check-point length.

C. The provisional ultrasonic requirements should be further modified to include defect height and possibly depth in the acceptance criteria.

---

1 Shipbuilders' comments suggest that this estimate is optimistic. Some reported UT cost up to 3/4 that of RT.

2 As mentioned in the Executive Summary and discussed in Appendix G , this may be impractical.

**The last recommendation requires additional fatigue analyses and experimental data, in addition to information on size, location, and frequency of weld defects. Because the liquid-filled wheel provided better coupling than existing wedge devices, further effort to develop the wheel concept is suggested in order to provide a more reliable, lower-cost inspection procedure.**

**An analysis of the inspection of pipe welds revealed that there is insufficient stress data for ship piping to conduct the stress and fatigue analyses required to justify relaxing the inspection sample or acceptance criteria. An evaluation of other techniques concluded that radiography is the most practicable at this time.**

## Section 2
## HULL-WELD INSPECTION

The current ABS requirements for hull-weld inspection and their practical application in the shipyards are reviewed in this section. The adequacy of the current requirements is discussed in the context of amount of inspection and . repair, ship hull stresses, brittle fracture behavior, and flaw growth theory to define possible changes that could lead to lower inspection and repair costs. Potential nonradiographic inspection techniques are experimentally evaluated for their technical applicability and cost impact.

### 2.1 CURRENT REQUIREMENTS AND PRACTICE

In 1965, after a two-year study, the ABS issued an informal guide for non-destructive (radiographic) inspection of hull welds (Reference 1). After several years of experience in the implementation of these guidelines, formal radiographic acceptance requirements were published by ABS in 1971 (Reference 2). The acceptance requirements were based on surveys of worldwide shipbuilding practice and on other related standards such as those of the ASME and the U. S. Navy, and reflect an assessment of commonly observed "good" quality welding, economically attainable by experienced shipbuilders [Reference 3).

In 1972, ABS issued a provisional guide to the use of ultrasonic nondestructive methods of hull weeld inspection (Reference 4). Ultrasonic methods may, on a case-by-case basis, be approved by the ABS as a substitute for radiography.

#### 2. 1. 1 Radiographic Inspection Requirements

The current ABS radiographic inspection requirements have the following features:

A. Sample Size – Only a portion of the hull welds is required to be inspected. The number of check points, n, is to equal or exceed

$$n = \frac{L(B+D)}{500}$$

where L, B, and D are the length, breadth, and depth of the hull, measured in feet, Each checkpoint presumably consists of one standard radiographic film, which typically includes about 1. 5 ft of weld.

B. Selection of Critical Locations — The minimum sample size, n, refers to the midship section (the central 0. 6L), where presumably the hull bending stresses are the highest. Within the midship 0. 6L, the specification directs attention to areas of high applied stress, high geometric stress concentration, and/or potentially high residual stresses, such as "intersections of hutts and seams in the shear strakes, bilge strakes, deck stringer and keel plates, and butts in and shout hatch corners in main decks and in the vicinity of breaks in the superstructure."

C. Specification of Radiographic Technique — These requirements assure a certain level of sensitivity, require the use of acceptance standards (penetrameters), require adequate weld surface quality, and require general conformance With accepted radiographic practices.

D. Reliance on Discretion of the Surveyor — The surveyor may require radiographic inspection outside the midship 0. 6L. When a radiograph reveals defects, and additional radiographs taken in adjacent areas also show defects, the extent of further adjacent radiography is at the surveyor's discretion. He may, instead of requiring further radiography, simply require that the entire weld joint be repaired. The extent of inspection of repaired welds is at the surveyor's discretion.

E. Two Levels of Acceptance — Acceptance to Class A is required for all radiographs taken within the midship 0. 6L of ships greater than 500 ft in length. Class B applies to shorter ships and to all radiographs taken outside the midship 0. 6L.

F. Definition of Unacceptable Defects

1. All cracks of any length revealed by the radiographs are unacceptable.

2. Incomplete fusion or incomplete penetration is rejectable according to the length of the radiographic indication by a standard that varies with plate thickness.
3. Slag is treated in essentially the same way as incomplete penetration, except that the acceptable lengths are larger and there is a distinction between Class A and Class B standards.
4. The maximum size of isolated pores is 25 percent of the plate thickness, or about 0. 1875 in., whichever is less.
5. Distributed porosity is limited to a pore area of about 1. 5 percent of the weld cross - sectional area in any given 6-in. length. Pores of less than 0. 015-in. diameter are disregarded.
6. Combined porosity and slag are limited in that the percentage of permissible slag plus the percentage of permissible porosity are not to exceed 150 percent.

G. Definition of Defect Extent — When a radiograph reveals unacceptable defects, adjacent areas are to be radiographed to define the extent of the defects.

H. Repair of Welds — Unacceptable defects are to be excavated and the areas are to be repaired by melding.

2. 1.2 Provisional Ultrasonic Inspection Requirements

The provisional ultrasonic specification is similar in scope to the radiographic inspection requirements. The sample size, the selection of critical locations, the reliance on the surveyor's discretion, and the requirements for definition of defect extent and for repair welding are the same as for radiography. The major differences between the radiographic and provisional ultrasonic specifications are:

A. The length to be inspected ultrasonically at each checkpoint is 50 in. versus about 18 in. for radiography.

R. The ultrasonic specification does not distinguish between defect types in generic terms such as slag, crack, etc. Instead, the intensity of signal and the length of defect indication are monitored.

c. The acceptable lengths of defect indications are greater in the ultrasonic specification (see Figure 2-1, for example).

D. The minimum length of defect indication rejectable in the ultrasonic specification is 0. 5 in. In the radiographic specification, all cracks are rejectable.

### 2. 1.3 Shipyard Inspection Practice

Interviews were held with personnel from nine major shipyards to survey current hull-weld inspection practice. All of the shipyards had extensive experience with the ABS requirements for radiographic inspection. Almost all of the shipyards had some experience with the ABS provisional requirements for ultrasonic inspection. The estimated usage of radiography and ultrasonic testing at each of-the shipyards is shown in Table 2-1. The estimates indicate that the average usage for all yards Was about 54 percent ultrasonic and 46 percent radiographic. However, each individual shipyard strongly favored one of the techniques, with four of the nine yards primarily employing ultrasonic inspection.

The shipyards with a large workload of both U. S. Navy and commercial ships used ultrasonic inspection almost exclusively. These shipyards used ultrasonic inspection because they had previous experience with the U. S. ,Navy requirements for ultrasonic inspection, and these requirements caused minimum interference with production on a three-shift-per-day schedule. The commercial shipyards with less than full workloads favored radiographic inspection, since it could be performed without interfering with production. However, these yards were beginning to develop an ultrasonic inspection capability. There was a definite trend toward increased usage of ultrasonic inspection at all yards visited.

## 2.2 ANALYSIS OF CURRENT HULL - WELD INSPECTION REQUIREMENTS

In addition to employing lower-cost techniques, an obvious May to decrease hull - weld inspection costs is to change the current ABS requirements to reduce the extent of inspection or the amount of repair required. The

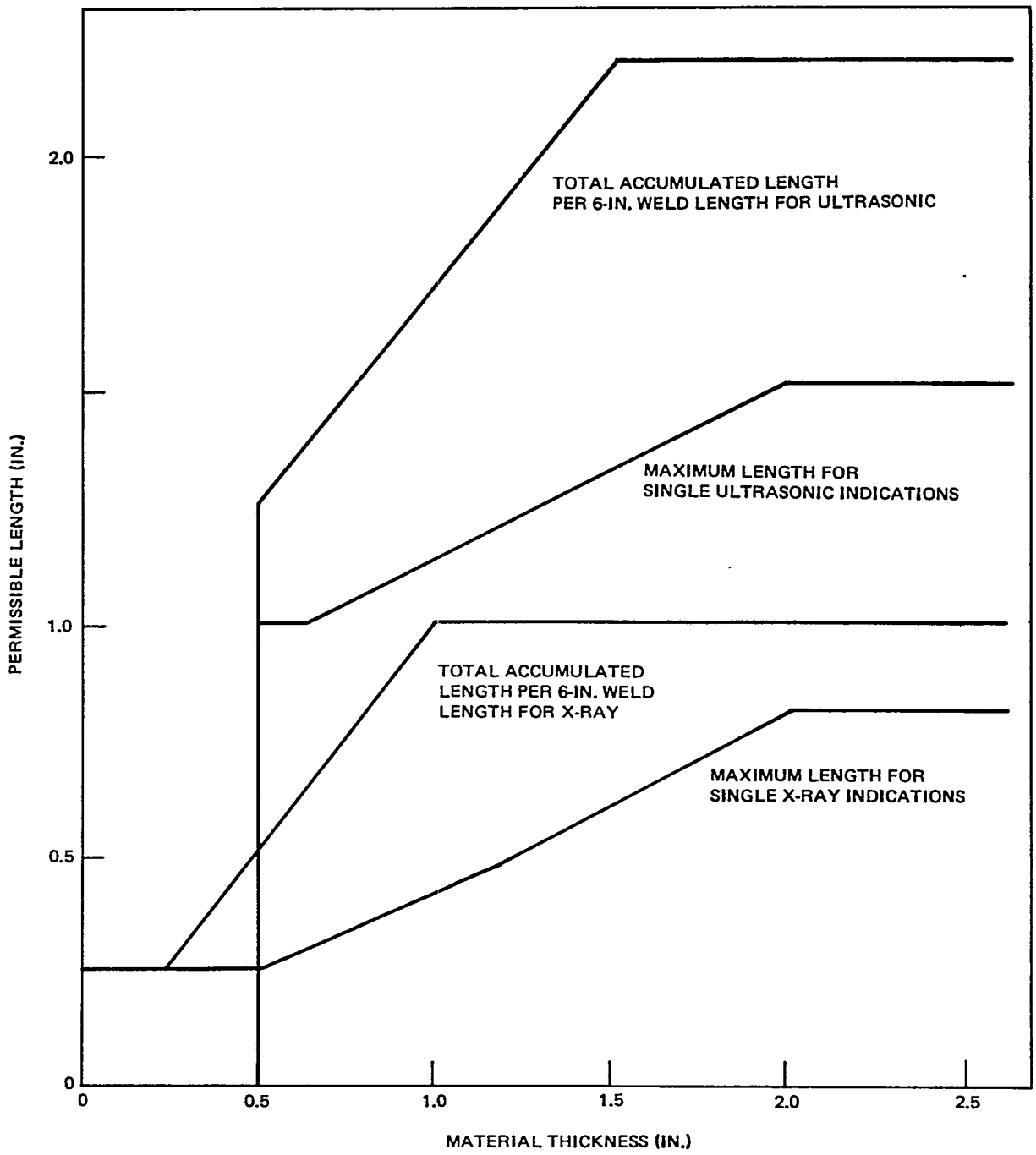


Figure 2-1. Comparison of Radiographic and Ultrasonic Acceptance Levels, Class A

**Table 2-1**

**COMPARISON OF HULL-WELD INSPECTION TECHNIQUES AT SEVERAL SHIPYARDS**

| Shipyard | Relative Usage (percent) | |
|---|---|---|
| | Radiography | Ultrasonics |
| 1 | 22 | 78 |
| 2 | 78 | 22 |
| 3 | 28 | 72 |
| *4 | 75 | 25 |
| **5 | 10 | 90 |
| **6 | 5 | 95 |
| **7 | 0 | 100 |
| 8 | 100 | 0 |
| 9 | 95 | 5 |
| Average | 46 | 54 |

*Mainly Navy experience
**Both Navy and merchant experience

following approach was employed to determine if the current requirements could be changed to result in lower inspection cost without significantly lowering the structural integrity or reliability of the resulting hulls:

A. Quantify current ABS requirements with respect to nondestructive inspection and repair.

B. Assess ABS sampling scheme in relationship to practice and ship failure history.

C. Identify probable failure modes (i. e. , brittle failure, fatigue, simple over load).

D. Evaluate role of defects in weld performance.

E. Identify sources and approximate magnitudes of stresses in hulls.

F. Perform analyses to define critical flaw types, sizes, and locations.

G. Compare results with ABS requirements to formulate possible changes.

## 2.2. 1 Implications of ABS Requirements

The quality of ship hull welds is assured by ABS rules regarding welder training, raw material requirements, joint preparation and welding practice, destructive tests (optional), leakage testing, and nondestructive inspection with subsequent repair. The rules regarding the latter, which comprise the subject approached in this analysis, include:

A. Visual inspection of all welds.

E. Specified radiographic and/or ultrasonic inspection of areas selected at surveyor's discretion.

C. Optional magnetic-particle and dye-penetrant inspection.

D. Repair and reinspection of rejected welds.

The specifications for radiographic and ultrasonic inspection were summarized in Section 2. 1. Eased on the minimum number of checkpoints specified in the rules, the fraction of the total hull weld-length requiring inspection was estimated. The estimates were made assuming that the typical plate in the 0. 6L midship section averaged 8 ft by 24 ft and that the area of openings (i. e. , hatches) was negligible. The results indicated that only approximately 1.5 per cent of the total hull weld length within the 0. 6L midship section require inspection by radiography. For ultrasonic inspection the required length of weld inspected increases to about 4.5 percent.

Another calculation indicated that if only weld intersections in the midships 0. 6L were inspected by radiography, the rules would require that about 22 per cent of the intersections be sampled. Similarly, if the inspection were limited to butt welds, only about 5 per cent of the total butt-weld length would be sampled.

These estimates were made to provide an understanding of ABS minimum sampling requirements and for comparison with typical shipyard inspection practice. A brief analysis was made of the acceptance radiographs of two vessels built in the United States. One was a 640-ft-long container ship built recently and inspected according to the current ABS radiographic specification. The second ship, a 528-ft-long cargo liner, was built in 1960-61 before radiographic standards were uniformly applied.

---

3 A shipbuilder commented that "too much emphasis has been placed on the 50 inch UT check point. Most check points are intersections and the UT requirements for intersections is only 30 inches (5 inches on each side of the butt and 10 inches each side of the seam). With over half of the check points intersections, the calculations using a 50 inch check point for UT are not valid". This supports the contention that the UT cost estimates in this report are optimistic.

The extent of hull welds inspected on the container ship, 580 ft, was approximately 3 to 4 percent of the estimated hull plating weld length in the midship 0. 6L. The number of locations sampled exceeded the minimum ABS requirements (1. 5 percent approximately) due to request of the purchaser. The radiographic sampling on the cargo liner, built prior to adoption of current ABS requirements, was estimated at just under 2 percent of the plating weld length in the midship 0. 6L.

The amount of inspection performed on the container ship compared well with the survey of current shipyard practice. Most builders indicated that they routinely inspected from two to four times the minimum required hull-weld sample to satisfy purchaser requests. The variation in the nine shipyards surveyed was from the minimum required to approximately 100 percent of the total hull-weld length. Some purchasers required 100-percent inspection of intersections, an amount greater than required by the ABS. It was apparent that increased confidence in the current ARS minimum inspection requirements on the part of both purchasers and builders would, in itself, lower the cost of nondestructive inspection. The only justification for more than the minimum inspection required should be the occurrence of problems with the weld process, as determined by abnormally high rejection rates.

Further analysis of these radiographs indicated that about 13 percent of the hull weld radiographs on the container ship and about 20 percent of the radiographs on the cargo vessel mere considered to detect rejectahle defects. This was consistent with the opinion of an informed source in the U. S. Coast Guard, who estimated that about 16 percent of all shipyard weld radiographs in the United States are rejected.

The evidence suggests that between 10 and 20 percent of all spots inspected contain flaws that require repair under current ABS standards. If the selection of spot locations were completely random, 10 to 20 percent of the uninspected weld (usually greater than 95 percent of the total) would contain rejectable defects. Interviews with shipyards, however, indicate that the selection was not completely random, with such factors as visual weld

appearance, welder's reputation, and estimated service stresses influencing the surveyor's spot selection. Nevertheless, the results of this limited investigation suggest that the presence of currently rejectable defects in uninspected hull welds, some located in highly stressed areas, is very probable. The safe operation of existing ships, inspected under current ABS standards or less severe rules and containing rejectable defects, indicates that the current rejection criteria may be conservative or that periodic maintenance procedures detect defects before they reach critical size.

### 2. 2.2 Structural Failure Modes

The purpose of the current ABS hull-weld inspection requirements is to prevent in-service structural failures in ship hulls caused by weld flaws. A rational critique of the current criteria requires a knowledge of the most likely structural failure modes in ship hulls and the participation of weld defects in the failure process. To this end, a literature survey was conducted and is presented in its entirety in Appendix A. The results particularly pertinent to this discussion are summarized below.

A. Structural hull-failure modes might include ductile rupture, brittle fracture, or fatigue-crack growth.

B. Ductile rupture of welds due to overload is unlikely because the weld metal is usually significantly stronger than the mild-steel hull plate, as shown in Figure 2-2.

C. Brittle fractures may initiate at weld defects, but catastrophic propagation almost always occurs in the less-tough hull plates.

D. Catastrophic brittle failure can occur, but rarely does, when a combination of severe conditions exists (such as low ambient temperature, inordinately high stresses, severe defects at critical locations, and high brittle-transition temperature of the steel).

E. Selection of plate ductile-to-brittle transition temperature significantly below the minimum expected service temperature ensures that cracks propagating in a flamed, embrittled, or high-stress area will be arrested in the plate. When the transition temperature is selected in this manner, cracks with lengths from 8 to 12 in. will not undergo brittle propagation even if stresses reach the yield strength.

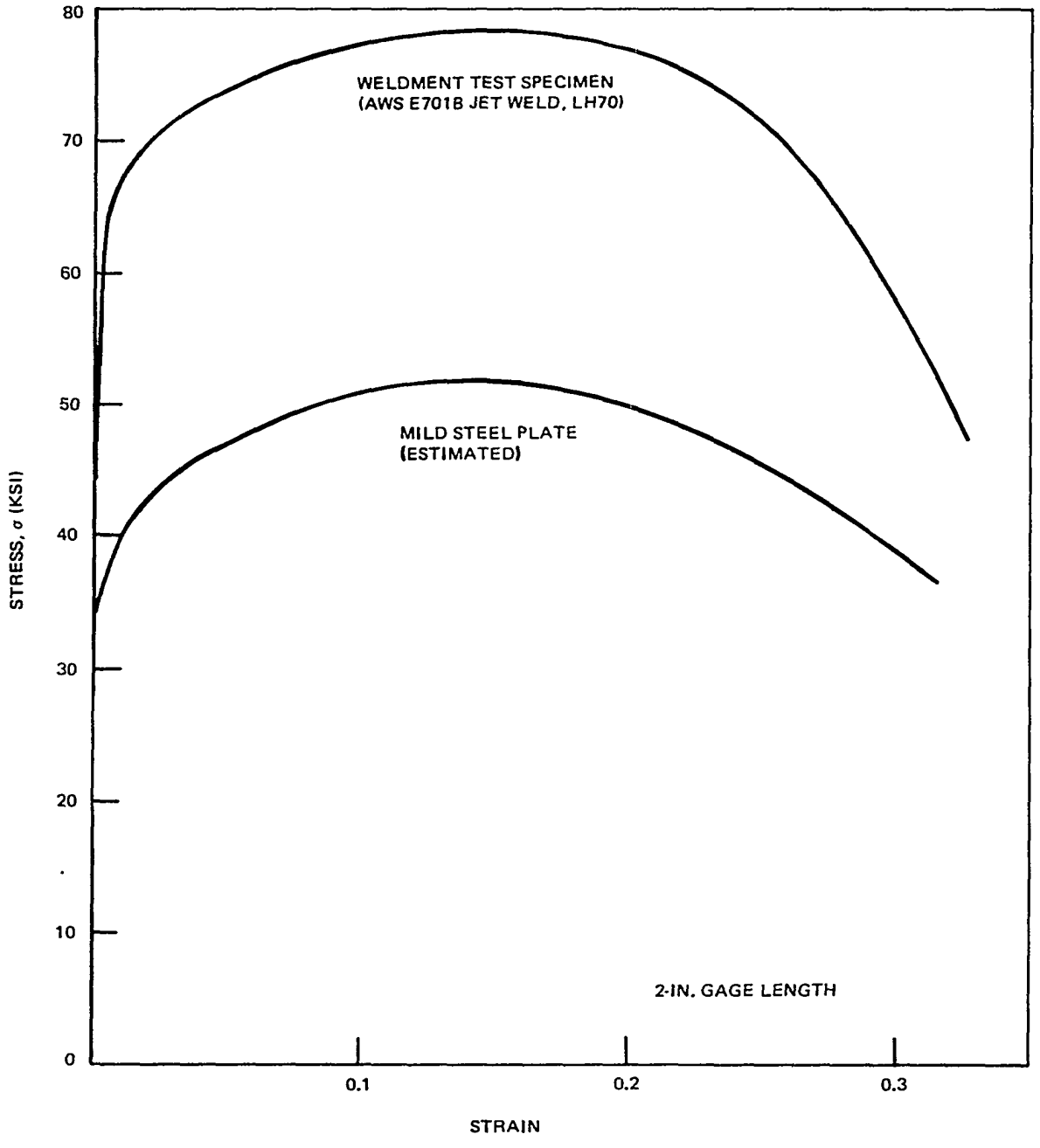


Figure 2-2. Stress-Strain Curves of Mild Steel Plate and Ship Steel Weld in Slow Tension at Room Temperature

F. The regulated control of steel-plate processing, chemistry, and/or toughness properties has all but eliminated the brittle-facture problem in present-day ships.

G. Several surveys of cracking observed in the hulls of in-service ships indicate that, excluding "external" factors such as collisions, weather, grounding, ice, fire, or corrosion, the primary cracking mechanism in ships is fatigue.

H. The most likely sources of fatigue cracks include structural members near welded discontinuities and welded joints associated with highly loaded areas such as corners. No tendency for. cracks to initiate at butt welds is evident.

1. Weld flaws are of concern because they are potential initiation sites for fatigue-crack propagation.

## 2. 2.3 Weld Defects and Their Effect on Performance

Defects commonly found in ship welds include porosity, cracks, slag, and incomplete penetration. An insight to the relative occurrence of these defects in typical ship hulls was obtained by analysis of the radiographs from the container ship and the cargo ship discussed in Section 2.2. 1. Figures 2-3 and 2-4 show the frequency of each defect type in inspected welds of the two ship hulls. Figures 2-5 and 2-6 give the flaw - length distributions of the defects. The following observations are made from the figures:

A. Defects frequently occur in combination. In Figures 2-3 and 2-4, the shaded portion of each bar represents the incidence of that defect alone. The unshaded portions represent combined defects and are marked uith a letter denoting the other type of defect.

B. In both ships, slag was the defect most frequently found. Cracks were also frequent. Incomplete penetration, incomplete fusion, and large voids were relatively rare.

C. Rejectable porosity was frequently found in the container ship and almost absent in the cargo ship.

D. Defects longer than about 3 in. are relatively rare, although there appears to be a finite probability of finding defects between 6 and 12 in. in length.

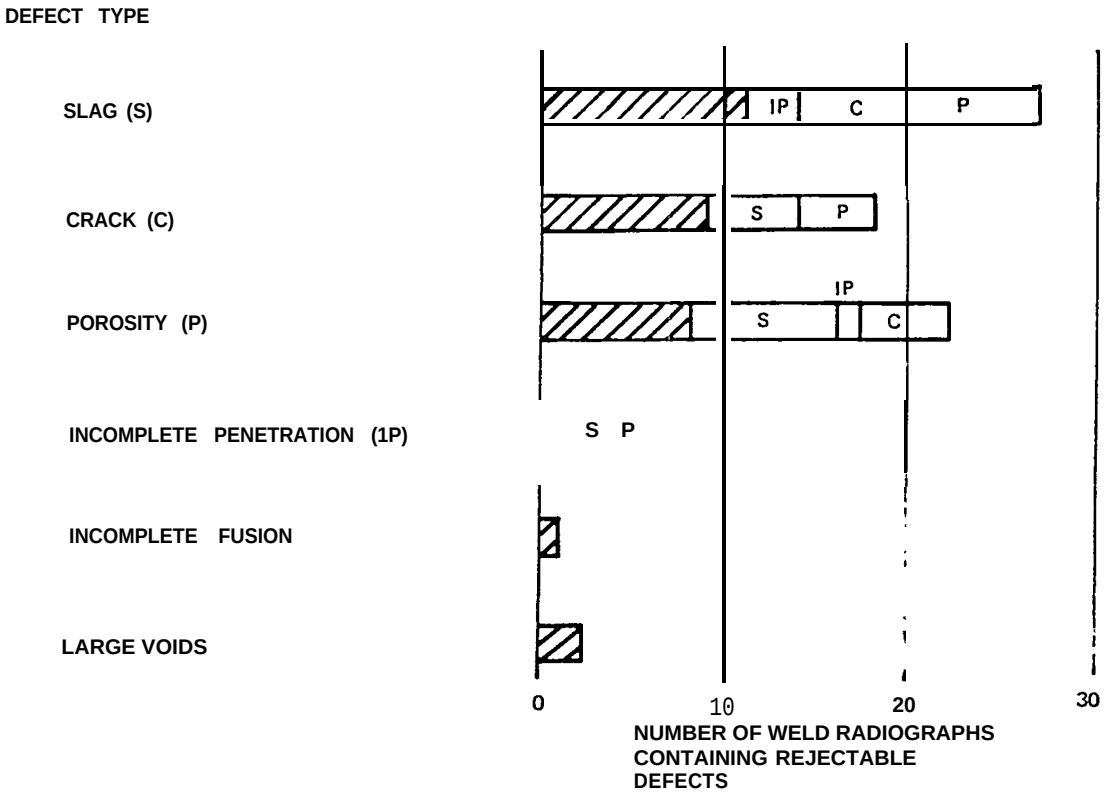


Figure 2-3. Incidence of Various Defect Types in the Container Ship

E. Most cracks are less than 1 in. long, and thus many might escape rejection under the provisional ultrasonic inspection criteria.

The results of a brief search for experimental data regarding the effects of the common weld flaws on the performance of welded structures are presented in Appendix B. The relevant aspects of the data for each flaw category can be summarized as follows:

A. Porosity — Because the weld is considerably stronger than the parent metal in steel welds, a large amount of porosity is required

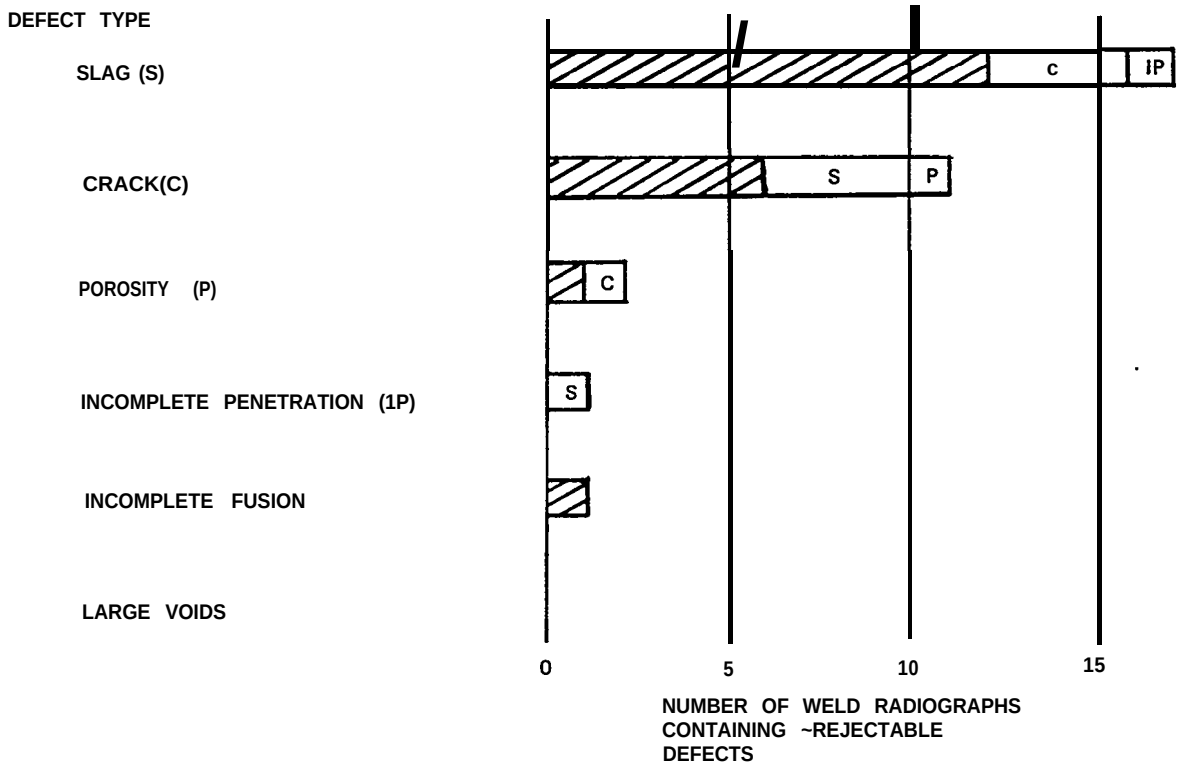


**Figure 2-4. Incidence of Various Defect Types in the Cargo Ship**

to lower the joint strength significantly. Up to 7 per cent porosity does not affect strength, ductility, or Charpy impact properties of the submerged arc-weld joints. Although evidence is conflicting, data indicates that porosity affects fatigue endurance limits.

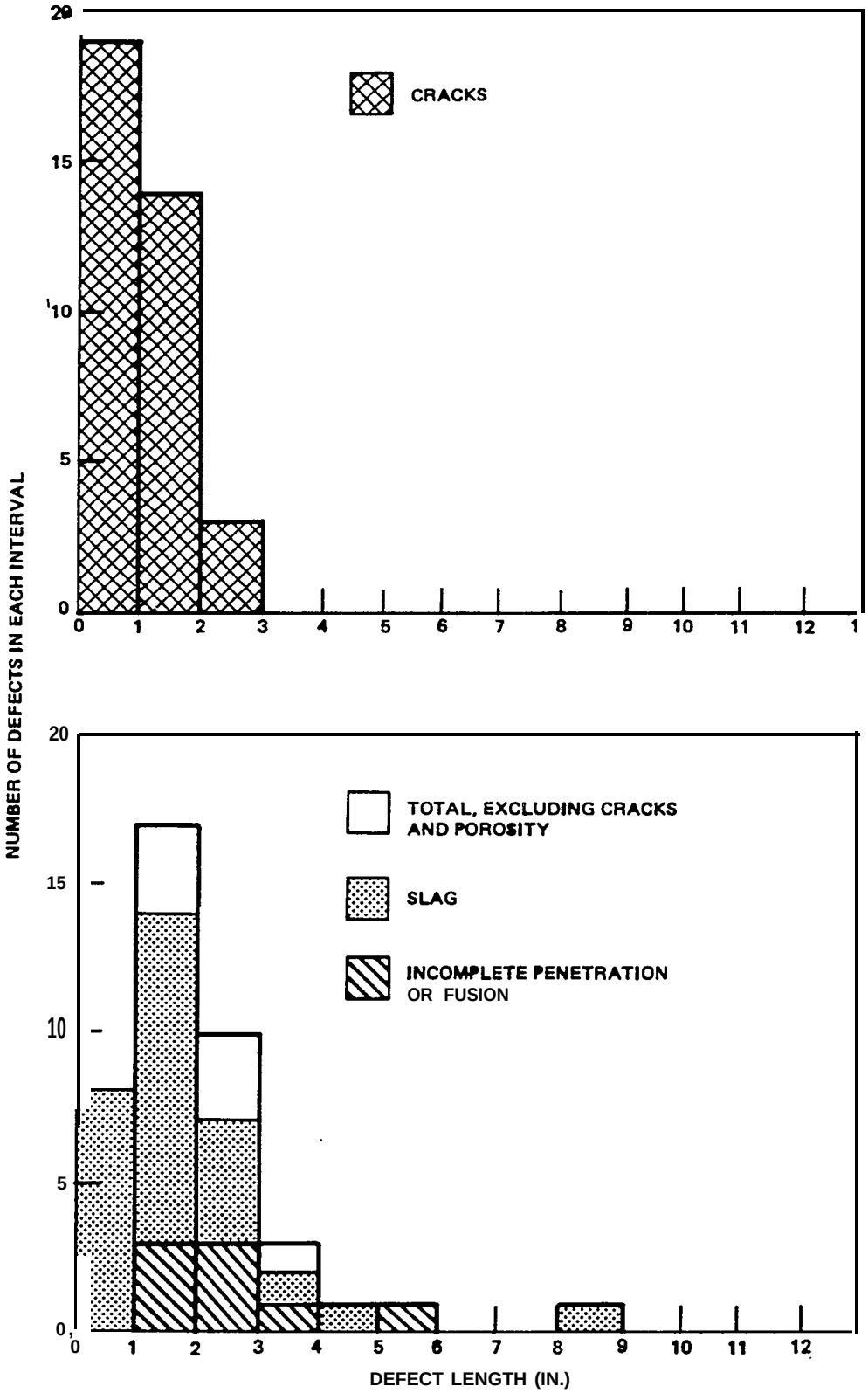


Figure 2-5. Lengths of Individual Defects in the Container Ship

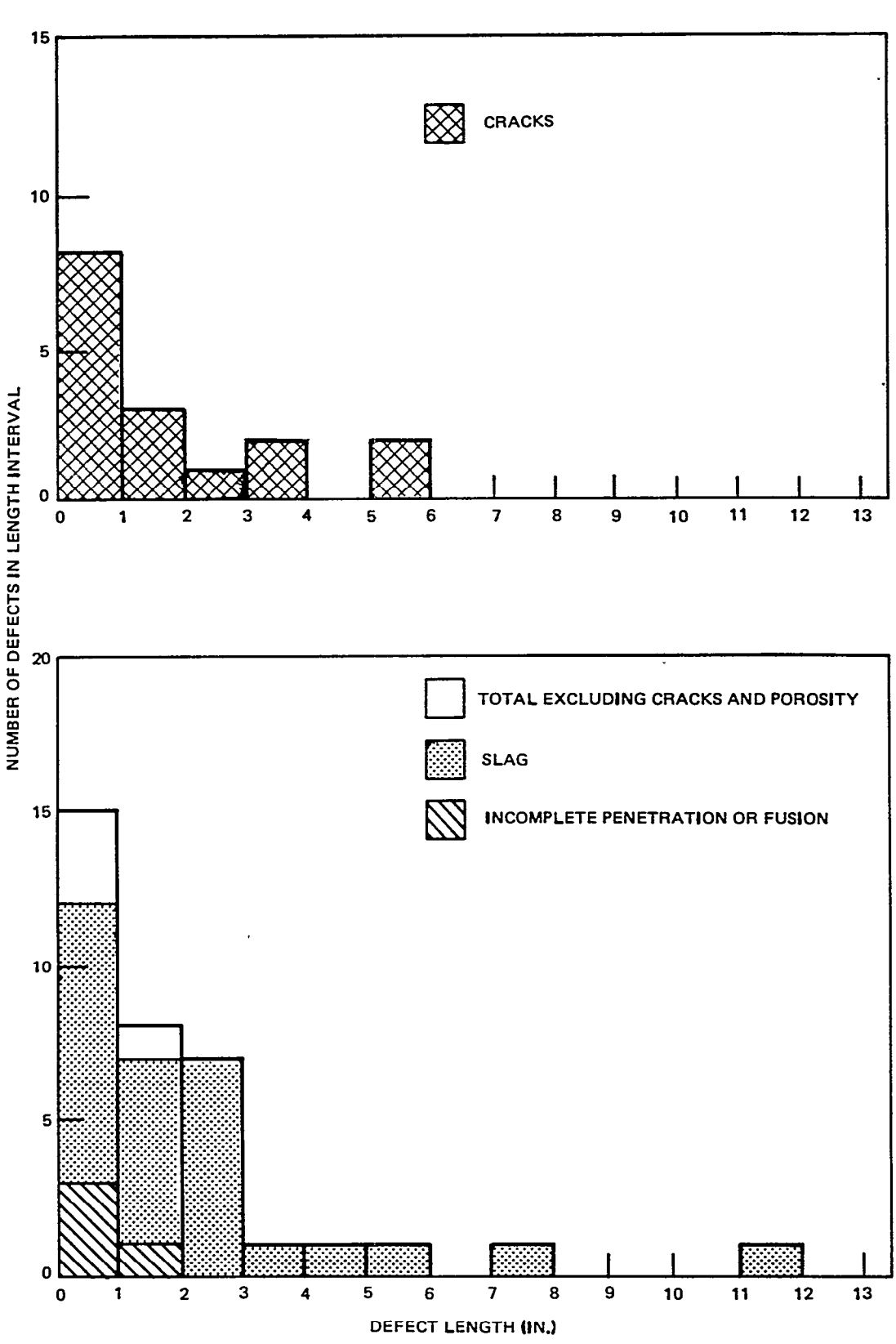


Figure 2-6. Lengths of Individual Defects in the Cargo Ship

B. Cracks —At stress amplitudes on the high side of those experienced in the hull plating of typical ships, limited data indicates that fatigue life is lowered in cracked weld specimens.

C. Slag — The presence of slag inclusions appears to increase scatter in fatigue life[4], due to the varying notch effects possible.

D. Incomplete Penetration — Incomplete penetration defects lower the endurance limit.

Thus, the limited data indicates that the primary effect of all flaw types was to lower the fatigue endurance limit.

### 2. 2.4 Fatigue Growth of Weld Defects

Fatigue has previously been identified as the most likely failure mode resulting from weld defects (Section 2.2. 3). In order to gain some insight into the relationship between flaw geometry, failure criteria, and weld inspection requirements, an approximate fatigue-growth analysis was performed. In making fatigue crack-growth calculations, the "fourth-power" law appears to correlate fairly well with data far many materials over a large range of stresses (References 5 and 6). The fourth-power law may be stated as

$$\frac{da}{dn} = C\ (\Delta K)^4 \qquad (1)$$

$$= \pi^2\, C(\Delta\sigma)^4\, a^2 \qquad (2)$$

and may be integrated to give

$$\frac{1}{a_o} - \frac{1}{a_f} = \pi^2 C \sum_i (\Delta\sigma_i)^4\, n_i \qquad (3)$$

where $n_i$ is the number of stress cycles that experience the stress range $\Delta\sigma_i$. For the purposes of this report, "a" is defined as the distance from a reference line in the crack to one growing edge. The location of the reference line is dependent on the crack's location and geometry. $a_o$ is the original distance; af is the final distance. Figure 2-7 presents some fatigue crack-growth data for steels (References 6 and 7) and also the crack-growth law assumed in the calculations.

---

4 e.g., for a case cited in Appendix Section B. 2, the fatigue life could be anything from 60, 000 cycles to more than $10^6$ cycles.

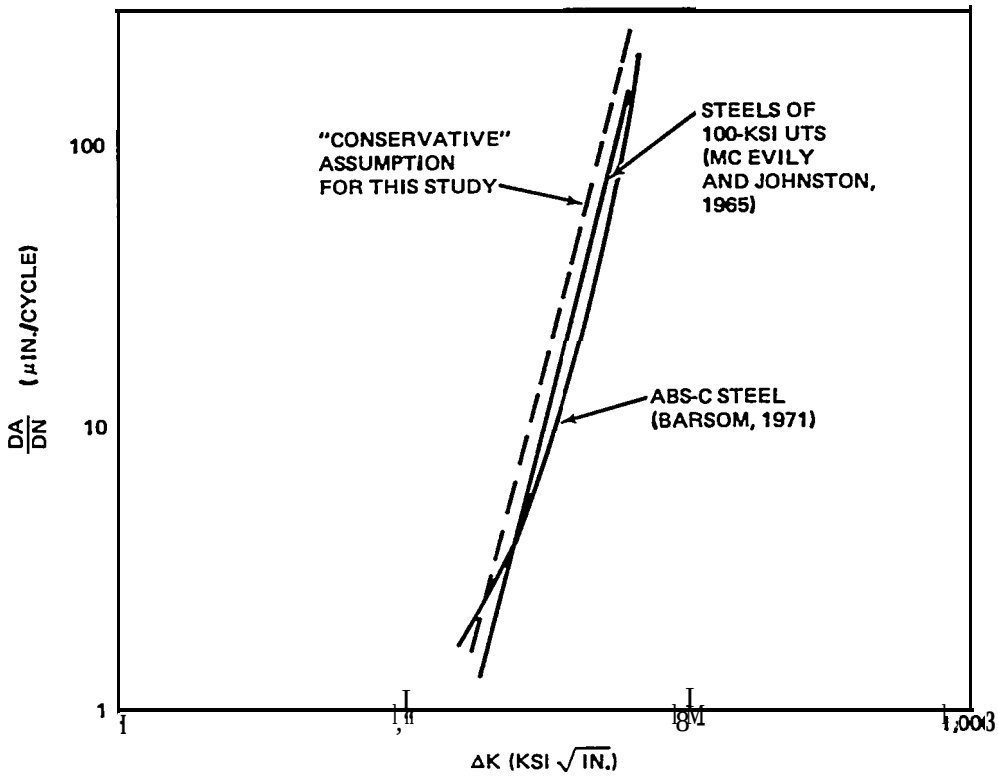


Figure 2-7. Crack Growth in Low-Carbon Steels

**Several assumptions are implicit in using Equation 3 and Figure 2-7 to estimate the growth of weld defects in a ship:**

**A. The weld metal is assumed to conform to Figure 2-7, which is based on plate steel.**

**B. The fourth-power law ignores both the order of varying-amplitude stress-cycle application and the effects that mean stress level may have on crack-growth rate.**

**C. It is assumed that the initial weld defect is a sharpened crack, which may not be true for incomplete penetration, slag, or porosity.**

**D. Much of the ship-hull lifetime is spent at extremely low stress amplitudes (Figure 2-8), at which little if any crack growth data has been obtained. It is assumed that Equation 1 and Figure 2-7 may be extrapolated to low amplitudes of stress -intensity factor.**

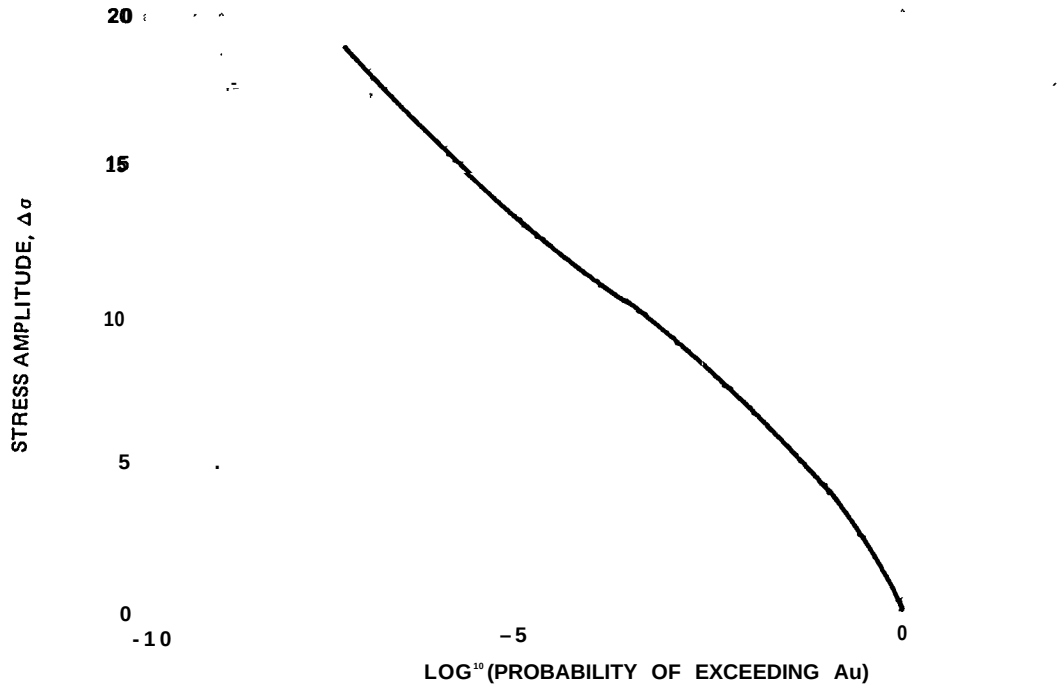


Figure 2-8. Assumed Curve of Stress Amplitudes Experienced in Deck Plates of Typical Merchant Vessels

E. In the case of cracks growing through the thickness of the weld, no account is taken in Equation 3 of the surface magnification effects, which tend to increase the effective stress -intensity factor.

The stress amplitudes, $A u_i$, to which butt (transverse) welds in the hull are exposed were estimated from Nibbering's "expected 95 percent confidence limit" for wave-moment stresses (Reference 8) and are shown here in Figure 2-8. The values of $A U_i$ and the corresponding number of cycles actually assumed in the fatigue calculations are shown in Table 2-2, together with the results in terms of ( $l/s. - l/a_f$) calculated from Equation 3. The result may be summarized as

$$\frac{1}{a_o} - \frac{1}{a_f} = 0.163Y$$

where Y is the time in years necessary to grow the crack from $a_o$ to $a_f$.

Table 2-2

ASSUMED CYCLIC STRESS AMPLITUDES

| $\Delta\sigma$ Peak-to-Trough Stress (ksi) | $n_i$ Number of Cycles in 20 Yr | $\pi^2 C (\Delta\sigma_i)^4 n_i$ Estimated Flaw Growth Factor* (20 yr) | Relative Contribution to Total Estimated Flaw Growth (%) |
|---|---|---|---|
| 22 | 1 | 0.00004 | |
| 19 | 10 | 0.002 | |
| 17 | $10^2$ | 0.0014 | 1 |
| 15 | $10^3$ | 0.0087 | |
| 12 | $10^4$ | 0.036 | 1 |
| 10 | $10^5$ | 0.17 | 5 |
| 8 | $10^6$ | 0.70 | 21 |
| 5 | $10^7$ | 0.95 | 29 |
| 3 | $10^8$ | 1.38 | 42 |
| | | $\sum_i$ 3.25 | 100 |

*Total Flaw Growth Factor = $\frac{1}{a_o} - \frac{1}{a_f}$ = 3.25 lover 20 years

or

$\frac{1}{a_o} - \frac{1}{a_f}$ = .163 in.$^{-1}$ over 1 year

In converting total number of stress cycles to years, it was assumed that approximately $10^8$ cycles are accumulated in 20 yr of service. This figure is based on the 10-sec period of the usual wave-induced-moment cycle (there are $0.63 \times 10^8$ 10-sec periods in 20 yr). A discussion of these and other stresses in ship hulls is presented in Appendix C.

Table 2-2 suggests that, contrary to general supposition (for example, References 9 through 11), the lower stress amplitudes motivate most of the fatigue-crack growth.

Figure 2-9 gives the estimated time needed for a crack that intially penetrates the plate, and has an initial length $2a_o$, to grow to a total length of 6 in. under the action of the stress-amplitude spectrum shown in Table 2-2 . The upper limit of 6 in. was selected because it seems large enough to be detected in

5 $a_o$ in this case is

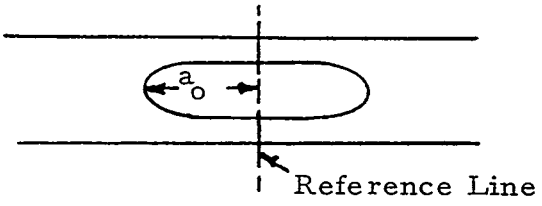

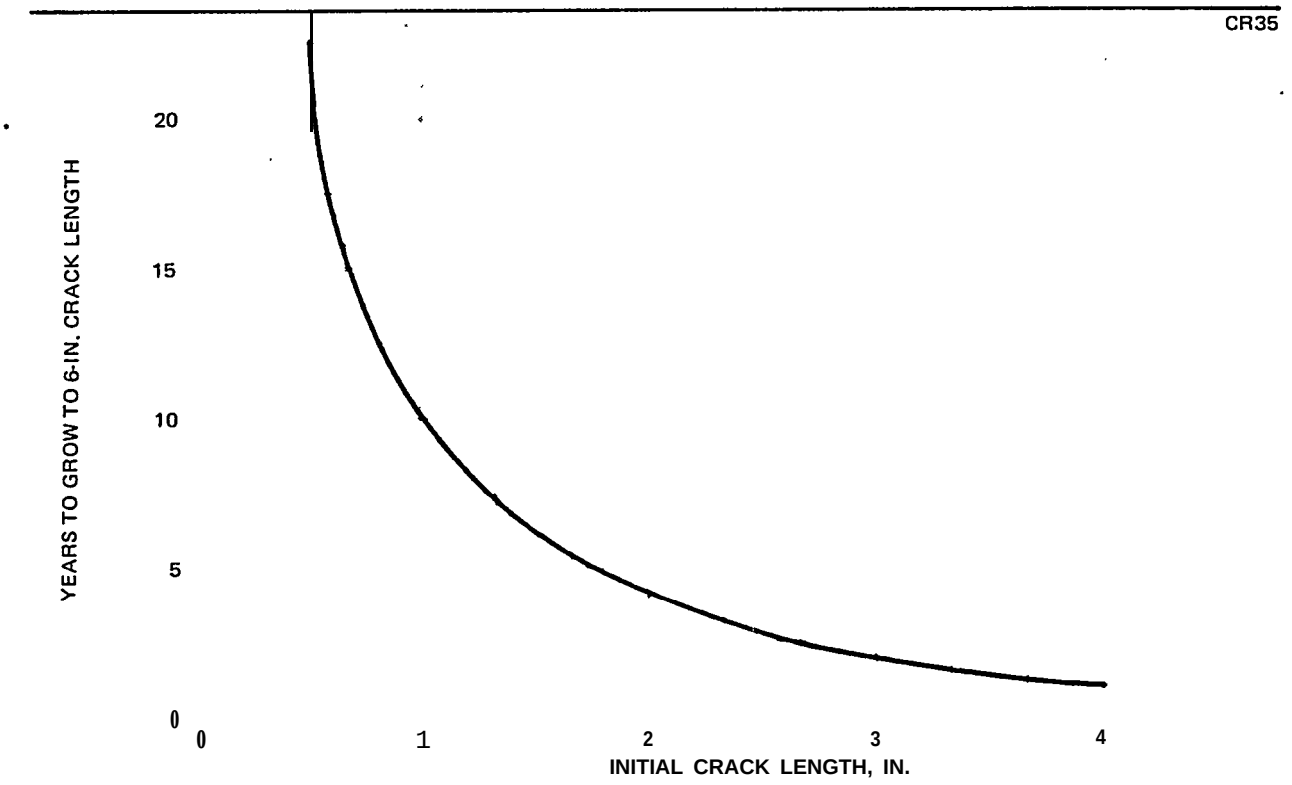


Figure 2-9. Calculated Service Life Before Attaining 6-in. Length for Through-Cracks of Various Initial Lengths

routine surveys and yet appears conservatively under the 8- to 12-in. length that would be critical with respect to brittle failure if an unusually high stress (in the vicinity of yield strength) occurred when the hull experienced low temperatures.

Figure 2-9 shows the length extension of a defect after it has grown to full penetration of the hull plate. In general, a submerged, elongated defect will-tend to grow heightwise (in fatigue) until it penetrates the thickness of the weld before it extends significantly in length. This is simply a consequence of the tendency for irregular defects to grow toward a circular shape. Once full penetration has taken place, the crack will tend to grow in length.

The off-center flaw of Figure 2-10b will grow to full penetration more rapidly than the mid-depth flaw shown in Figure 2- 10a. Calculated re suits are in Figure 2-11.

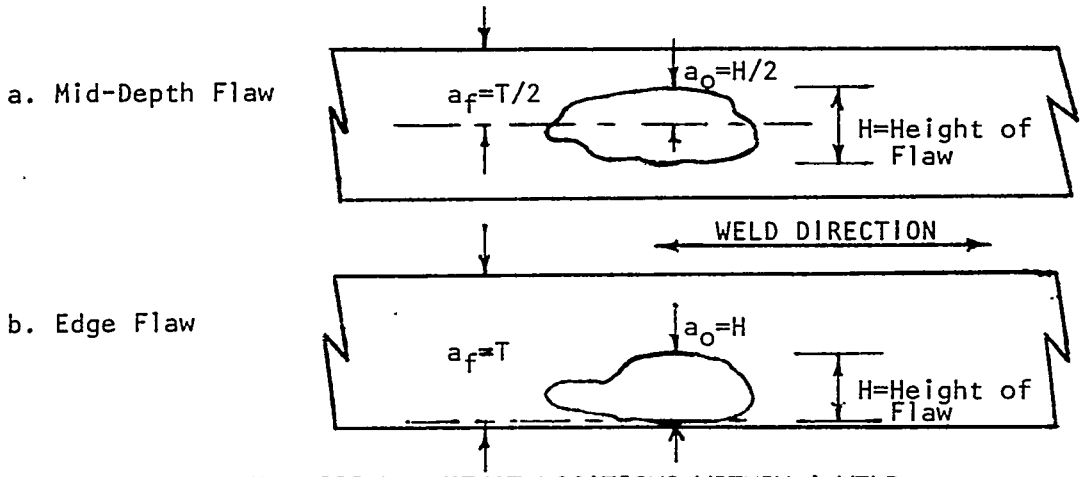


FIGURE 2-10: TWO POSSIBLE DEFECT LOCATIONS WITHIN A WELD

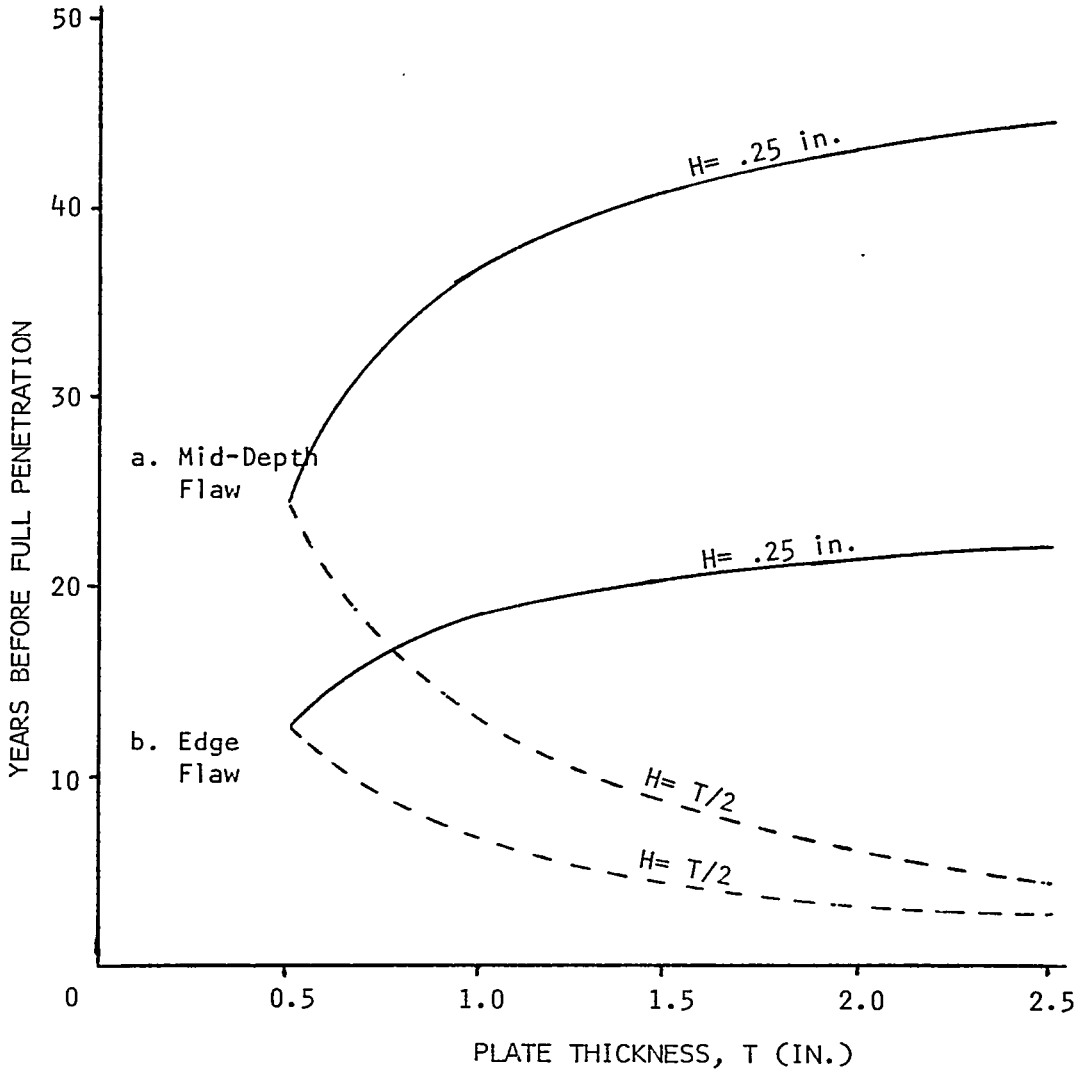


FIGURE 2-11:
CALCULATED SERVICE LIFE BEFORE ATTAINING PENETRATION OF WELD THICKNESS

It is apparent from Figure 2-11 that the fatigue life can be considerable for many fairly large defects before full penetration. It is obvious, as illustrated also in Figure 2-12, that the original height of a flaw will significantly influence its life before full penetration.

One implication relevant to the current ABS weld inspection requirements is suggested by the above results. The fatigue life of a weld flaw can be defined either as the time required for growth to full penetration (leakage) or as the time for growth to a length where brittle fracture is possible. If growth to full penetration is considered the criterion for criticality, the ' results of the analysis indicate that original flaw height is the primary factor determining fatigue life. If the prevention of catastrophic (brittle) failure is the sole criterion, original flaw height (see Figure 2-10) and original flaw length determine the time (cycles) to reach critical size. In both cases, information regarding flaw height is desirable in making rational weld-inspection accept - reject decisions. In the current ABS weld-inspection requirements, only flaw length is included in the criteria for acceptance or repair. Assuming the availability of a suitable nondestructive inspection technique, the inclusion of flaw eight in the criteria could lower the frequency of rejection and repair. [2]

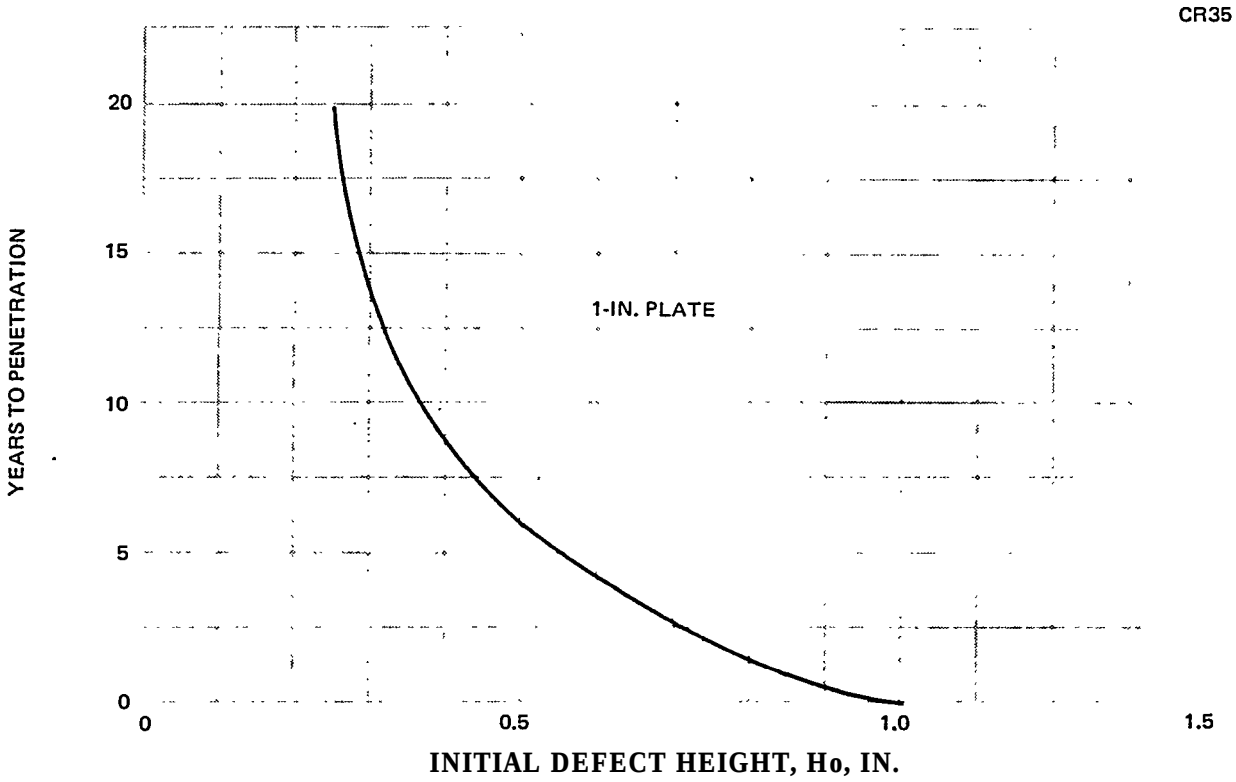


FIGURE 2-12. CALCULATED EFFECT OF DEFECT HEIGHT ON LIFE TO PENETRATION FOR l-IN. PLATE

6 A reviewer's analysis, Appendix G, indicates that the use of height and depth criteria may not be practical.

The discussion so far has been based on stress amplitudes (Figure 2-8) representing simple shell butts. In regions of load concentration, such as at corners of hatch openings, significantly higher stresses may occur. Based on the simple fourth-power relationship (Equation 1), the effect of stress concentrations on fatigue life may be estimated as in Figure 2-13. For commonly observed stress concentrations of about 2, the fatigue life (however defined) of a given defect will be decreased by more than a factor of 10. This observation suggests the importance of screening detail design to eliminate high stress concentrations in high load areas.

The results of the fatigue analyses were employed to evaluate the current ABS radiographic and provisional ultrasonic inspection acceptance-rejection criteria. The longest acceptable single flaw was determined from Figure 2-1

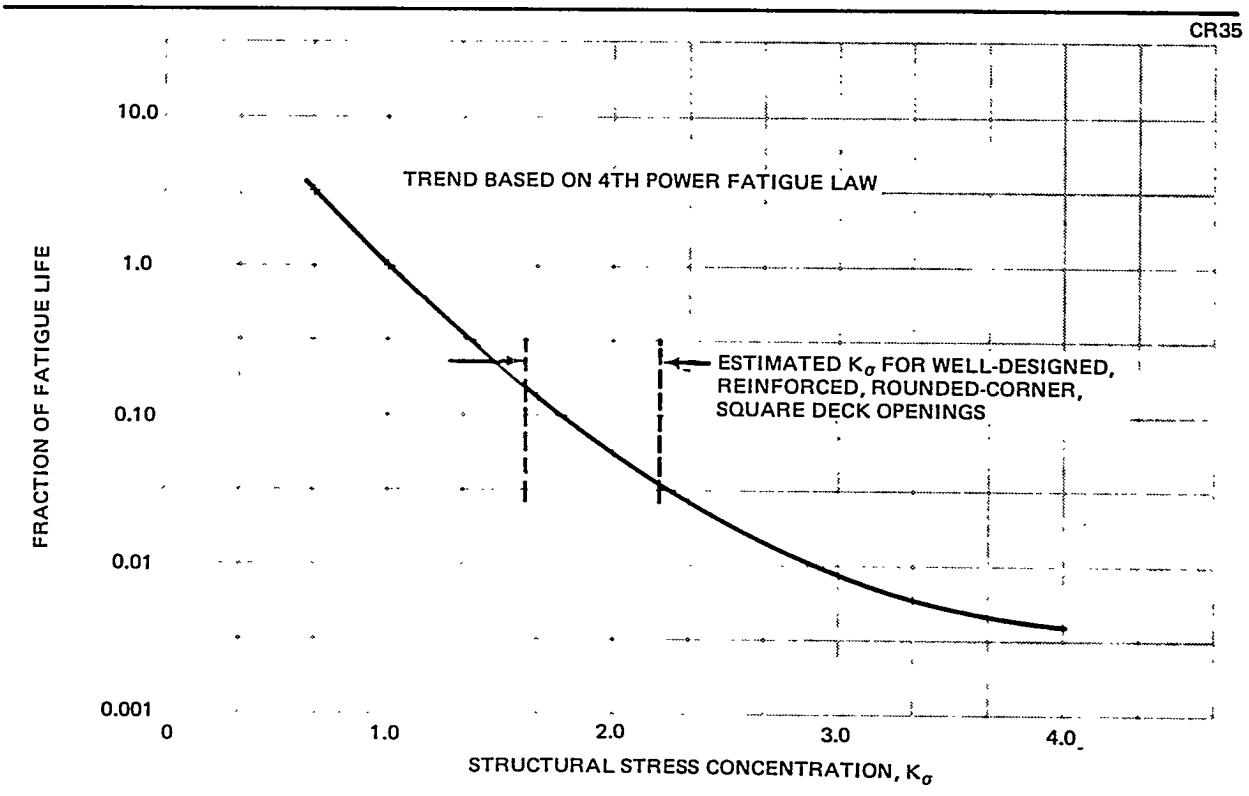


Figure 2-13. Effect of Elastic Stress Concentrations on Fatigue Life of Defective Welds

for plate thicknesses from 1/2 to 2 in. The initial flow width was assumed to be 1/4 in. for all plate thicknesses. The estimated times to reach both full penetration (leakage) and an assumed (conservative) critical length of 6 in. are shown in Figure 2-14. Two cases, with and without stress concentration, are illustrated.

The effect of initial flaw height on fatigue life is shown for l-in. -thick plate welds in Figure 2-15. The longest acceptable initial flaw lengths from the current radiographic and provisional ultrasonic criteria were employed. Several implications relevant to the weld inspection requirements are suggested by this very approximate analysis which tends to overpredict fatigue growth:

A. For most cases in areas of no stress concentration, the current radiographic acceptance-rejection criteria appear to be conservative with respect to assuring no brittle failure of inspected welds during a 20-y-r lifetime. However, high initial flaws in thick plate may penetrate the thickness prior to 20 years.

B. The greater initial defect length presently acceptable for ultrasonic inspection leads to significantly less conservative criteria if indicated length is synonymous with actual length, as the inspection results of this program suggest (see Section 2.3. 4).

C. Different heights of flaws can preduce wide variations in the time required for acceptable flaws of the same initial length to grow to a potentially dangerous size, as illustrated in Figure 2-15. The current radiographic and ultrasonic requirements do not distinguish between flaws that are short in height and the potentially more harmful high flaws. The inclusion of length and height criteria in the ultrasonic requirements could remove this concern.

D. For areas of high stress concentration, both current radiographic and ultrasonic criteria might accept flaws that could grow to dangerous sizes in short times (Figure 2-14). It should be emphasized that in all cases, full penetration should occur prior to extension to critical fracture length. Therefore, the currently required periodic service inspections should result in detection and repair of the penetrated flaws before they become potentially harmful to the hull structural integrity.

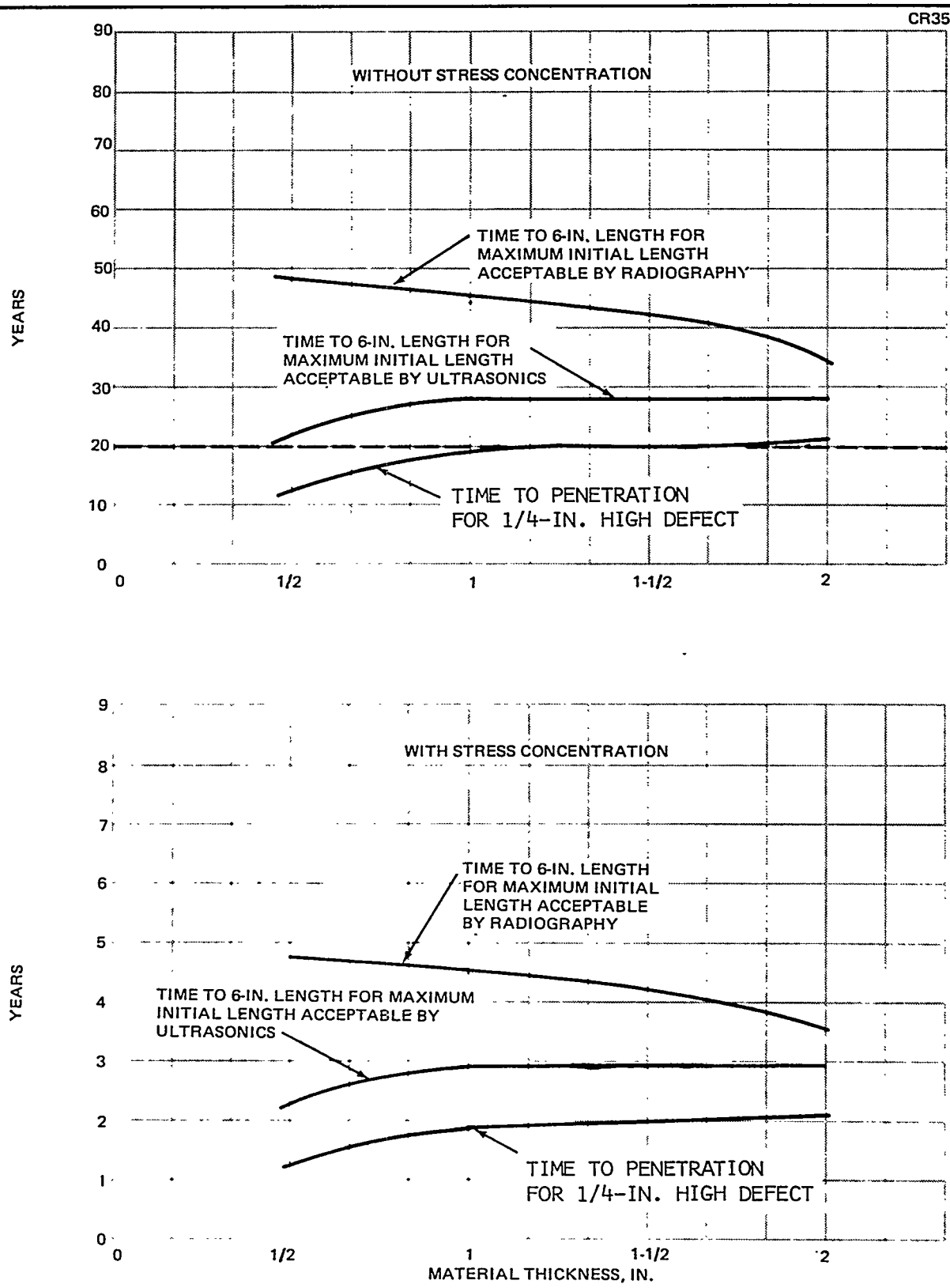


FIGURE 2-14. ESTIMATE TIME TO PENETRATION AND TO 6-IN. LENGTH FOR 1/4-IN. HIGH DEFECT OF MAXIMUM ACCEPTABLE LENGTH FOR VARIOUS PLATE THICKNESSES

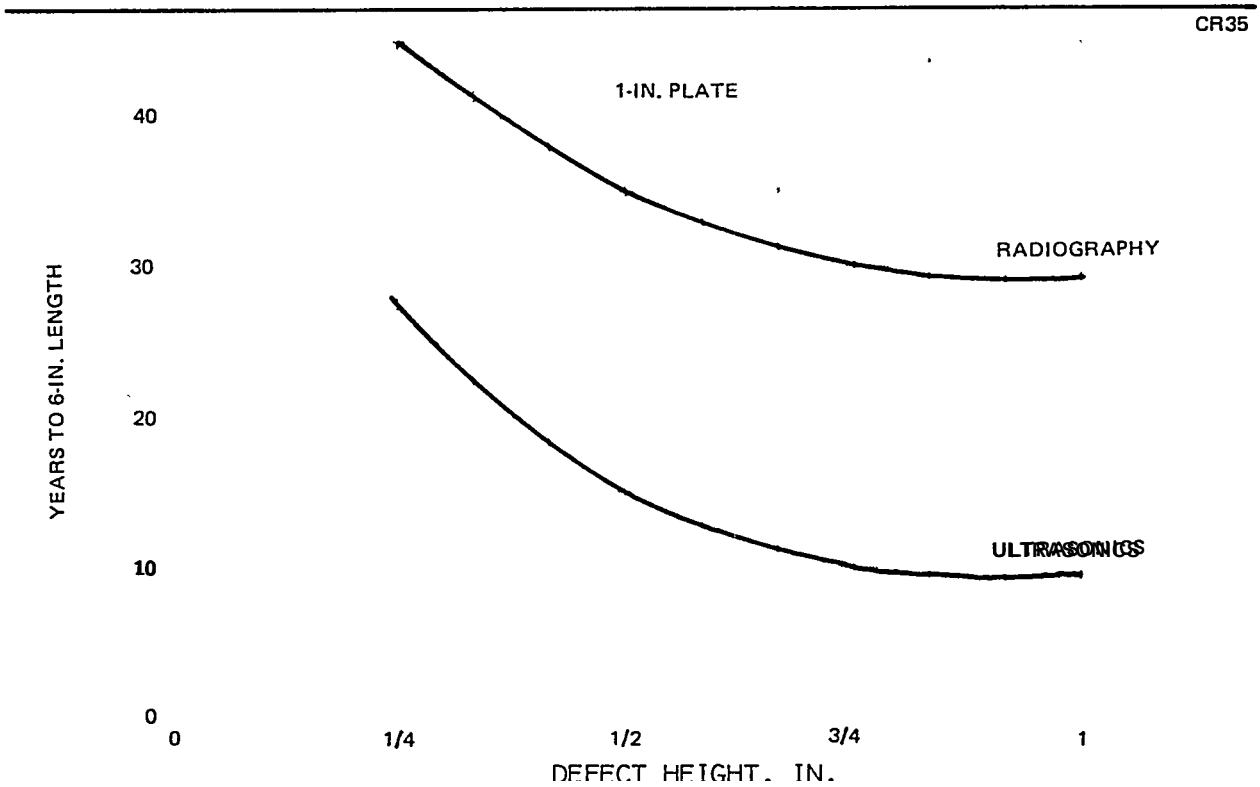


**FIGURE 2-15. ESTIMATED TIME TO 6 IN. LENGTH FOR DEFECTS OF VARIOUS HEIGHTS AND MAXIMUM ACCEPTABLE FOR l-IN. PLATE-APPROXIM4TELY 0.45" FOR RT AND 1.15" FOR UT; SEE FIG. 2-1**

## 2.3 EVALUATION OF TECHNIQUES

**One of the ways of reducing the cost of nondestructive inspections to change the inspection method. The alternative method must detect the presence and magnitude of internal defects as required by the acceptance criteria. The method must also be less expensive to employ than radiography. An experimental evaluation was conducted to determine the relative effectiveness and costs of possible alternative techniques.**

Wedge ultrasonic shear-wave inspection, ultrasonic shear-wave inspection using a liquid-filled wheel, ultrasonic delta scan, acoustic holography, and acoustic emission techniques were selected as well developed methods that could potentially be applied in a shipyard environment. The inspection results for these techniques were compared to those of X-ray using welded test specimens with purposely introduced weld defects. The detected defects were also compared directly with actual defects as revealed by the fracture of selected weld sections.

### 2.3. 1 Nondestructive Testing Specimens

Thirty-one test panels with purposely introduced weld defects were provided by Todd Shipyards Corporation—Los Angeles Division. There were three types of panels, as illustrated in Figure 2-16. Four types of weld defects were introduced: porosity, slag inclusions, incomplete penetrations, and cracks. The panel dimensions and defect types were distributed among the types of panels as described in Table 2-3. The test panels were intended to be representative of weld geometry and defect types that might occur in shipyard practice. Fabrication details are given in Appendix D.

CR35

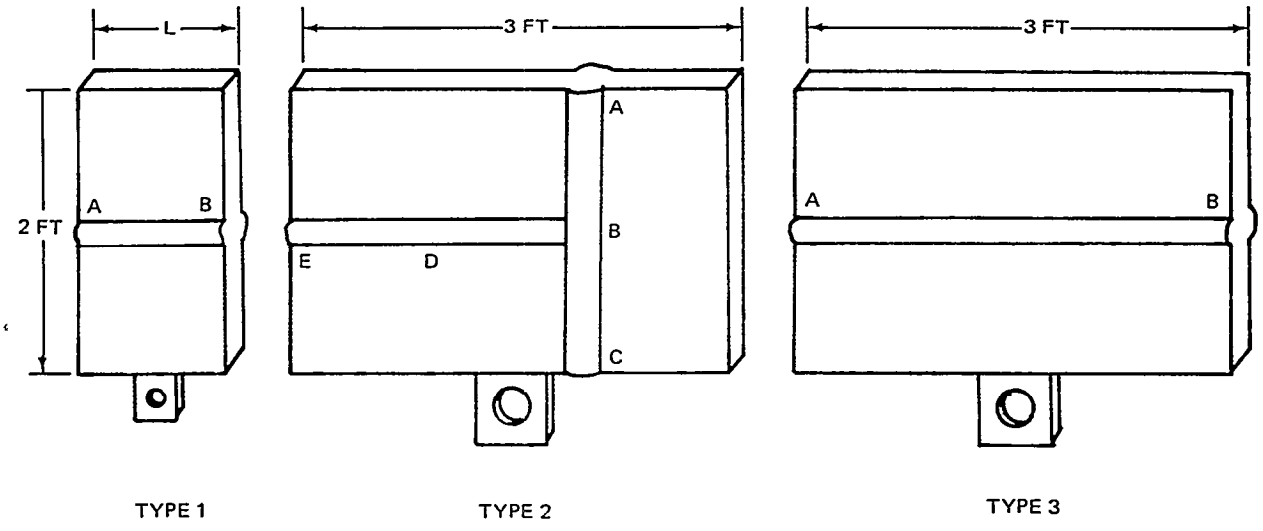


Figure 2-16. Panel Specimens

Table 2-3

TEST PANEL DESCRIPTION

| Panel Type | No. of Panels | Dimensions (in.) L | W | T | Defect Type P | S | LP | C[j,k] |
|---|---|---|---|---|---|---|---|---|
| 1 | 15 | 6-1/2 to 12 | 24 | 1/2, 1, 1-1/2, | 2 | x | x | x | x |
| 2 | 14 | '36 | 24 | 1/2, 1, 1-1/2, | 2 | x | x | x | x |
| 3 | 2 | 36 | 24 | 1/2, 2 | | | | | X |

Key

P = porosity, S = slag inclusion, LP = lack of penetration, C = crack

*The majority of the cracks were parallel to the weld centerline.

### 2.3.2 Nondestructive Inspection Techniques

The test panels were inspected using the alternative techniques as indicated in Table 2-4. Details of the calibration and inspection procedures are given in Appendix E. A brief description of each technique evaluated is presented in the following sections.

Table 2-4

INSPECTION PLAN

| Panel Type | Inspection Technique: X-Ray | Ultrasonics: Wedge (Shear-Wave) | Ultrasonics: Wheel (Shear-Wave) | Ultrasonics: Delta | Acoustic Holography | Acoustic Emission |
|---|---|---|---|---|---|---|
| 1 | X | X | X | | X | |
| 2 | X | X | X | X | | |
| 3 | X | X | X | | | X |

### 2. 3.2.1 Film Radiography

All of the test panels were inspected using film radiography as specified by the ABS radiographic inspection requirements. There were two exceptions to general ship practice. First, an x-ray source was used rather than a gamma-ray source. Second, for all but the 2-in. -thick panels, extra-fine-grain film (Kodak Type M) was used rather than fine-grain film (Kodak

Type AA). These steps guaranteed a sensitivity sufficient to protide an accurate basis of comparison for evaluation of the alternative techniques. [7]

### 2. 3.2.2 Wedge Shear-Wave Inspection

All of the test panels were inspected using conventional shear-wave techniques as specified by the ABS provisional ultrasonic inspection requirements. An Automation Industries Model 725 Immerscope was used as the pulse r- receiver. An Automation Industries 1/2 in. -diameter, Type SFZ, Style 57A3134, 2.25-MHz longitudinal-wave transducer was used both as a transducer for reference during the program for comparing other transducers and for pulse r-receiver setup and lamination inspection. Three Automation Industries Type STL, 2. 25-MHz angle-beam transducers were used for shear-wave inspection.

The shear-wave transducers were selected because they have active elements of the same size (1/2 in. wide by 1 in. long) as the liquid-filled wheel. The inspection angles used for each material thickness are presented in Table 2-5. These angles were chosen to make the results directly comparable to those for the liquid-filled wheel.

Table 2-5

INSPECTION ANGLES

| Material Thickness (in.) | Shear-Wave Angle in Steel (deg) |
|---|---|
| 1/2 | 70 |
| 1 | 60 |
| 1-1/2 | 45 and 60 |
| 2 | 45 and 60 |

Some difficulty was experienced in obtaining the proper distance-amplitude correction using the sensitivity time control on the pulse r-receiver. A simpler calibration method (Appendix E) was developed that provided the necessary discrimination levels.

---

Shipbuilders commented that the combination of extra-fine grain film and using X-ray could lead to a misleading conclusion that RT is always more sensitive than L-T. The use of fine grain film and gamma ray sources, generally employed in shipyards, would have disclosed that RT is only more sensitive to linear type flaws such as cracks, cold shuts and lack of fusion.

8

Although the necessary discrimination levels were achieved, one shipyard tried the calibration method described and commented that it

The surface condition of the test panels was often less than adequate for shear-wave inspection. These panels were disc-sanded to remove weld splatter and to smooth regions of primed surface adjacent to unprimed surface.

Considerable care was required for the correct interpretation of reflections from the weld beads. Small errors in the calibration procedure could lead to the incorrect interpretation of these signals as defect indications.

Position and length measurements were recorded for each defect detected. The maximum signal-amplitude distance of the transducer from the weld and the position of the signal on the oscilloscope screen were also re - corded for each defect. Thus, information about the position, length, and height was available for each defect.

### 2.3.2.3 Liquid-Filled Wheel Shear -Wave Inspection

All of the test panels were inspected using an Automation Industries Type SOB, Style 50 D340, 2. 25-MHz, variable-angle wheel search unit. The ultrasonic transducer was oriented within a liquid-filled wheel to perform shear-wave inspection at right angles to the rolling direction of the wheel, as shown in Figure 2-17.

The calibration and inspection procedures (Appendix E) were similar to those for wedge shear-wave inspection.

.Special procedures for calibrating the internal angle were developed using wedge-angle blocks. The angle was adjusted by maximizing the reflected signal from the face of a 45°, 60°, or 70° wedge. The method was simple, accurate, and repeatable.

The operation of the wheel was hindered by the presence of two internal reflections within the wheel. One reflection due to improper backing of the piezoelectric element was eliminated by bonding a piece of closed-cell sponge to the back of the element. The other reflection occurred after a reflection from the liquid-tire interface, as shown in Figure 2-18. This reflection interfered with inspection of the top 1/2 in. for 2-in-thick material at 45 degrees after a reflection from the bottom surface of the test panel. Elimination of this reflection would require modification of the transducer holding mechanism to introduce an absorber along the internal sound-beam path.

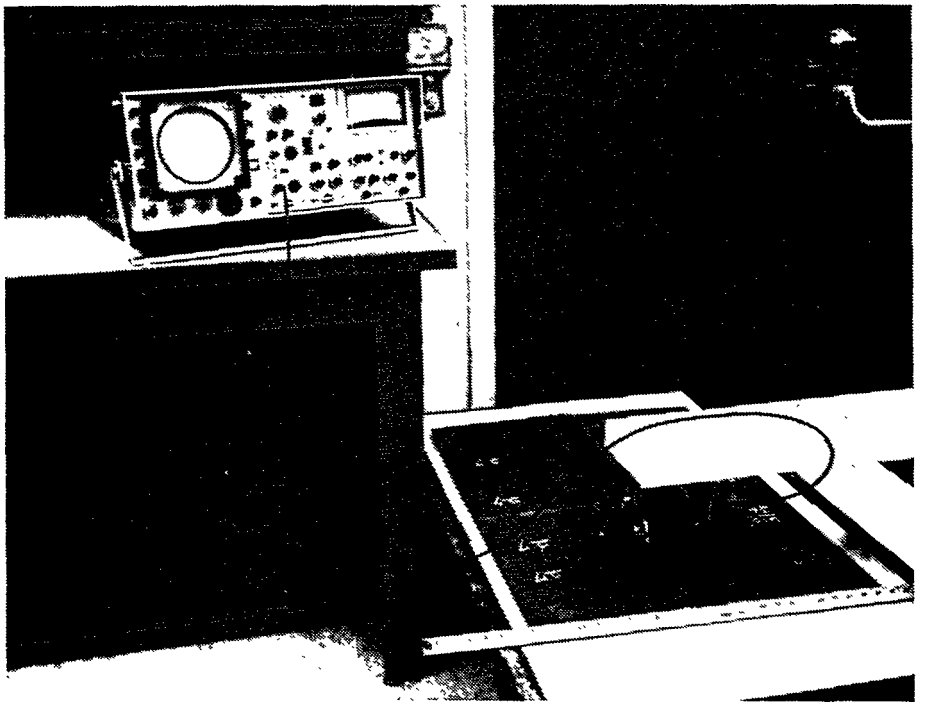

Figure 2-17. Liquid-Filled Wheel Shear-Wave Inspection

Several passes of the wheel were required to inspect the weld volume completely, as shown in Table 2-6. The spacing between passes was determined by the projected length of the 1/2 in. -wide transducer element on the steel surface.

The wheel was somewhat involved and cumbersome to operate because of the internal angle adjustment and pass indexing required. On the other hand, interpretation of the reflected signal was easier because of the fixed distance of the wheel from the weld.

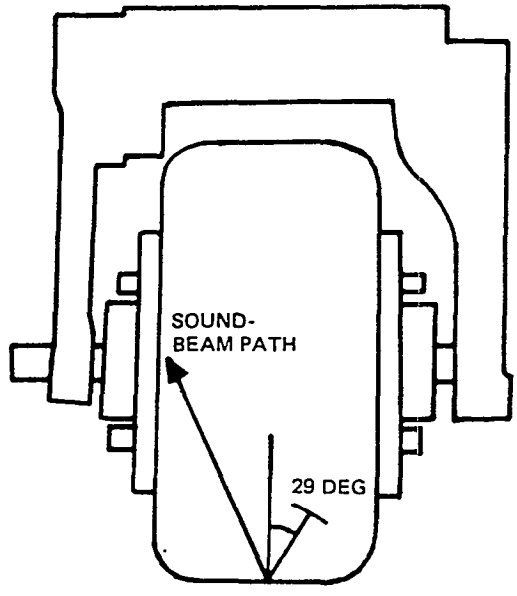


Figure 2-18. Internal-Reflection Sound-Beam Path

Table 2-6

DISTANCE FROM WELD FOR WHEEL PASSES

| Material Thickness (in. ) | Angle (deg) | Distance From Weld (in. ) |
|---|---|---|
| 1/2 | 70 | 1-1/4, 1-7/8, 2-1/2 |
| 1 | 60 | 1-5/16, 1-7/8, 2-7/16, 3, 3-9/16 |
| 1-1/2 | 45 | 2-9/16, 3-1/8, 3-11/16 |
| | 60 | 1-9/16, 2-1/8, 2-11/16 |
| 2 | 45 | 3-1/4, 3-13/16, 4-3/8 |
| | 60 | 2, 2-9/16, 3-1/8 |

Position, length, and height measurements were recorded for each defect in the same manner employed for wedge shear-wave inspection.

### 2. 3.2.4 Delta Scan

An attempt was made to inspect a few of the Type 2 test panels using the delta-scan technique. An Automation Industries Delta Scan Manipulator, Style 57 A4957, was used to position two transducers, a transmitter, and a receiver. The transmitter was oriented to produce shear waves in the weld metal. A focused receiver was used to detect any signals redirected by the presence of a defect.

Several transmitters and receivers were tried in a variety of different orientations without success. The technique provided excellent detection of through holes in the sensitivity calibration standard, but the relatively irregular weld-bead surfaces reflected or reradiated sound that could not be excluded through normal gating procedures. Personnel at Automation Industries and General Dynamics agreed that irregular weld-bead surfaces present a problem for delta-scan inspection (Reference 12). Accordingly, further evaluation of delta scanning was terminated.

### 2. 3.2.5 Acoustic Holography

All of the Type 1 test panels were inspected using a Model 200 Holscan Digital Mechanical Scanner manufactured by Holosonics in Richland, Washington. A technical report on this work has been published, (Reference 57).

The scanner was designed for very thick metal sections. The scanning aperture of 6 in. by 6 in. , scanning velocity of 3 in. /see, and increment step of 0. 018 in. resulted in a rather slow inspection rate.

Sensitivity standards have not been established for acoustic holography. The inspection was performed at a resolution level determined by the 3-MHz transducer frequency.

### 2. 3.2.6 Acoustic Emission

Using acoustic emission techmques, two Type 3 test panels with 4-ft-long welds were monitored for crack formation during welding and weld cooldown. One panel was 1/2 in. thick, the other was 2 in. thick. The weld was contaminated using cast-iron filings to generate cracks. The panels were subsequently trimmed to a 3-ft length for further evaluations.

A Dunegan-Endevco Model 902 flaw locator, Model 802 PC preamplifiers, and Model S750B transducers were used to detect and locate the acoustic emissions from crack formation or growth. One transducer was placed at each end of the weld. The instrumentation determined the difference in arrival time of an acoustic emission event.

Background noise and attenuation measurements were taken to help select the correct transducer frequency and threshold gain. The instrumentation was very sensitive to extraneous mechanical and electrical noise. Transducers with a resonant frequency of 750 kHz were selected for their reduced sensitivity to extraneous noise from long distances. Nearby electrical activity was halted during the monitoring to reduce the electrical interference. Better shielding and the use of differential transducers should eliminate the electrical interference.

It was difficult to select the proper threshold gain. A total system gain of 60 dB provided very little indication of crack formation, whereas a system gain of 80 dB was so high that the instrumentation primarily detected extraneous noise. Even a procedure using a simulated emission event introduced at one transducer location to adjust the gain of the opposite transducer, which resulted in less than 80 dB gain, still resulted in extreme sensitivity to extraneous noise. Emission events from cracks were not distinguishable from the background noise using either the flaw locator or from a plot of count rate versus time. Acoustic-emission detection of defects other than cracks was not examined. Acoustic-emission monitoring during welding was not satisfactory for inspection of ship-hull welds.

### 2. 3.3 Fracture Testing

Selected specimens were cut from the test panels to fracture the weld metal and reveal the presence of any defects. The specimens primarily contained crack and lack-of-penetration defects, as it was felt that radiography provided reliable indications for slag and porosity. The specimens were 3 in. wide by 2 ft long, with a flat area machined on one side of the weld bead and a sharp notch machined on the other side to a depth of 1/4 the panel thickness, as shown in Figure 2-19. The specimens were cooled below the ductile-brittle

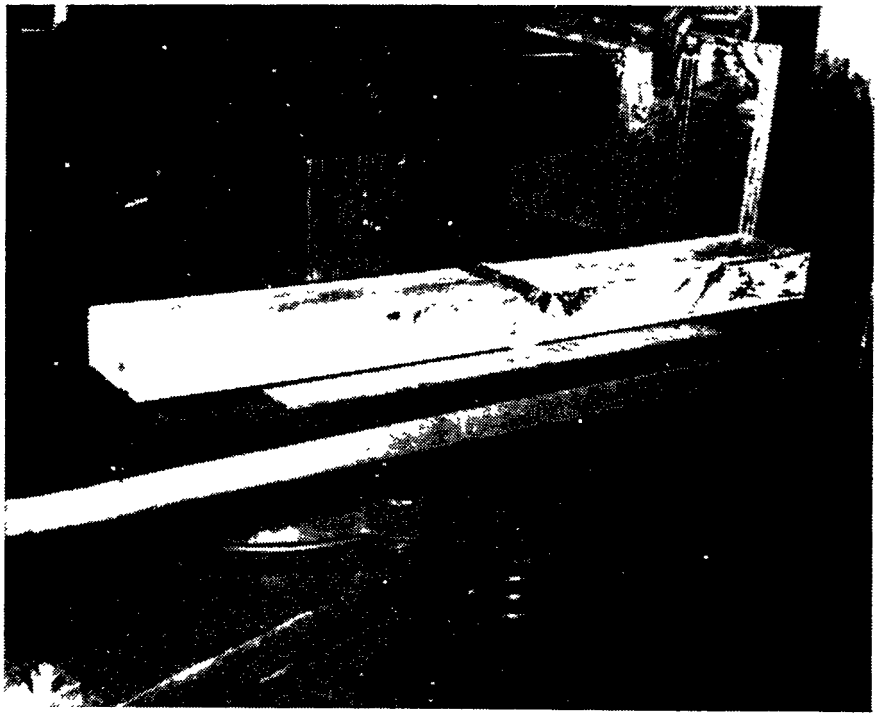

Figure 2-19. Fracture Specimen

transition temperature using liquid nitrogen and were fractured in three-point bending with the center load applied opposite the notch. This method of testing was employed to ensure that the fracture would occur through the weld.

### 2. 3.4 Inspection Results

The alternative techniques were compared to a laboratory radiographic technique as the standard. Radiography was chosen because of its history of acceptance for inspection of steel welds in a shipyard environment. The results of the inspections were tabulated by the length of defect indications by technique and by the length of defect indications found by both a given technique and radiography.

An example of the data obtained from a typical weld, along with definitions of the parameters used in the technique comparison calculations, is shown in Figure 2-20.

### 2.3.4.1 Comparison of Inspection Results by Technique

As discussed previously, delta scan and acoustic -emission monitoring were not satisfactory for inspection of ship-hull welds. Comparison calculations for the remaining techniques are presented in Table 2-7. The calculations are presented for two different groups of specimens. The first group consisted of specimens inspected by acoustic holography, while the second group consisted of the first group plus additional specimens not inspected by acoustic holography.

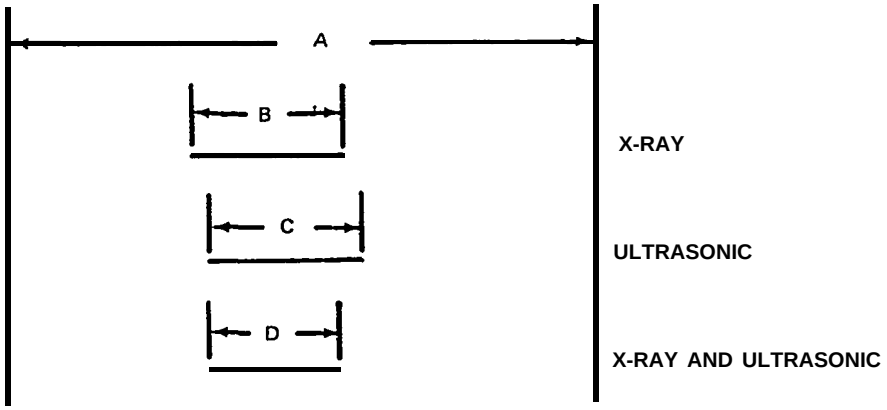


A = TOTAL LENGTH OF WELD
B = LENGTH OF DEFECT FOUND BY X-RAY
C = LENGTH OF DEFECT FOUND BY ULTRASONICS
D = LENGTH OF DEFECT FOUND BY BOTH X-RAY AND ULTRASONICS

(1) $100\,\frac{B}{A}$ = PERCENT OF WELD FOUND DEFECTIVE BY X-RAY

(2) $100\,\frac{C}{A}$ = PERCENT OF WELD FOUND DEFECTIVE BY ULTRASONICS

(3) $100\,\frac{A-(B+C)+2D}{A}$ = PERCENT CORRELATION BETWEEN X-RAY AND ULTRASONICS

(4) $100\,\frac{D}{B}$ = PERCENT OF DEFECT FOUND BY X-RAY THAT WAS ALSO FOUND BY ULTRASONICS

(5) $100\,\frac{A-(B+C)+D}{A-B}$ = PERCENT OF DEFECT-FREE WELD FOUND BY X-RAY THAT WAS ALSO FOUND TO BE DEFECT-FREE BY ULTRASONICS

Figure 2.20. Types of Comparison Calculations

The comparison calculations show that:

A. Wedge shear-wave inspection rejected less than the wheel technique.

B. The wedge shear-wave technique was better than the wheel for cracks, the wheel was better than wedge shear-wave inspection for porosity, and both were equally sensitive for incomplete penetration and slag.

C. Acoustic holography rejected more than the X-ray reference but detected only half the defects and had the lowest correlation with X-ray.

D. Of the alternative techniques, the wheel detected the greatest percentage of X-ray-detectable defects and had the best correlation with X-ray reference.

The reduced sensitivity of wedge shear-wave inspection was noted during inspection as a 1oss in sensitivity to defects in the test panels, as compared to the through holes in the sensitivity calibration standard. The reflected signals from many defects were present but of insufficient amplitude to be considered detectable. This effect was probably due to poorer coupling on the test panels as compared to the calibration standard. Procedures to compensate for these coupling variations should increase the sensitivity and rejection rate of wede shear-wave inspection to at least the same levels as those of the wheel.[5]

---

9

A shipbuilder made the important comment that:

"Considerable attention is given in the report to comparing RT and UT reject rates where in almost all cases RT appears to be the more sensitive NDT method. Sensitivity is claimed to be lowest in UT because of lack of proper coupling on the actual test surface as compared with that on the calibration surface. It has been the shipyard's experience that sensitivity difference between RT and UT is less pronounced than that stated in the report. . . . . Since the crack-like discontinuity is considered to be the most serious, it has generally been considered by us that UT represents the most sensitive test and is preferred for critical applications. It is our opinion that any sensitivity difference observed during the project could have been nullified by increasing the UT sensitivity and therefore, a more direct comparison could have been made between RT and UT. This increase in sensitivity could have been used in the final recommendations for proposed revisions to the ABS 'Provisional Requirements for UT Inspection of Hull Welds' and that sensitivities being proven equal, length of inspection at each inspection point could be justified as being the same for the 'standard' RT and UT."

Table 2-7

COMPARISON CALCULATIONS FOR REJECTABLE DEFECTS

| Criteria | 15 Specimens | | | | 31 Specimens | | |
|---|---|---|---|---|---|---|---|
| | | Ultrasonic Shear-Wave | | | | Ultrasonic Shear-Wave | |
| | X-Ray* | Wheel | Wedge | Acoustic Holography | X-Ray* | Wheel | Wedge |
| Percent weld found rejectable | 30 | 39 | 28 | 44 | 35 | 29 | 17 |
| Percent x-ray-rejectable (4)** found rejectable | 100*** | 68 | 51 | 49 | 100 | 55 | 34 |
| Percent x-ray-acceptable (5) found acceptable | 100 | 73 | 81 | 58 | 100 | 85 | 92 |
| Percent correlation with (3) x-ray (all defects) | 100 | 72 | 72 | 55 | 100 | 74 | 72 |
| Percent correlation with x-ray for cracks | 100 | 59 | 64 | 49 | 100 | 68 | 74 |
| Percent correlation with x-ray for incomplete penetration | 100 | 82 | 76 | 62 | 100 | 77 | 77 |
| Percent correlation with x-ray for slag | 100 | 76 | 73 | 53 | 100 | 79 | 79 |
| Percent correlation with x-ray for porosity | 100 | 71 | 78 | 55 | 100 | 61 | 45 |

*X-ray used as a reference for comparison with respect to other NDT methods — *** 100 percent does not imply that 100 percent of the defects were detected.

**Numbers in parentheses refer to comparison calculations of Figure 2-20.

While ultrasonic inspection is less sensitive than radiography to rounded discontinuities, the larger ultrasonic check-point length results in more repair. Experience indicates (see Section 2. 2) that the amount of repair required by radiographic inspection has been sufficient to ensure reliability of the ship hull. Assuming that the rejection rate for contact shear-wave inspection (with sensitivity compensated for coupling variations) is the same as for the wheel, the check-point length should be reduced from 50 in. to approximately 22 in. to keep the amount of repair the same as that resulting from radiographic inspection of the same welds.

### 2. 3.2.2 Fracture Testing Results

Comparison calculations made employing the fracture results as the basis of comparison are presented in Table 2-8. These calculations show that:

A. As expected, the X-ray reference found the greatest percentage of defects and had the best correlation with the fracture surface. However, its correlation with the flaws exposed by fracture was not as high as might be expected.

B. The results from the wheel were nearly as good as those from X-ray.

C. Wedge shear-wave inspection was less sensitive than either the wheel or X-ray.

**Table 2-8**

**COMPARISON CALCULATIONS FOR FRACTURE SPECIMENS**

| Criteria | Fracture | X-Ray | Ultrasonic Shear-Wave | |
|---|---|---|---|---|
| | | | Wheel | Wedge |
| Percent weld found defective | 46 | 43 | 36 | 33 |
| Percent correlation (3)* with fracture | 100 | 70 | 66 | 59 |
| Percent defects found (4) | 100 | 63 | 52 | 42 |
| Percent undefective found (5) | 100 | 75 | 78 | 74 |

*Numbers in parentheses refer to comparison calculations of Figure 2-20, using the fracture surface as the basis of comparison

A comparison was made of the defect lengths determined by the X- ray reference and by ultrasonic inspection for the defects detected. Half the time the X-ray length was larger than the ultrasonic length, and half the time the ultrasonic length was larger than the X-ray length. Thus, on the average, there was little difference in the lengths detected by either.

### 2.3.4.3 Inspection Results of a Similar Study

In a study conducted at Ingalls Shipbuilding (Reference 13), a number of welds were inspected by both film radiography and ultrasonic shear-wave. Of 103 radiographic intervals inspected, 28 were rejected by shear-wave and 26 were rejected by radiography. Of these, 11 were rejected by both shear-wave and radiography. The corresponding comparison calculations are presented in Table 2-9. This comparison was made on the basis of number of check points, not rejectable defect lengths. Ingall's study indicates that a shipyard ultrasonic technique yields results at least equivalent to those of a shipyard radiographic technique.

### 2. 3.4.4 Detectability Versus Material Thickness

The comparison calculations for detectability versus material thickness are summarized in Figures 2-21 and 2-22. The calculations were made by grouping the panels by thickness. The results indicate that:

A. The wheel provided better correlation with the X-ray reference and detected a greater percentage of X-ray -rejectable defects than did wedge shear-wave inspection for all but the 2-in. -thick panels.

B. The ultrasonic techniques' performances are nearly independent of material thickness.

---

This supports the shipbuilders comments that the X-ray technique used in this report was more sensitive than accepted RT techniques. See page 33, footnote 7.

Table 2-9

COMPARISON CALCULATIONS FOR INGALLS INSPECTION RESULTS

| Criteria | Wedge UT |
|---|---|
| Percent weld found rejectable | 27 |
| Percent correlation with radiography (3)* | 69 |
| Percent radiography - rejectable found rejectable (4)** | 42 |
| Percent radiography - acceptable found acceptable (5)** | 78 |

*Numbers in parentheses refer to comparison calculations of Figure 2-20.
**Using RT as the basis for comparison does not mean that it is more accurate. In fact, UT rejected more weld check points than RT.

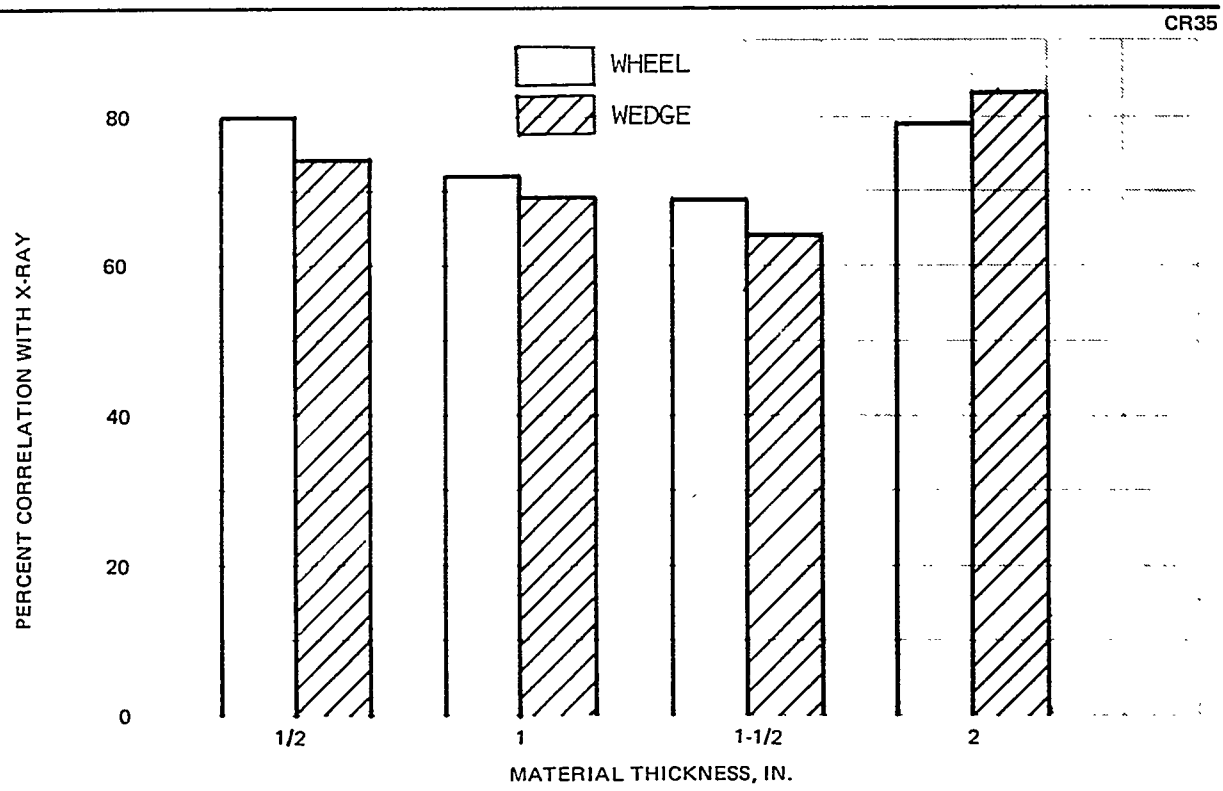


FIGURE 2-21. PERCENT CORRELATION WITH X-RAY FOR THE WHEEL AND WEDGE INSPECTION FOR VARIOUS MATERIAL THICKNESSES

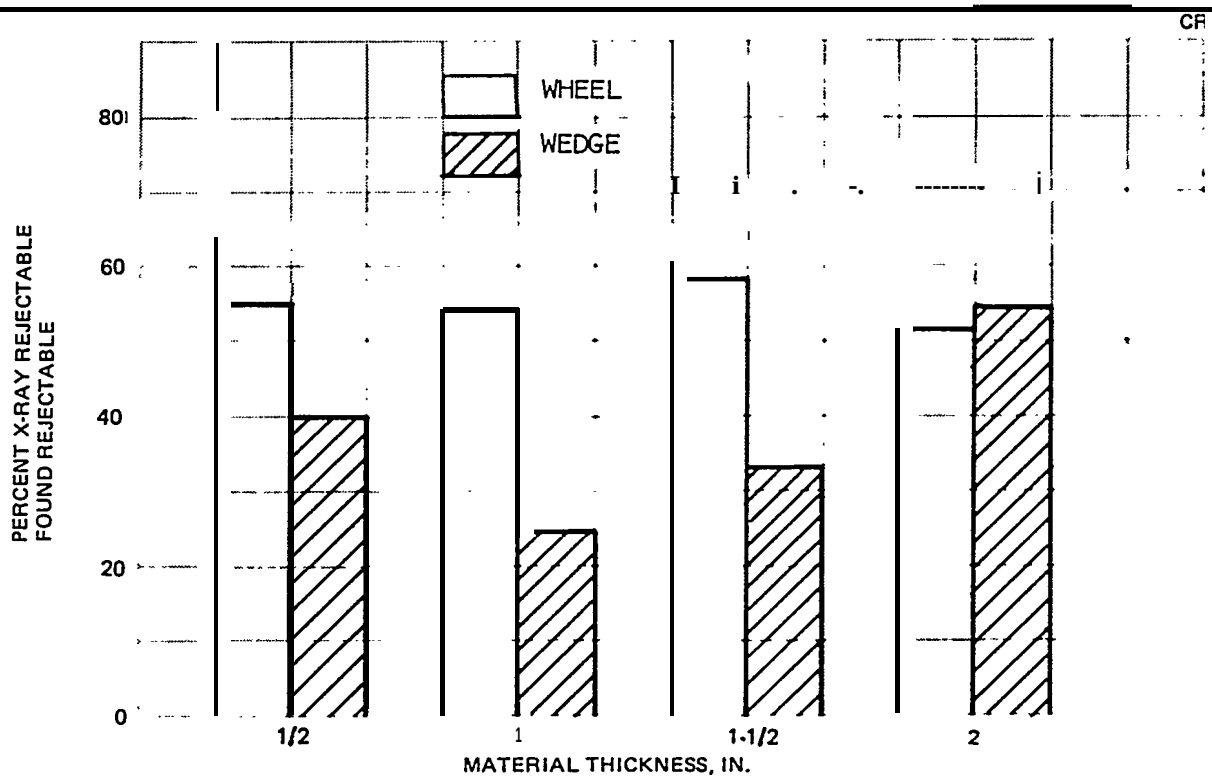


FIGURE 2-22. PERCENT OF X-RAY-REJECTABLE DEFECTS ALSO FOUND REJECTABLE BY THE WHEEL AND WEDGE INSPECTION FOR VARIOUS MATERIAL THICKNESSES

### 2.3.5 Cost Considerations

**The costs associated with the nondestructive testing of hull welds were difficult to determine. Interviews with shipyard inspection personnel did not provide any information about total inspection costs. Shipyard personnel generally had the impression that radiographic inspection was slower and more expensive than ultrasonic inspection. Several of the shipyards were just becoming familiar with ultrasonic inspection costs and did not have any information on the relative costs of ultrasonic versus radiographic inspection. Of the shipyards with experience, the estimates for the cost of ultrasonic inspection ranged from 1/5 to 2/3 that of radiographic inspection.**

**A tanker 786 ft long, 105 ft wide, and 57 ft deep was selected as an example to estimate the absolute and relative costs of nondestructive inspection. For a tanker of this size, the radiographic and ultrasonic specifications require at least 255 inspection points. This amounts to 457 ft of weld for radiographic inspection and 1, 063 ft of weld for ultrasonic inspection. Additional inspection points may be required by the regulatory bodies or purchaser.**

The cost of radiographic inspection was estimated to be approximately $28 per inspection point. The cost of taking the exposure, developing the film, and reading the film was estimated at $8 per shot by a radiographic inspection service. It was estimated that an additional 2 hr at a labor rate of $10/hr was required to determine the film and source positions, record the results, and mark the defect locations on the weld.

The radiation hazards of radiographic inspection imply additional costs. These costs were neglected in this discussion, with the. understanding that the estimated costs will be higher when the inspection presents a radiation hazard.

The cost of ultrasonic inspection was estimated to be approximately $6 per inspection point. The cost is lower than for radiographic inspection due to the higher inspection rate, immediately available results, and ease of locating defects on the inspected weld.

For the ship selected and the above inspection costs, the cost of radiographic inspection would be $7, 140, and the cost of ultrasonic inspection would be $1, 530. The cost of repair and reinspection should be added to these costs.

It is also difficult to estimate the cost of repair welds. Assuming that 20 percent of the weld was found rejectable by radiographic inspection, 91 ft of weld would be repaired. Using the ratio of percent weld rejectable by ultrasonic inspection to percent weld rejectable by radiographic inspection found in this program, 10 percent of the ultrasonically inspected weld would be repaired. This amounted to 106 ft of weld due to the greater amount of weld inspected ultrasonically.

The percentage of weld found rejectable depends upon the overall quality of the weld. Interviews with shipyard inspection personnel indicate that the rejection rate varies from 3 percent to 28 percent or more of the weld inspected. One average estimate from the U. S. Coast Guard was that 16 percent of the inspected weld is rejected.

The cost of the repair weld depends upon a number of factors.[11] The main factor is the amount of weld metal involved. Generally, more metal would need to be removed and rewelded for a 2-in. -thick weld than for a 1 /2-in. -thick weld. Since the distribution of rejectable weld length by weld thickness is not known, calculations will be made for both the best and worst cases. The least expensive repair would be for a 1 /2-in. -hick submerged arc weld, and the most expensive repair would be for a 2-in. -thick manual weld.

Assuming a weld-metal removal rate of 8.5 lb/hr, a submerged arc weld deposition rate of 10 lb/hr, and a manual weld deposition rate from 1.5 to 5 lb/hr, the costs for repairs would be $2. 87/ft for submerged-arc repair of 1 /2-in. -thick welds and $61.32 /ft for manual repair of 2-in. -thick welds. The actual average repair rate would be somewhere between these two extremes. These rates assume that on the average, nearly three-quarters of the defective weld needs to be removed to eliminate the defects present. Using these rates, the repair required by radiographic inspection could range from $261 to $5, 580. Similarly, the repair required by ultrasonic inspection could range from $304 to $5, 400. Clearly, in some cases the repair could cost more than the inspection itself.

Finally, assuming that the repair welds are reinspected and found acceptable, the costs of reinspection would be $1, 428 for radiography and $153 for ultrasonics. The total expenses could range from $8, 829 to $14, 148 for radiography and from $1,987 to $8,183 for ultrasonics.

The substitution of ultrasonics for radiography would result in a cost saving of approximately $6,400 for a tanker of this size. This saving is based on performing the minimum amount of inspection currently required by the ABS radiographic and ultrasonic specifications. If the ultrasonic checkpoint length is reduced to that of radiography (about 1- 1/2 ft), the savings would increase to about $9,800 for the tanker considered.

---

11 One aspect not included was identified by a shipyard: "UT has a capability of determining the total extent of rejectable weld during the initial inspection and does not require repeated expansion radiographs at separate inspection times to determine the total defective weld. UT has proven to be a time saver during repair by locating the side nearest the defect to minimize the amount of gouging and rewelding. “

One of the primary ways of reducing the cost of inspection is to convince the purchasers that more inspection than required does not make the ship more reliable. Performing the minimum amount of inspection, rather than three times the minimum as often requested, would itself result in a saving per tanker of up to $28,000 for radiography and $16, 000 for ultrasonics. On the other hand, if three times the minimum is requested, the substitution of ultrasonics for radiography would result in a cost saving of $19,000 to $30,000 per tanker.

Shipbuilders comment:

"The general content of the report, cost and time used to perform the inspections on field locations, concurs somewhat with our figures on actual work being performed in our yard."

"The costs referred to are not identifiable and could be confusing considering the substantial variations in conditions under which both tests and repairs must be made in a shipyard."

"No account for check points being at intersections (shorter inspection lengths) was taken. The cost of the lengths inspected therefore would be less. No consideration of the fact that radiographic costs are based on exposures (film length may vary between 7 and 17 inches) rather than length inspected. We find UT inspection costs about 75 per cent of RT inspection and the principal advantage for using UT is related to less interference with other trades and no safety hazard of radiation."

"The radiographic inspection costs stated appear to be realistic; however, the $6 per inspection point cost allotted for UT inspection appears to be considerably low, especially since the cost refers to inspection of a 50-inch inspection point. UT of a 12-inch segment (inspection point) costs approximately one manhour (approximately $9 ). This would increase total cost for UT inspection of the 786 ft. long craft cited from $1, 530 to $4, 845 compared to the stated $7,140 for radiography. However, there are some cost savings related to repair which were not reported. UT has a capability of determining the total extent of rejectable weld during the initial inspection and does not require repeated expansion radiographs at separate inspection times to determine the total defective weld. UT has proven to be a time saver during repair by locating the side nearest the defect to minimize the amount of gouging and rewelding."

## Section 3
## PIPE-WELD INSPECTION

### 3.1 ANALYSIS OF CURRENT REQUIREMENTS

Shipboard piping systems are governed by the standards of the U. S. Coast Guard (Reference 14), which require mandatory nondestructive inspection of the butt welds joining certain types of pipe if the pipe conforms to Class I, I-L, or II-L requirements. Figure 3-1 summarizes some of the conditions that determine whether a pipe is to be classified within these classes, and Figure 3-2 summarizes the inspection requirements by class. No inspection is required if the pipe falls outside these classes.

Where radiographic inspection if called for, it is to be in accordance with the ASME Code, Section I, Paragraph PW-51 (Reference 15). This code provides for rejection of welds with the following features:

A. Any crack, incomplete fusion, or incomplete penetration.

B. Elongated slag inclusions greater in length than 1/4 in. for thicknesses (T) of 3/4 in. or less, l/3T for T between 3/4 in. and 2-1/4 in. , and 3/4 in. for T greater than 2-1/4 in.

C. Porosity area greater than 1 percent.

Ultrasonic inspection is permitted by the Coast Guard regulations as a substitute for radiography only in those cases where 20-percent radiography is required (Figure 3-2), and even then only upon special approval of the procedures in each instance.

In addition to nondestructive inspection, the Coast Guard regulations require hydrostatic proof and leak checks at 1 -1/2 times the maximum working pressure for certain classes of piping. After the ship is placed in service, periodic leak checks are conducted on critical runs of piping. For example, the main steam piping is checked at 1- 1/4 times the allowable working pres - sure every 1 to 4 yr (depending on ship and boiler type), and liquified petroleum gas pipes are to be leak-checked once a month.

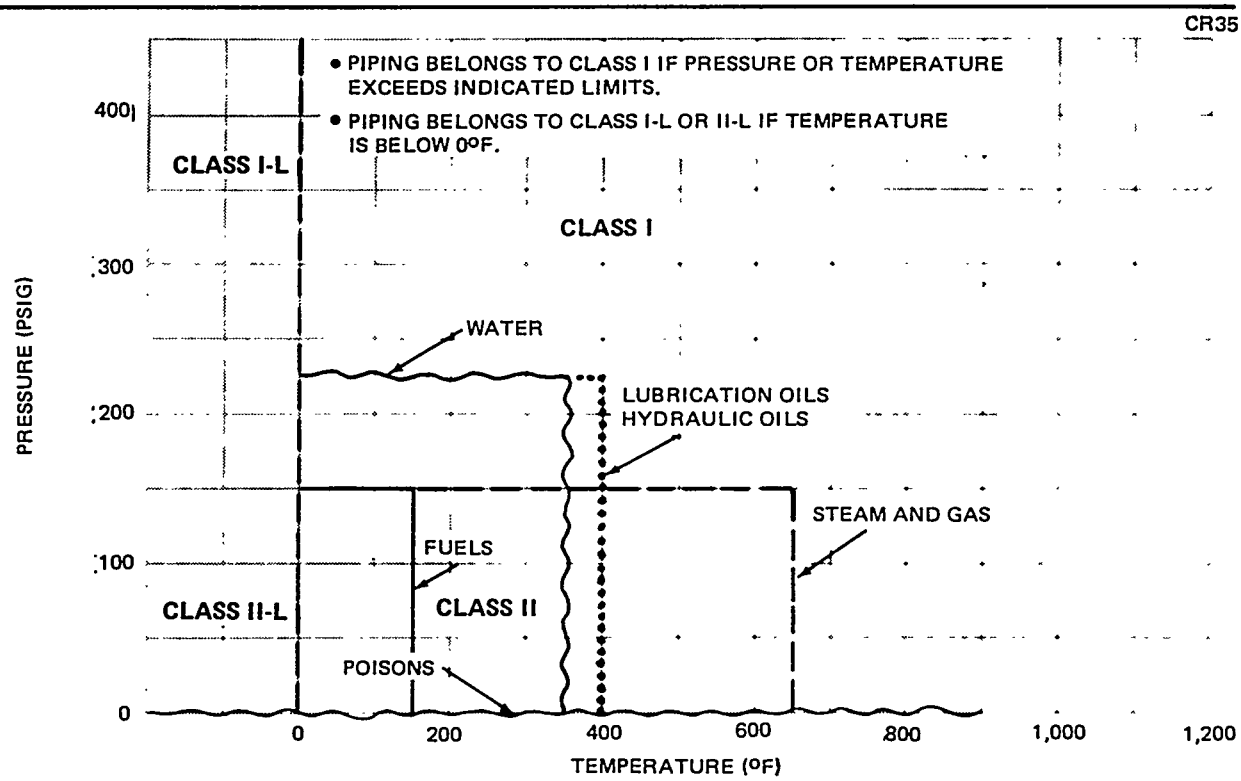


Figure 3-1. Definition of Some Pressure and Temperature Conditions for Classifying Pipes Carrying the Indicated Fluids

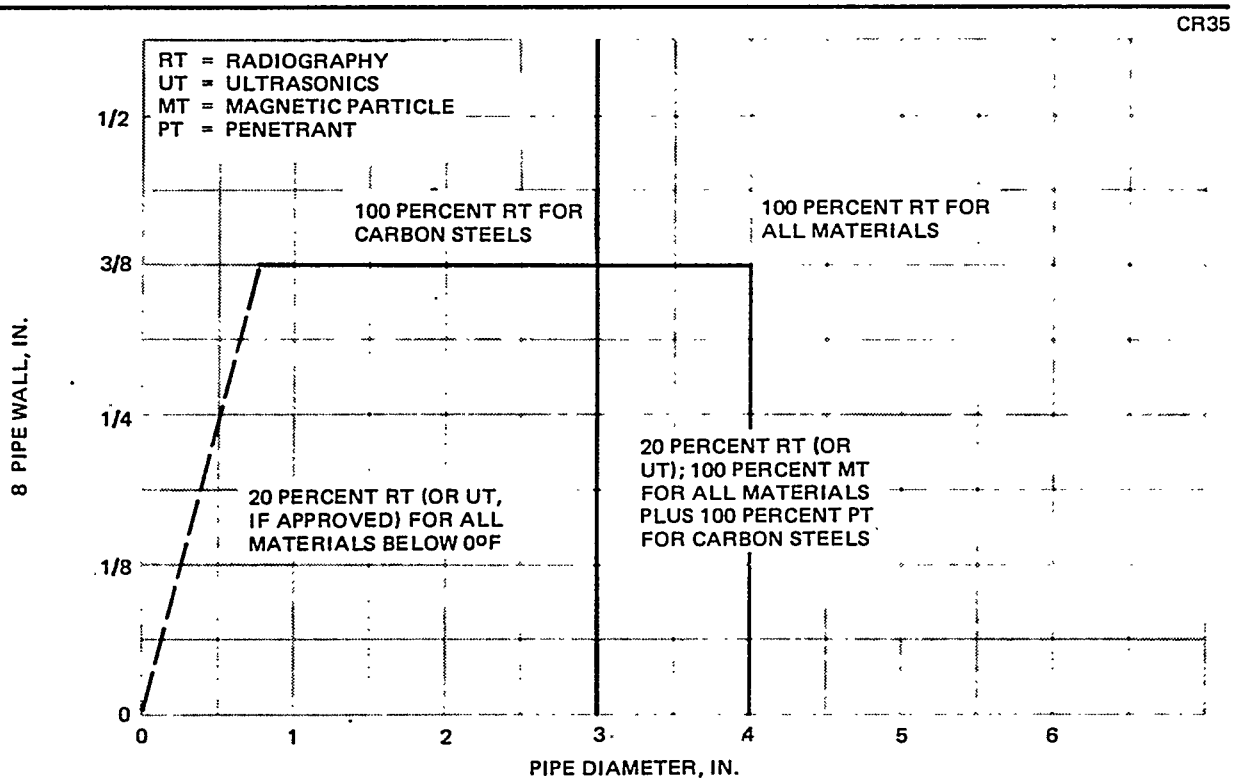


Figure 3-2. Marine Regulations: Summary of Inspection Required as a Function of Pipe Dimensions for Class I, I-L, and II-L Piping

The allowable working pressures in shipboard pipes have as an upper limit the allowable set by the American National Standards Institute (ANSI, Reference 16) for land-based pipe. The effect of shipboard motions must be taken into account in order to obtain Coast Guard approval. If an adequate calculation of shipboard effects such as collision, wave motions, and vibration, in addition to pipe pressure, is made, the pipe can be designed to the working stresses allowed by the ANSI code. However, if such a calculation is not made, then the working pressure cannot exceed 80 percent of the ANSI allowable.

Additional consideration for the special needs of shipboard service is shown by Figure 3-3, which compares various codes as to the requirements for 100-percent radiographic inspection of butt welds. The pipe sizes (thicknesses and diameters) that are designated as needing mandatory inspection under Coast Guard rules (Reference 14) are smaller than those designated by ANSI (Reference 16) or by the ASME (Reference 15). One justification for the fact

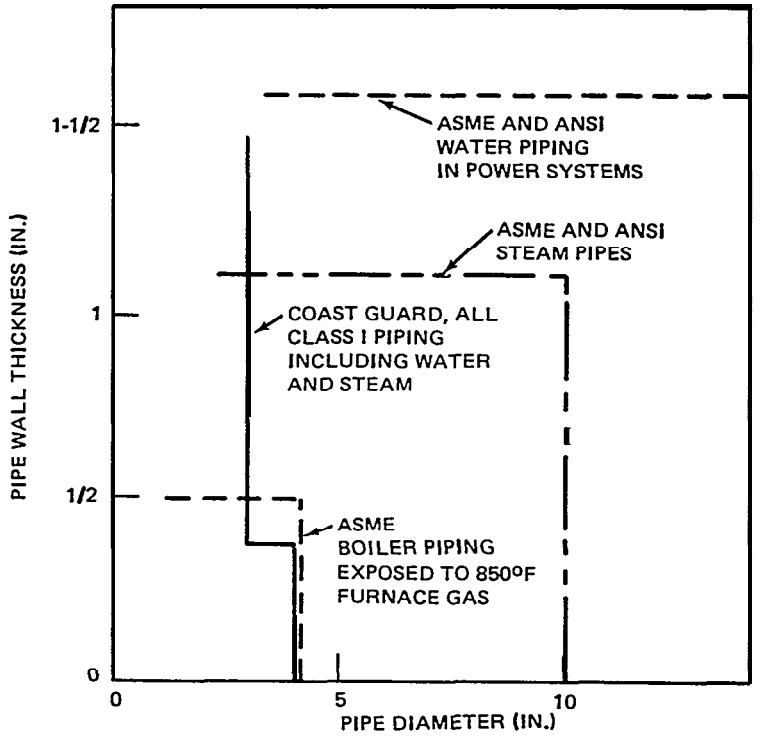


Figure 3-3. Comparison of Marine and Land Codes: Limits on Pipe Diameter and Thickness Beyond Which 100-Percent Weld Radiography is Required

that more radiography is specified for marine piping than for land-based piping is the greater degree of uncertainty in working stresses in marine piping. In addition to the pressure, temperature, and vibratory environments that apply to land piping, the marine pipes endure additional stresses of unknown magnitude and frequency transmitted from the hull.

Another, and perhaps overriding, consideration is the problem of reducing to a practical minimum the danger to people and property that might result from pipe ruptures in case of collisions or other unplanned impacts. This danger is essentially absent in most land-based piping.

Because the loads transmitted to pipe welds from the hull under normal service conditions or during a catastrophic external occurrence, such as a collision, are virtually impossible to calculate in any deterministic fashion, no attempts Were made in this study to duplicate for pipes the stress and fatigue analyses conducted for hull welds. It appears that cutting costs by inspecting less pipe welds and/or loosening the acceptance-rejection criteria for detected defects would be difficult to justify.

From interviews held with the personnel of several shipyards, it is estimated that approximately 80 percent of ship piping welds are made and inspected in the shop before being installed in the hull. The remaining 20 percent must be made and inspected during the assembly of the hull. The factors that make radiography expensive in the case of hull-plate welds are also operative in the case of pipe welds, particularly those made in the hull. Since pipe Welds account for an appreciable fraction of the hull-melding costs, the motivation for considering alternate inspection techniques is clear.

The emphasis of the current study was to evaluate the utility of potentially less costly inspection methods such as ultrasonic shear-wave inspection, ultrasonic delta scan, acoustic holography, and acoustic emission monitoring. The intent was to determine the ability of these alternate techniques to detect the pipe-weld defects currently considered rejectable on the basis of radiography.

## 3.2 EVALUATION OF TECHNIQUES

The evaluation of delta scan, acoustic holography, and acoustic-emission monitoring for hull-weld inspection (Section 2. 3) indicates that these techniques would not be suitable for pipe-weld inspection. Ultrasonic shear-wave inspection was evaluated as an alternative to radiographic inspection of pipe welds.

### 3.2.1 Nondestructive Testing Specimens

Eight pipe specimens with purposely introduced weld defects were provided by Todd Shipyards Corporation — Los Angeles Division. Half of the pipe specimens had an outside diameter of 5 in. and a wall thickness of 7/16 in. The other half had an outside diameter of 8 in. and a wall thickness of 5/8 in. The pipe sections were 15 in. long with a butt weld in the center.

Defects in the pipe welds were generated in much the same way as for the panel welds. One type of defect was introduced into each pipe. Porosity was generated using a heliarc without gas shielding, and sometimes with oil contaminant as well. Slag inclusions were manually welded in place, and then the weld was completed as usual. The incomplete-penetration defects were made by preparing the weld edges with the appropriate weld lands for the incomplete penetration and the appropriate groove for the complete penetration on either side. Crack defects were generated using a broken tack-weld approach. All of the welds employed heliarc and manual welding with 7018 electrode material.

### 3. 2.2 Nondestructive Inspection Techniques

The test pipes were inspected using film radiography and wedge shear - wave inspection. A brief description of each technique is presented in the following sections.

#### 3. 2.2.1 Film Radiography

All of the pipe welds were inspected using film radiography as specified by the ASME code. The same x-ray source and film were used as for the test panels. Additional exposures were made through one wall thickness for improved sensitivity, as the inside of the pipe was readily available.

### 3. 2.2.2 Wedge Shear-Wave Inspection

All of the pipe welds were inspected using shear-wave inspection as specified by the ABS provisional ultrasonic requirements. The same pulser-receiver and master transducer were used as for the test panels. A 70-degree, 2. 25-MHz Krautkramer transducer originally designed for use with the Krautkramer Model USK5 flaw detector was used for contact shear-wave inspection. This transducer was chosen for its narrow width of 3/8 inch.

A narrow transducer was used because a good portion of the sound from a wider transducer would be reflected away from the transducer by the curved inside surface of the pipe. This effect would occur even if a curved contact wedge were used for a wider transducer. A greater percentage of the incident sound will be reflected for a narrow transducer. Thus, the sensitivity calibration using a through-hole standard will more nearly be the same as for inspection of flat material. Also, a sufficiently narrow transducer would not require the use of a curved contact wedge. While the coupling would be improved by such a wedge, if the pipe radius became even slightly larger than the radius of the curved contact wedge, the coupling would suffer greatly. Also, a curved contact wedge would not allow an oscillatory motion of the transducer.

The narrow transducer was fairly easy to manipulate. A slight rocking motion was included to help ensure that the maximum reflected signal from the bottom surface was being obtained.

### 3.2.3 Inspection Results

Comparison calculations for the pipe specimens are presented in Table 3-1. The results indicate that shear-wave inspection was not reliable for pipe. The technique was particularly insensitive to porosity defects. The detailed inspection results and tabulations of detected defects are presented in Appendix E.

**Table 3-1**

**COMPARISON CALCULATIONS FOR DETECTABLE DEFECTS IN PIPE SPECIMENS**

| Criteria | X-Ray | Wedge |
|---|---|---|
| Percent weld found defective | 49 | 27 |
| Percent correlation with x-ray (3)** | 100* | 57 |
| Percent x-ray-detectable (4) found detectable | 100 | 33 |
| Percent x-ray-undetectable (5) found undetectable | 100 | 78 |

* 100 percent does not imply that 100 percent of the defects were detected.

** Numbers in parentheses refer to comparison calculations of Figure 2-20.

## Section 4

## CONCLUSIONS

This program explored possibilities for lowering the cost of ship-weld inspection without adversely affecting ship reliability. The current requirements for weld inspection and repair were reviewed and analyzed. The possibility of achieving lower inspection costs through adjusting the requirements and employing more efficient nondestructive inspection. methods was explored. The following conclusions were derived from the results of this investigation.

### 4.1 HULL WELDS

#### 4. 1.1 Relationship of Defects to Failures

Conclusions reached regarding the relationship of defects to failures are:

A. The most probable consequence of weld defects on structural integrity is fatigue growth to full penetration. Sub sequent slow growth to lengths which may cause brittle failure is improbable due to regular survey inspections.

B. Fatigue cracks in modern ships occur primarily in the hull skeleton and not in the more critical hull plating.

C. Typically, from 10 to 20 per cent of the inspected weld is rejected and repaired. Assuming that the inspection points are selected in at least a partially random manner, it is likely that a similar fraction of the uninspected weld contains rejectable defects. However, the low incidence of fatigue cracks in modern ships implies that these unrepaired rejectable defects seldom cause failures.

#### 4. 1.2 Fatigue Analysis

Conclusions regarding fatigue analysis are:

A. Fatigue growth at low stress amplitudes is the most important factor in flaw growth, although ship- steel data in this regime is not available.

B. For the majority of hull welds, defects acceptable by the current radiography criteria will not grow to a length where brittle failure is possible during 20 years of service. In regions of high structural stress concentrations, fatigue growth is increased by factors of 10 or more.

C. Flaw height is as important as flaw length in determining the fatigue life of welds.

### 4. 1.3 Evaluation of Nondestructive Inspection Techniques

Conclusions concerning nondestructive inspection techniques are:

A. In their current state of development, ultrasonic delta scan, acoustic holography, and acoustic emission techniques are not practicable for shipyard inspection of hull welds.

B. Of all the alternative techniques evaluated, ultrasonic shear-wave provided the most sensitivity and best definition of weld defects. It is a viable alternative to radiography for hull-weld inspection and can characterize defect height and depth. Ultrasonic length indications, on the average, are nearly the same as those of radiography.

C. The liquid-filled wheel is more sensitive than the wedge but is cumbersome to operate. The reduced sensitivity of the wedge transducer is due to poorer coupling on the test specimens, as compared to the calibration standard.

### 4. 1.4 Cost Analysis [11]

Conclusions resulting from the cost analysis are:

A. Neglecting the cost of the radiation hazard for radiography, the cost of radiographic inspection were estimated to be up to approximately five times that of manual-contact shear-wave inspection.

B. While ultrasonic inspection is less sensitive than radiography, the increased ultrasonic sampling requirements result in more repair. The cost saving (including repair) of ultrasonics over radiography for a 786- ft-long tanker under these conditions ranges from about $6,400 to $19,000 for minimum and typical amounts of inspection, respectively. A decrease in ultrasonic check-point length to that of radiography would increase the cost saving to between $9,800 and $29,400.

---

11 For shipbuilders' comments, see footnotes on pages II and 49.

### 4. 1.5 Conclusions Pertinent to Current Requirements

Conclusions concerning current requirements are:

A. Although only a few percent of the hull welds are required to be inspected, shipyards often inspect several times the minimum required. The additional inspection appears unwarranted unless problems with the weld process occur, as determined by abnormally high rejection rates.

B. Provisional ultrasonic requirements result in about three times more inspection than with radiography. The checkpoint length could be reduced to result in the same amount of repair as for radiographic inspection without reducing reliability.

C. For the majority of hull welds, the current radiographic acceptance criteria appear to be conservative. The provisional ultrasonic acceptance criteria are somewhat less conservative than those for radiographic inspection due to the larger acceptable defect sizes for ultrasonic inspection. The addition of meaningful height triteria to the requirements for ultrasonic inspection could result in less repair and, at the same time, would make the requirements more conservative.

## 4.2. PIPE WELDS

Conclusions concerning pipe-weld inspection are:

A. The U.S. Coast Guard requirements for radiographic inspection of marine pipe welds are more severe than those of ANSI or ASME due to uncertainty in the working stresses and potential danger to ship personnel.

B. In the absence of any information on the stresses in marine piping, reducing the cost of inspection and repair through less inspection or relaxed acceptance requirements cannot be justified.

C. Evaluation of delta scan, acoustic holography, and acoustic emission techniques for panel welds suggests that these techniques would not be suitable alternatives to radiography for inspection of pipe welds. Experimental evaluation of ultrasonic shear-wave inspection indicated that this technique also is not a suitable alternative.

## Section 5

## RECOMMENDATIONS

The results and conclusions of this program lead to the following recommendations pertinent to inspection of hull and pipe welds.

### 5.1 HULL WELDS

#### 5. 1.1 Radiographic Inspection

The results of the program indicate that there is no reason to increase the minimum amount of inspection required. It is recommended that no more than the minimum be performed.

#### 5. 1.2 Ultrasonic Inspection

In order to lower costs, the increased usage of ultrasonic inspection is recommended. The provisional requirements for ultrasonic inspection should-be accepted with the following changes:

A. Reduce the check-point length to 22-inches in order to achieve the same amount of repair as for radiography.

B. Compensate for coupling variations from the sensitivity calibration standard to the production material. These procedures are detailed in a forthcoming ASTM E164 revision.

C. Base the acceptance criteria on the length, height and depth of the defect. [14]

---

14 See Appendix G for a reviewer's analysis which indicates that the use of height and depth criteria may not be practical.

### 5. 1.3 Recommendations for Further Study

A. Conduct an analytical and experimental study of high- cycle/low-stress fatigue as required to supp'ort selection of the weld acceptance triteria.

B. Conduct a statistical analysis of the inspection results for several ships before and during service to determine the incidence, size, and fatigue growth of defects. Use the results of this analysis to help develop a checkpoint sampling strategy.

c. Develop a practical ultrasonic inspection method using a liquid-filled wheel to further reduce the cost of weld inspection. This system would improve coupling, lessen the skill required of an operator and significantly increase inspection speed.[15]

## 5.2 PIPE WELDS

No change in the requirements for inspection of ship pipe welds is recoin - mended at this time. It is recommended that stress data be obtained from instrumented pipes on actual ships and that the possible failure modes of pipe welds be examined using such data as a first step toward providing the rationale for possible modification of the inspection requirements.

---

15 The researcher included a recommendation for an automated ultrasonic inspection system employing electronic signal processing to eliminate interpretation by an operator and to provide a permanent record; see Appendix F. Shipbuilders commented that in their judgment the advantages of an automated system would be insufficient to justify development and later procurement costs.

## REFERENCES


1. Circular No. 145, Index 3.3.2, American Bureau of Shipping, 25 May 1965.

2. American Bureau of Shipping, Requirements for Radiographic Inspection of Hull Welds, 1971.

3. Interviews with ABS personnel.

4. American Bureau of Shipping, Provisional Requirements for Ultrasonic Inspection of Hull Welds, Circular No. 254, 3 Jan 1972.

5. A. S. Tetelman and A. J. McEvily, Jr., Fracture of Structural Materials, John Wiley & Sons, 1967.

6. A. J. McEvily, Jr. and T. L. Johnston, The Role of Cross -Slip in Brittle Fracture and Fatigue, Proceedings, of the First International Conference on Fracture, Sendai, Japan, Vol 2, 1966.

7. J. M. Barsom, Fatigue Crack Propagation in Steels of Various Yield Strengths, submitted for presentation at the First National Congress on Pressure Vessels and Piping, San Francisco, May 1971.

8. Nibbering, Ship Structure Committee, Report SSC-206.

9. F. Steneroth, Low-Cycle Fatigue, in proceedings of First International Ship Structures Congress, University of Glasgow, Sept 1961.

10. Report of Committee 7 on Low Cycle Fatigue, Proceedings, Second International Ship Structures Congress, Vol 1, Delft, Netherlands, 1964.

11. Report of Committee 3d on Discontinuities and Fracture Mechanics, Proceedings, Third International Ship Structures Congress, Vol 1, Oslo, 1967.

12. Personal communication with H. E. Van Valkenburg, Automation Industries Inc., Danbury, Corm. , and Bill Yee, General Dynamics, Fort Worth, Tex.

13. J. D. Theisen, Comparison of Ultrasonic Test and Radiographic Test Results of Surface Ship Weld Inspection, Ingalls Shipbuilding Corporation, Jan 1968, and letter of 23 January 1972 to Todd Shipyards.

14. U. S. Coast Guard, Marine Engineering Regulations, Subchapter F, Part 56, 1970.

15. American Society of Mechanical Engineers, ASME Boiler and Pressure Vessel Code, Section I.

16. American National Standards Institute, Code for Pressure Piping, Power Piping, USAS B31. 1.0-1967, published by ASME.

17. E. R. Parker, Brittle Behavior of Engineering Structures, John Wiley & Sons, 1957.

18. G. Murray Boyd, Fracture Design Practices for Ship Structures, in Volume V of Fracture, Edited by H. Liebowitz, Academic Press, 1969.

19. W. S. Pellini, Notch Ductility of Weld Metal, Welding Research Supplement, May 1956.

20. W. H. Munse, Brittle Fracture in Weldments, in Fracture, Vol IV, edited by H. Liebowitz, Academic Press, 1969.

21. A. A. Wells, Effects of Residual Stress on Brittle Fracture, in Reference 20.

22. K. Masubuchi, et al. , Interpretative Report on Weld-Metal Toughness, Ship Structure Committee Report SSC - 169.

23. S. R. Heller, et al. , Twenty Years of Research Under the Ship Structure Committee, Transactions of SNAME, 75 332-384, 1967.

24. E. A. Lange, The Cost of Fracture Control, Machine Design, 7 Sept 1972.

25. G. E. Bockrath and J. B. Glass co, A Theory of Ductile Fracture, McDonnell Douglas Report MDC G2895, Aug 1972.

26. J. D. Lubahn, Strain Aging Effects, Trans ASM, 44, 643-666, 1952.

27. A. K. Shoemaker and S. T. Rolfe, Static and Dynamic Low Temperature KIc Behavior of Steels, Trans. ASME, J. Basic Energy, Sept 1969.

28. W. S. Pellini and P. P. Puzak, Fracture Analysis Procedures for the Fracture-Safe Engineering Design of Steel Structures, Naval Research Laboratory Report 5920, 15 Mar 1963.

29. W. S. Pellini, Criteria for Fracture Control Plans; Naval Research Laboratory Report NRL 7406, 11 May 1972.

30. Rules for Building and Classing Steel Vessels, American Bureau of Shipping, 1972.

31. J. Vasta and P. M. Palermo, An Engineering Approach to Low-Cycle Fatigue of Ship Structures, Trans. SNAME, 1965.

32. G. Vedeler, Discussion of Reference 31, Trans. SNAME, 1965.

33. J. M. Murray, Discussion of Reference 31, Trans. SNAME, 1965.

34. Principles of Naval Architecture, edited by J. P. Comstock, Sot. Naval. Architects and Marine Engineers, New York, 1967.

35. S. Hawkins, et al. , A Limited Survey of Ship Structural Damage, Ship Structure Committee, Report SSC-220, 1971.

36. V. Weiss, Problems in the Analytical Approaches to Weld Strength, Op. Cit. in Ref 39.

37. H. Thielsch, Defects and Failures in Pressure Vessels and Piping, Reinhold, 1965.

38. W. Soete and A. Sys, Influence of Weld Defects on High-Fatigue Behavior, Proceedings of First International Conference on Pressure Vessel Technology, Part II, Page 1147, ASME, 1969.

39. H. Thielsch, The Sense and Nonsense of Weld Defects, in A. R. Pfluger and R. E. Lewis, editors, Weld Imperfections, Addison -Wesley Publishing Company, 1968.

40. W. G. Warren, Fatigue Tests on Defective Butt Welds, Welding Research, Vol 6, Dec 1952.

41. Ship Design and Construction, edited by A. M. D'Arcangelo, Sot. Naval Architects and Marine Engineers, New York, 1969.

42. J. R. Henry, et al. , Slamming of Ships, A Critical Review, Ship Structure Committee Report SSC -2o8, 1970.

43. D. Hoffman and E. V. Lewis, Analysis and Interpretation of Full Scale Data on Midship Stresses of Dry Cargo Ships, Ship Structure Committee Report SSC-196, June 1969.

44. ABS Program for the Collection of Long-Term Stress Data From Large Tankers and Bulk Carriers, Final Report, American Bureau of Shipping, 1971.

45. J. Clarkson, Survey of Some Recent British Work on the Behavior of Warship Structures, Ship Structure Committee, Report SSC-178, Nov 1966.

46. R. S. Little and E. V. Lewis, A Statistical Study of Wave Induced Bending Moments on Large Oceangoing Tankers and Bulk Carriers, Transactions SNAME, 1971.

47. B. T. Cross and W. M. Tooley, Advancement of Ultrasonic Techniques Using Reradiated Sound Energies for Nondestructive Evaluation of Weldments, Automation Industries, Inc. , Technical Report 67-53, Aug 1967.

48. B. T. Cross, K. J. Hannah, W. M. Tooley, The Delta Technique—A Research Tool—A Quality Assurance Tool, Automation Industries, Inc. , Technical Report TR 68-11, Mar 1968.

49. B. G. W. Yee, A. H. Gardner, L. Hillhouse, D. R. Russel, Evaluation and Optimization of the Advanced Signal Counting Techniques , on Weldments, General Dynamics, Report Number FZM-5917, Jan 1972.

50. C. K. Day, An Investigation of Acoustic Emission From Defect Formation in Stainless Steel Weld Coupons, Battelle Northwest, Richland, Wash. , Report BNNL-902, 1969.

51. W. D. Jolly, An In-Situ Weld Defect Detector-Acoustic Emission, Battelle Northwest, Richland, Wash. , Report BNWL-817, 1968.

52. W. D. Jolly, Acoustic Emission Exposes Cracks During Welding Process, Welding Journal (New York), 48, 21, 1969.

53. W. D. Jolly, The Application of Acoustic Emission to In-Process Weld Inspection, Battelle Northwest, Richland, Wash. , Report BNWL-SA-2212, 1969.

54. W. D. Jolly, The Use of Acoustic Emission as a Weld Quality Monitor, Battelle Northwest, Richland, Wash. , Report BNWL-SA-2729, 1969.

55. C. E. Hartbower, Application of Swat to Nondestructive Inspection of Welds, Aerojet-General Corporation, Sacramento, Calif, Technical Note, 1969. ,

56. D. Prine, NDT of Welds With Acoustic Emission, General American Research, Niles, Ill., presented at the U. S. /Japan Joint Symposium on Acoustic Emission, 5 July 1972.

57. Acoustical Holography Inspection of Ship Hull Weldments, Report 1023-73, Holosonics, Inc. , Richland, Wa. , 25 May 1973.

# Appendix A
# BRITTLE FRACTURE AND CRACKING IN SHIPS

## A. 1 THE BRITTLE-FRACTURE PROBLEM

The statistics of ship failures during the 1940's presented by Parker (Reference 17) show that 47 percent of major (Group I) fractures in T-2 tankers originated at defective butt welds in the deck and sheer strakess in the shell mostly at the bilge, and in the bilge keel. In Liberty ships, the percentage of butt-weld origins was lower (23 percent), but this simply may be a reflection of the severity of the hatch-corner problem in these vessels.

Parker claims that at the time of his writing (1956-57), postwar welded tankers had experienced no Group I fractures. He attributes this record in part to the favorable effects of the use of radiography to check welds in many of these newer ships. In the summary of his book, Parker wrote, "The need for completely sound welds has been repeatedly demonstrated."

Laudable though it is, the desire for completely sound welds is probably not attainable within realistic economic constraints.

While the fact that weld defects played a role in originating fractures cannot be disputed, other factors appear necessary if the fracture is to propagate. Charpy impact testing of steel plates taken from fractured ships showed an overwhelming correlation between transition temperature (defined then in terms of the 15 ft-lb energy level) and the fracture path (Reference 17). Plates containing, or adj scent to, the fracture origin had the highest transition temperature; plates through which fractures propagated had intermediate transition temperatures. The implication is clear: fractures may initiat, at weld defects, but catastrophic propagation is improbable unless the adjacent plate material has a transition temperature higher than the service temperature.

Boyd (Reference 18) suggests that chance plays a significant role in the catastrophic fracture of ships. He notes that "It is almost certain that many of the structures that have not failed contain features known to be conducive to brittle fracture and have sustained similar failure conditions to those which have failed." To calculate the probability of failure of a steel structure, one must consider the statistical distributions of such conducive factors as low ambient temperature, high stresses (from such variable sources as wave action and thermal stress), presence and severity and location of defects, the brittle transition properties of the steel , and so on.

To obtain a serious brittle fracture, each of these statistically distributed factors must coincidentally be at a low-probability extreme.

After reviewing the various steps taken to reduce the ship fracture problem, Boyd concludes, in part, that:

> "Many of the fractures have emanated from notch effects due to design features, Workrmanship, or accident. It is therefore important to avoid such effects by careful attention to detail design and workmanship. Attention to such details also reduces the liability to fatigue cracking. It is recognized, however, that it is impossible to eliminate all forms of poten - tial crack initiators. . . The most effective and economic precaution against brittle fracture lies in improving the notch ductility of the steel. . . To be suitable for ships, the steel must be capable of tolerating the potential crack ini- tiators that are inevitable in practical ship construction, over the range of temperatures experienced by ships in service. "

It may be of interest to note that the weld itself is usually at least as tough as the plate steel. This may be inferred from a variety of evidence:

A. It is noted in Reference 19 that "in a number of cases, far out of proportion to the relative areas of weld and base metal, the ship fracture stopped at or near welds. "

B. Brittle cracks initiated in welds but always propagated out of the weld and ran in the plate metal some distance away (References 18, 20, and 21).

C. Reference 22 notes that the toughness (Charpy) requirements for weld filler metals in ABS-class construction are as stringent as those for the plate steel.

The general realization of the importance of steel-plate properties led to studies of ship-steel specifications during the 1950' s (Reference 18). In 1955, ABS was the first classification society to formally amend the steel rules. The changes were with reference to chemistry and processing.

Other societies also introduced changes, including requirements for notch toughness determinations. In 1959, the requirements of several major socie - ties were unified. The result was an internationally accepted series of five grades of ordinary (58- to 71-ksi ultimate tensile strength) ship steel: A, B, C, D, and E, of which the first three, in deference to U. S. steelmaking practice, have no impact test requirement but are controlled as to process and chemistry, and the last two, in deference to European and Japanese practice, are controlled by Charpy impact requirements.

The majority of ship-hull construction makes use of these ordinary-strength steels. In addition, the ABS rules permit the use of the "H32 Series" of higher- strength steels (68- to 85-ksi ultimate, 45. 5-ksi minimum yield, grades AH32, DH32, and EH32) and the "H36 Series" of 'higher- strength steels (71 - to 91 -ksi ultimate, 51 -ksi minimum yield, grades AH36, DH36, and EH36). With the exception of grade AH steels, the higher-strength steels have more stringent Charpy requirements than the ordinary- strength steels (Table A- 1).

Table A-1
CHARPY REQUIREMENTS

| Steel Grade | Charpy Requirement | |
|---|---|---|
| | Energy (ft-lb*) | Temperature (°F) |
| D (similar to C) | 35/23 | 32 |
| E | 45/30 | 14 |
| DH32 and DH36 | 25/17 | -4 |
| EH32 and EH36 | 25/17 | -40 |

*First number is for longitudinal specimens, second number is for transverse specimens.

The use of the higher-strength steels is said (Reference 3) to be fairly common in decks of dry-cargo hulls with large deck cutouts, but absent in large tankers. Welds in higher-strength steels are covered by the same inspection requirements (References 2 and 4) as ordinary steel welds.

Until 1972, it was possible to say (References 18 and 23, for example) that no ship built since 1955 (when the new ship steels became mandatory) had suffered a catastrophic brittle fracture. Considering that there are estimated to be some 54, 000 merchant vessels of various ages operating today, this information would suggest that the brittle fracture problem has essentially been solved.

However, in 1972, a 42, 000-ton oceangoing gasoline barge split in two in still water. Lange (Reference 24) suggests that the cause was inadequately tough steel, which can occasionally result even under the modern ABS grades (A, B, C, and AH). Whatever the cause (the matter is believed to be as yet unresolved), this one occurrence does not change the conclusion that catastrophic brittle fracture in ships is statistically exceedingly unlikely.

At ordinary temperatures, and in the absence of dynamic impact loading, mild steel is relatively insensitive to cracks. This is illustrated by the relationships between fracture stress and crack size shown in Figures A-1 and A-2 for plate and weld, respectively. In the absence of appropriate test data, these graphs were computed from static tensile stress-strain curves (Figure 2-2) using the procedures developed in Reference 25.

However, low temperature and high rates of loading can make the stress-strain response of mild steel considerably less ductile (References 5, 26, and 27, for example) and thereby allow brittle behavior in some circumstances. The ships that broke in half between 1942 and 1965 (Reference 18) did so at relatively low ambient temperatures (and were built before 1954).

The major factors involved in the brittle fracture of mild steel may be indicated by the fracture analysis diagram developed by Pellini and Puzak (Reference 28). The effects of temperature, flaw size, and stress are schematically indicated on such a diagram in Figure A-3 for a plate of given thickness in tension.

CR35

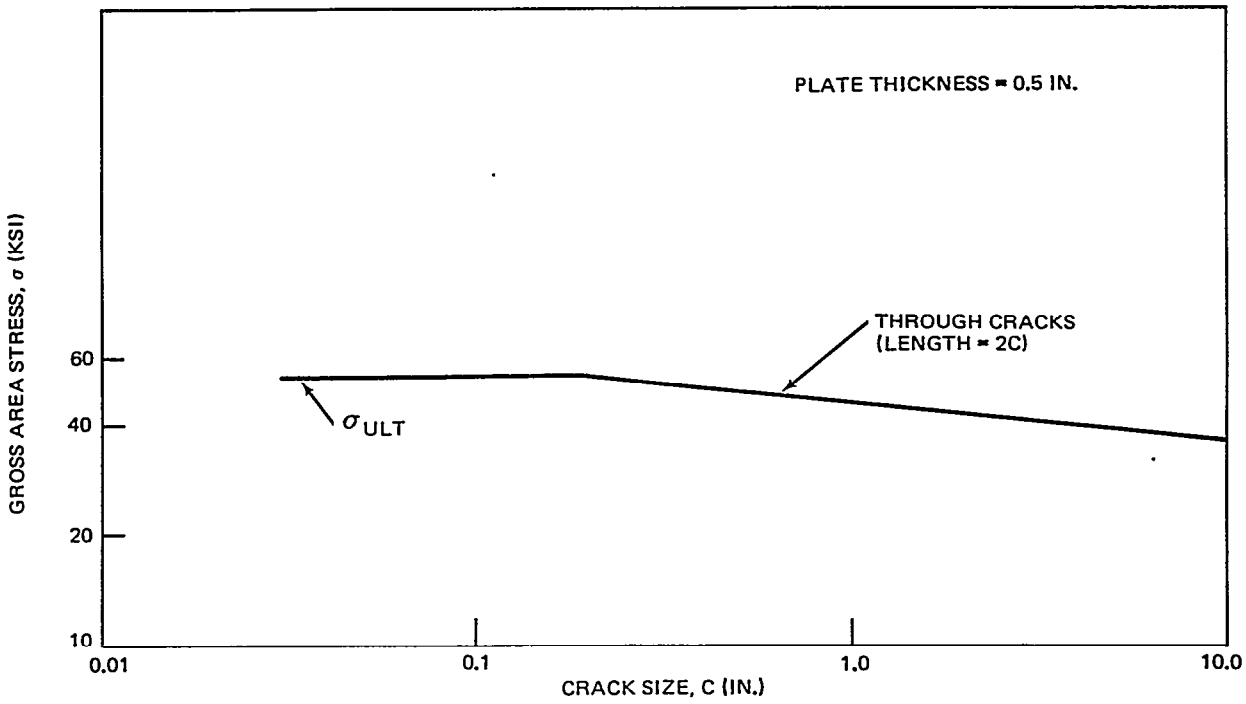


Figure A-1. Computed Fracture Curve, Mild Steel Plate at Room Temperature

CR35

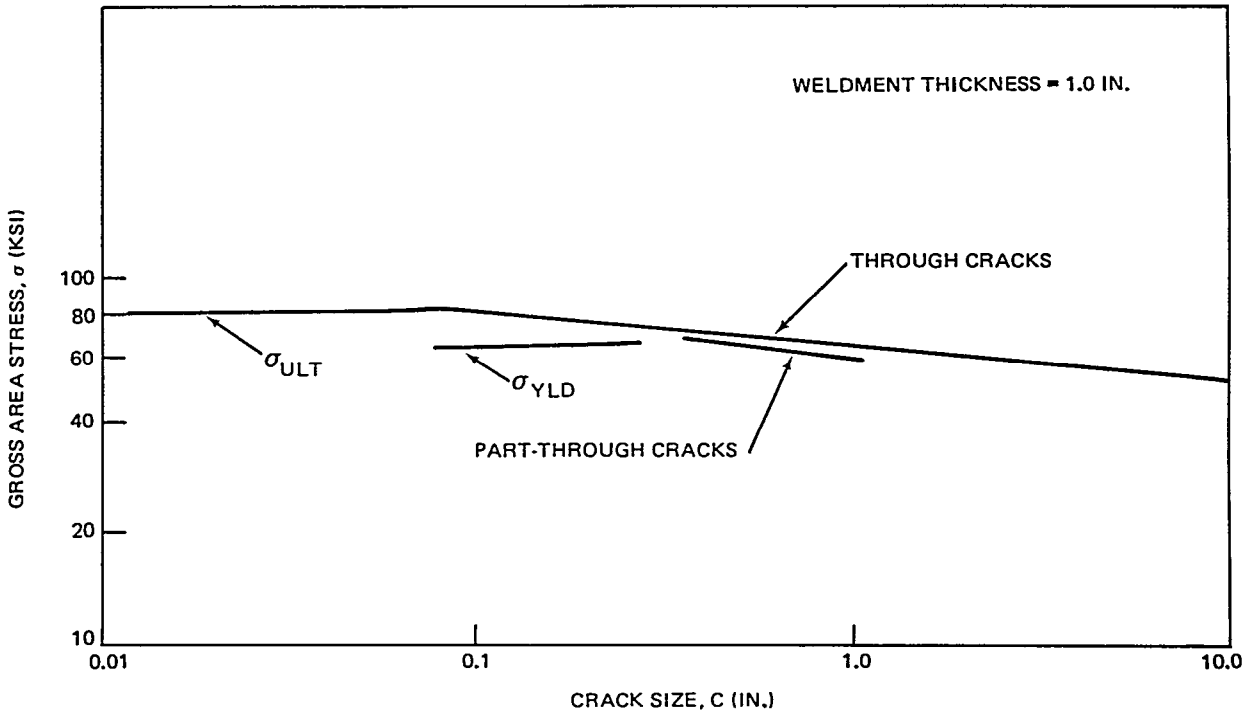


Figure A-2. Computed Fracture Curves, Ship-Steel Weld at Room Temperature

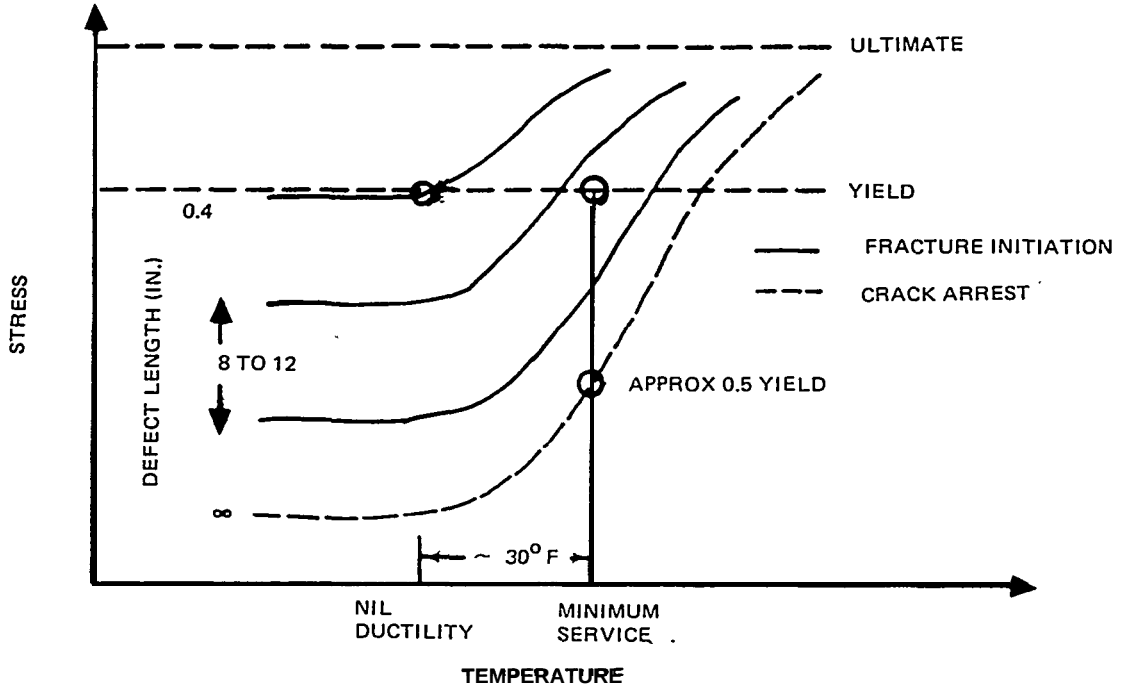


Figure A-3. Fracture Analysis Diagram (After Pellini)

**In discussing the application of the fracture analysis diagram, Pellini (Reference 29) notes that large, complex steel structures, such as ship hulls, are designed to relatively low stress levels (less than O.5 yield strength). Therefore, steel-plate material selection such that the nil-ductility temperature is at least 30 °F below the minimum expected service temperature will provide safety by ensuring that any small cracks that start to propagate in a zone of flawed or embrittled material, and high residual stress or high geometric stess, will be arrested in the plate.**

**If we assume that most ship-hull plate conforms to this requirement regarding its nil-ductility temperature, the fracture analysis diagram shows that crack lengths between 8 and 12 in. would be necessary to initiate brittle-fracture propagation if the local structural stresses reach the yield strength of the plate. Stresses of this magnitude would only occur near welds (residual stresses) and/or near structural stress concentrations. A brittle crack that started in this manner would theoretically be arrested once it became long enough to extend to regions of lower tensile stress.**

It should be noted that the specifications for most ship steels (Reference 30) do not require a determination of the nil-ductility temperature. The assumption that these steels generally do conform to Pellini's criterion is therefore based on successful service experience since 1955 or so.

## A. 2 CRACKING IN MODERN SHIPS

Several surveys of cracking observed in the hulls of ships in service have been referred to in the literature (References 9, 10, 11, 18, 31, 32, and 33).

British experience (ships classed by Lloyd's Register) cited in Reference 33 has been that for ships built between 1957 and 1964, the number of cracks observed in 635 tankers over 400 ft long was 1.6 cracks per hundred ship-years, and in 1965 for dry cargo ships over 300 feet long was 4.6 per hundred ship- years. Few of these cracks were serious; the great majority were trivial. Boyd (Reference 18), describing the same Lloyd's study, notes that the vast majority of cracks were found in regular surveys and repaired, that 81 percent of the ships studied reported no cracks at all, and that the survey covered more than 8, 000 ship-years.

Norwegian experience (ships classed by Det Norske Veritas), cited in Reference 9 and 10, revealed 66 cracks in the hull shells or decks of 210 tankers over 400 feet long built after World War II. Of these, only one was attributed to brittle crack propagation. The rest were considered to be fatigue cracks originating in regions of high stress concentration. More recently, Vedeler of Det Norske Veritas comments (Reference 32) that in newer ships, very few cracks are observed in the hull shell (deck, sides, and bottom), but there is an increasing tendency for cracking to appear in the inner skeleton (in girders, for example). He notes no tendency for cracks to initiate at butt welds.

Japanese experience (Yamaguchi's survey cited in Reference 11) shows cracking to occur near deck-house connections to deck and bulwark, and in inner structural members primarily near welded structural discontinuities. A survey of 97 oil tankers between 1950 and 1962 showed that most of the cracking occurred before the ships were 5 yr old. The cracking was attributed to fatigue under the action of approximately $10^7$ stress cycles of varying

amplitude, of which about $10^5$ were of "high" amplitude. Welded joints were found to be one of the most likely sources for fatigue cracks, but only when associated with structural disco ntinuities and highly stressed areas such as corners.

Notable in these surveys is the absence of mention of weld defects as primary sources of fatigue cracks. Emphasis of the International Ship Structures Congress (References 9 through 11) has been on low-cycle (defined as under $10^5$ cycles) fatigue related to structural stress concentrations. When welds have been considered, it is because welds are unavoidably present in complex structural details and because sound welds often (especially in higher-strength steels) have less fatigue life than plate metal.

Nevertheless, the impression persists in some circles that weld defects are an important source of fatigue cracks in ships and that the repair of fatigue cracks represents a major item of ship maintenance costs (Reference 34).

The impact of hull cracking on ship maintenance costs can be inferred to be relatively small, on the basis of a recent survey of structural damage observed in cargo ships built in the U. S. after 1955 (Reference 35). The results of this survey, published in 1971, show that in 86 percent of the 824 cases investigated, structural damage was caused by "external" factors such as collisions (67 percent), heavy weather, grounding, ice, fire, and corrosion. These causes accounted for the major damage. In the remaining 14 percent of the cases, damage was usually minor, was due to miscellaneous causes, and usually was discovered during the routine surveys required by ABS regulations. In spite of the fact that ships are not explicitly designed to withstand collisions (the "hull girder" concept typically leaves the areas susceptible to collision, such as forward and aft ends and the waterline, relatively weak), less than I percent of the damage due to collisions involved fracture of the hull shell. Of the damage from all causes, 87 percent of the cases involved deformation and/or buckling without fracture, and 6 percent involved fracture attributable to excessive deformation. Fractures unaccompanied by deformation accounted for about 3 percent of the cases; however, weld failures were

not mentioned in this context. Instead, weld failures were listed as belonging to another 3-percent category, which also included "cracks," "wire- cutting," and "holing."

From these data, it may be inferred that defective welds account for a minimal fraction of ship repair costs. Therefore, there is probably room for modification of weld acceptance criteria toward less rigorous and (hopefully) less costly standards.

## Appendix B
## EFFECTS OF INTERNAL DEFECTS ON WELD PERFORMANCE

The information found in a brief search for experimental data regarding the effects of weld defects on the strength and fatigue life of welded structures is summarized here. The categories of weld defects considered are porosity, cracks, slag, and incomplete penetration.

### B. 1 POROSITY

Porosity does weaken a metal. Theory and measurements on porous metals are presented in Reference 36. However, in mild steel, the weld is considerably stronger than the plate (Figure 2-2). Therefore, a large amount of porosity is necessary before the joint strength is affected significantly. Reference 37 presents data to show that up. to 7-percent porosity does not affect the strength, ductility, or Charpy energy of submerged-arc welded joints in mild steels.

However, porosity has been found to influence fatigue strength. The evidence is conflicting. The study reported in Reference 38 showed no fatigue-crack growth from weld porosity in a mild-steel pressure vessel cycled 100, 000 times to a tensile stress level of about 85 percent of yield, whereas slag inclusions and incomplete penetrations did result in crack growth. On the other hand, Reference 37 cites data which shows that 7-percent porosity causes a 40-percent reduction in the endurance limit of mild-steel welds.

Thielsch, in Reference 39, complains that porosity is the defect most readily detected radiographic ally, the least harmful in service, and the most common cause for weld rejection. As may be seen from Section 2.2.3, the last part of this statement does not seem true in the case of ship welds, but the general sentiment is one to which many welding engineers will subscribe.

## B. 2 SLAG AND INCOMPLETE PENETRATION

A study of the role that weld defects play in fatigue of mild steel is reported in Reference 38. A large number of defects, including slag inclusions and incomplete penetrations, were incorporated in a pressure vessel that was cycled repeatedly to a tensile stress equal to 85 percent of the yield strength. The criterion of failure was leakage by penetration of the pressure vessel wall (O. 7 in. ) by the fatigue crack. It was found that incomplete penetrations less than 0.4 in. long and slag inclusions that represented less than O. 16 in. 2 of area on the radiograph were not able to cause failure in 100, 000 cycles. Defects of these dimensions would have been rejected by the current ABS criteria (Reference 2), even though the stress cycling of Reference 38 probably is more severe than that experienced by most hull welds and the criterion of failures is quite conservative.

Another study (Reference 40), using 6-in.- wide, transversely welded tensile coupons of O. 5-in. thickness, found that incomplete penetration defects lowered the endurance limit (taken as the stress at which $10^7$ cycles did not produce failure) from about ±12 ksi to about ±7, 500 psi.

The evidence of Reference 40 with respect to slag was not as clear-cut. At a cyclic stress of ±17, 600 psi, heavy slag patches gave great scatter in fatigue life, from about 60, 000 cycles to more than 106 cycles. The scatter was attributed to the various detailed geometries or notch effects that are possible with slag inclusions.

## B. 3 GRACKS

In the same study referred to under "Slag and Incomplete Penetration" above, Reference 40 presents fatigue data on transversely welded ship- steel specimens (1 /2-in. plate 6 in. wide). Fine longitudinal cracks were introduced during the welding. The single fractograph of a cracked specimen shows a (typical ?) crack of about 1. 5-in. length and O. 1 -in. height. The cracked specimens were tested in fatigue at various stress levels. Results show that alternding stress of less than ±4, 500 psi did not result in fracture of the specimen in $10^7$ cycles. At a stress level of ±7, 000 psi, fracture occurred in $1\,0^5$ cycles. These stress amplitudes (9, 000 psi and 14, 000 psi, respectively) are on the high side of those experienced in the hull plating of typical ships.

## Appendix C
## STRESSES IN SHIP HULLS

A knowledge of hull stresses during service is required to make quantitative judgments pertaining to the criticality of weld flaws in order to evaluate the current acceptance- rejection criteria. A consequence of the traditional approach to hull design is that the actual stresses are not well known, since ship design is based on experience rather than on detailed stress analyses.

The general approach to sizing is to consider the hull as a beam loaded both with its own weight, cargo, ballast, etc. , and by forces from "standard" waves (References 18 and 41). The calculated primary bending stress is limited to about A20, 000 psi for mild-steel hulls. Metal fatigue over a nominal 20-yr design life is not specifically considered in design {Reference 30), although the problem is generally recognized (References 31 and 34).

Recently, increased information on hull loads and stresses has been obtained from new oceanic data, improved wave-prediction methods, continuously monitored instrumented ships, and ship-model testing (Reference 41). Instrumented ship data (References 8, 23, and 42 through 46) is particularly useful for the purpose of this study.

The major stresses acting on the hull plating are longitudinal, are due to bending, and tend to be at a maximum in the deck and bottom within the midship region. Based on the currently available information, the major sources of stress are:

A. "still-water" stresses resulting from cargo and ballast distribution. The level of still-water stress varies every several days as the vessel enters new ports and accepts or discharges cargo, etc. The changes in still-water stresses appear in the range of 5, 000 to 10, 000 psi (Reference 45) .

B. Thermal stresses resulting from differences between air and water temperature and from the effects of direct sunlight on the steel temperature. The thermal stresses tend to vary on a daily cycle. Also, unlike the other stress components, they tend to be at a maximum near the waterline, where the greatest temperature gradients occur (Reference 23). At the deck, thermal stresses account for a daily fluctuation of about 5, 000 psi (Reference 46).

c. Wave-action stresses depend on the sea state and tend to fluctuate on approximately a 10-sec cycle. The maximum amplitudes of wave-action stress recorded on vessels of ordinary steel appear to be under 20, 000 psi (References 8 and 16). Such large stress amplitudes occur rarely. Most of the time, wave-action stresses are less than 3, 000 psi.

D. Vibration stresses occur on approximately a 1- to 2-see period and represent the first-mode vibration of the hull girder in response to excitation by wave action (Reference 46) and/or slamming (Reference 4.2). Vibratory or "springing" stresses are extremely sensitive in magnitude to the design of the vessel and in most cases are relatively low (Reference 46). In one exceptional case, the maximum springing stresses were of the same general magnitude as the maximum wave-induced stresses.

E. Residual stresses result primarily from the thermal contractions of welding. These are highest in the longitudinal direction (with respect to the weld) and can approach tensile yield in a narrow band (3 to 6 in. ) around the weld; however, they decrease rapidly away from the weld and become slightly compressive a few feet away (References 20 and 21). Residual stresses transverse to the weld also exist, but they tend to be low (Reference 17) except at weld intersections, where an improper sequence of welding can significantly affect the stresses (Reference 41).

F. Reaction stresses are a special case of residual stress. The term refers to long-range residual stresses such as those introduced into a plate when it is attached to the rest of the structure. Reaction stresses cannot be very large if the structure is appropriately supported and if the assembly tolerances are reasonable.

Because of unknowns such as residual and reaction stresses, existing data from instrumented ships reveals only stress fluctuations. However, the maximum tensile stress seen by the hull plating (away from stress concentrations) may be estimated roughly by adding together the maximum fluctuations from the various sources and dividing by 2:

| Source | Fluctuation, psi |
|---|---|
| Still water | 10, 000 |
| Thermal | 5, 000 |
| Wave-action | 20, 000 |
| Springing | 5, 000 |
| Total | 40, 000 |
| Maximum tensile = 1/2 (Total)= | 20, 000 |

This estimate, which represents a little more than half the yield strength, is in surprisingly good agreement with the design stress level obtained by the "standard-wave" approach. The influences of stress concentrations at structural discontinuities and horizontal bending stresses are not included in the above value.

Treating the hull as a beam subjected primarily to vertical bending moments implies that the longitudinal stresses are highest near the deck and bottom and nearly zero at the "neutral axis" of the beam. However, shear stresses in the side shell tend to be at a maximum near the neutral axis and have been measured to be approximately half the maximum longitudinal stress. This suggests that brittle fracture is less likely near the neutral axis. However, the yield strength in shear is approximately half that in tension, and fatigue cracking problems may be just as severe near the neutral axis as at the extremes of the hull girder section.

## Appendix D
## FABRICATION OF TEST PANELS

Type 1 panels were prepared by flame-cutting from a Type 3 panel that was 2 ft wide by 3 ft long. Type 2 panels were prepared by first welding together two panels, each measuring 1 ft by 2 ft. The panel was completed by welding on additional l-ft by 4-ft sections. The panel specimens contained a total of approximately 73.5 ft of weld.

Unprimed, ABS Grade C normalized steel was used to fabricate the test panels. The majority of the welds were made using the submerged arc-welding process with some manual welding to fabricate certain types of defects. After welding, the weld beads were masked with tape. The panels were then primed with the standard zinc primer used at Todd Shipyards. Each panel was provided with a padeye for handling purposes. The panel dimensions were chosen to provide a generous amount of weld for evaluation of nondestructive testing techniques, yet still be capable of being handled in the nondestructive testing laboratory. The Type 1 specimens were made smaller, as these panels were inspected by Holosonics and MDAC did not have the necessary material-handling equipment for larger samples. The heaviest specimens weighed approximately 480 lb.

Four types of defects were introduced into the welds: porosity, slag inclusions, incomplete penetrations, and cracks. It was desired to generate the minimum size of defects rejectable by radiography. Welding procedures were developed to generate these defects for each defect type and panel thickness. The weld joints were prepared as shown in Figure D-1. The welds were made with Lincoln Electric Company 7/32-in. -diameter L60 electrode and 760 flux (AWS F62-EL12). The welds were made using a Lincoln Electric Company three-wheel, tractor- type submerged arc-welding machine. The voltage, current, and travel-speed settings were varied for each pass, and no two welds were made in exactly the same manner. Nevertheless, typical settings can be given for each of the panel thicknesses.

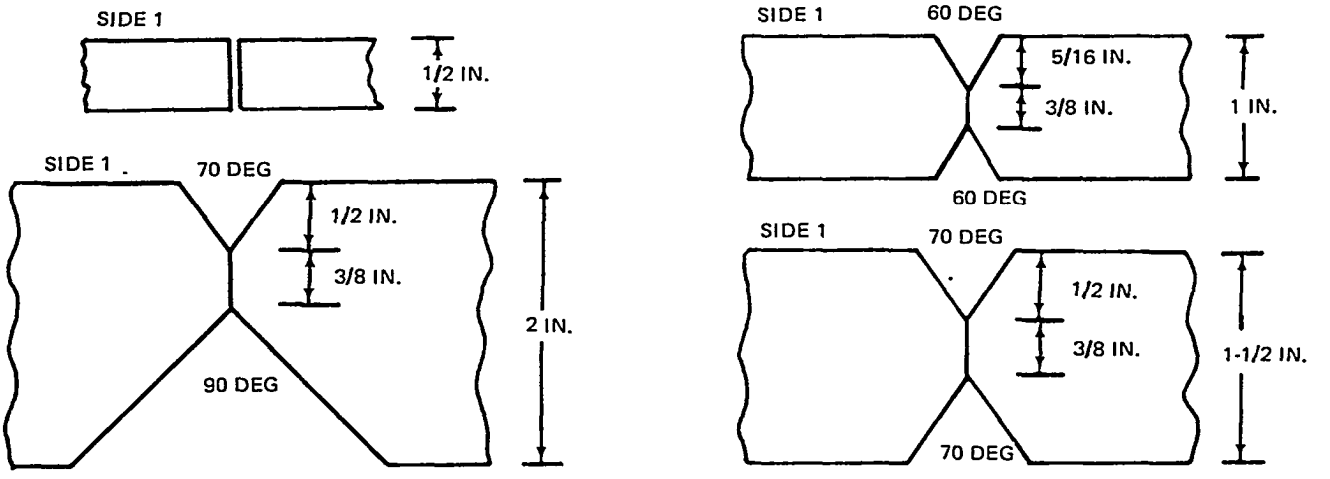


Figure D-1. Weld Joint Preparations

For 1 /2-in. - thick plate, the parameters for Side 1 were 600 amp, 36 v, and 24 in. /min. Similarly, for I - in. - thick plate, the parameters for Side 1 were 950 amp, 38 v, and 18 in. /min. For l-l /2-in.- and 2- in. -thick plate, multiple passes were required from each side. Generally, for 1-1/2-in. - thick plate, the first pass from each side used the same parameters as were used for the l-in. -thick plate. Subsequent passes generally used lower currents but the same voltage and travel speed. For the 2-in. -thick plate, the parameters for the first pass for each side were 975 amp, 38 v, and 18 in. /min. Subsequent passes used a lower current, but the same voltage and travel speed. These parameters were used to make good weld material. Contaminants were added or the welding parameters were changed to generate the desired defects.

Several methods of contamination were used to generate porosity. These included a few drops of oil or water placed in the weld joint, water placed in 1/8-in. - diameter drilled holes, water and graphite mixture placed in the weld groove, oil and graphite mixture placed in the weld groove, zinc primer

sprayed on the panel edges prior to fitting, and wet flux placed in the groove ahead of the submerged arc. Of these methods, a combination of zinc primer and wet flux appeared to work best in creating purposely introduced porosity defects.

The procedure for generating slag inclusions consisted of several steps. First, the weld joint was air-arc-gouged approximately 3/8 in. deep. Next, a piece of fused, submerged- arc flux of the desired size was placed in the groove. The slag inclusion was then sealed in place by manually welding over the inserted slag using either 6011 or 7018 electrode material. Finally, the weld was completed using the submerged-arc process.

Incomplete penetration defects were generated by three different techniques. For 1/2-in. - thick plate, the incomplete penetration defects were generated by temporarily reducing the welding voltage to 500 v over the areas where the incomplete penetration was desired. The subsequent welds were made with limited penetration to avoid destroying the incomplete penetration defect previously generated. For the 1- in. - thick plate, the welding machine was temporarily jogged from 1/2 in. to 3/4 in. from the centerline of the weld and then jogged back to the centerline of the weld after the correct length of incomplete penetration had been generated. Again, subsequent passes were made with limited penetration to avoid destroying the incomplete penetration defects. For the l-1/2 -in.- and 2-in. - thick plates, the procedure was to first seal in incomplete penetration defects using 6011 electrode material. Next, air-arc grooves were made on either side of the incomplete penetration defects. These grooves were made to allow complete-penetration manual welding using 7018 electrode material. Subsequent submerged arc-welding passes were made with limited penetration in order not to destroy the defects previously generated.

Two methods were used to generate crack defects. One method was to insert copper into the weld groove. A piece of copper approximately 1/16 in. in diameter by 1/16 in. long was inserted in the weld area for 1/2-in. - thick plate. This method did not seem to generate the desired cracks, as determined by radiographic examination. The final method selected was to air-arc-gouge some grooves into which tack welds were made with N90

electrode (Stelyte). This tack-weld material was very hard and brittle. The tack welds were broken to generate cracks. The broken tack welds were tightly fitted together, and the areas between the tack welds were manually welded using 6011 electrode material. The remainder of the welding was done using 7018 electrode material. While these defects are not necessarily representative of crack defects that occur in practice, this method was used because the crack position and size could be controlled. If enough contaminant material were added to the weld, cracks could be generated, but their location and size would not be well controlled.

The broken tack-weld approach for generating cracks was not suitable for evaluation of acoustic emission monitoring. Cast-iron filings were used as a contaminant to generate cracks in the welds that were being monitored by acoustic emission techniques. The welding details for these specimens are described in the section on acoustic-emission monitoring.

## Appendix E

## NONDESTRUCTIVE INSPECTION TECHNIQUES *

Details of the calibration and inspection procedures for each technique are given in the following sections.

### E. 1 FILM RADIOGRAPHY

A 300-kV Norelco Model NG300 x-ray source with 4-mm focal-spot size was used for all exposures. Lead-backed Kodak Type M film was used for all but the 2-in. - thick panels. Lead-backed Kodak Type AA film was used for the 2-in. - thick panels. The film was 4- 1/2 in. wide by 17 in. long. The exposure parameters are presented in Table E-1.

All of the films were processed using a Kodak X- Omat automatic film-developing machine. All of the films were clearly marked as to the specimen number and location of the exposure. Penetrameters were used to verify that the procedure yielded at least a 2-2T sensitivity level.

### E. 2 MANUAL-CONTACT ULTRASONIC SHEAR WAVE

Machine oil was used as a couplant for all calibration and inspection. The oil provided good shear-wave coupling without becoming viscous with time, and helped to prevent rust at the completion of inspection.

The amplitude linearity, distance linearity, and resolution of the Model 725 Immerscope were determined to be adequate using a transducer as a reference and an International Institute of Welding (IIW) block. The Model 725 Immerscupe was chosen for its extremely good amplitude and distance linearity.

The as-received surface condition of the test panels was often less than adequate for contact shear-wave inspection. One of the problems was that a zinc primer coat was applied after welding. Masking tape placed over the weldment left a region where primed material was adjacent to unprimed

* The terminology used in this appendix differs from that used in the main body of the report: "manual contact" is substituted for "wedge", "depth" for "height" of flaw; "depth" as used in the report is not discussed in this appendix.

Table E- I

EXPOSURE PARAMETERS FOR PANELS

| Panel Thickness (in.) | Voltage (kV) | Current (mA) | Focus-Film Distance (in.) | Exposure Time |
|---|---|---|---|---|
| 1/2 | 240 | 10 | 36 | 30 sec |
| 1 | 270 | 10 | 30 | 2 min |
| 1-1/2 | 270 | 15 | 30 | 4 min 30 sec |
| 2 | 280 | 14 | 30 | 6 min 30 sec |

material. The very slight change in thickness from one region to the other was sufficient to destroy coupling, even with the use of a relatively viscous oil couplant. Also in many cases, weld splatter was present. These small pieces of splatter were sufficiently large to pry up the contact transducer and destroy the necessary coupling. In both cases, an air-powered disc sander was used to remove the weld splatter and taper the jump from primed to non-primed surface sufficiently to allow contact shear-wave inspection.

The pulse r-receiver was calibrated to check for plate laminations by placing the master transducer on the IIW block to generate multiple internal reflections in the 1 -in. direction. The sweep speed and sweep delay controls were then adjusted to provide a convenient spacing betwen reflections. For example, the first and second back reflections could be positioned on the 1 and 2 scale-division marks. The sensitivity or gain control was adjusted to provide a nearly full- scale indication from the first back-reflection signal. The area adjacent to the weld was inspected for laminations using the master transducer. Only one specimen, Panel 12, was found to have any laminations. In this case, the multiple internal reflections either disappeared or became more closely spaced. The extent of the lamination was mapped, and a scale drawing of the area detected is shown in Figure E-1 .

The following calibration procedure was used for a given angle transducer. First, the master transducer was placed on the IIW block to display a series of multiple internal reflections for a sound path of 3. 6 in. This sound path for longitudinal waves is equivalent to a sound path of 2 in. for shear waves

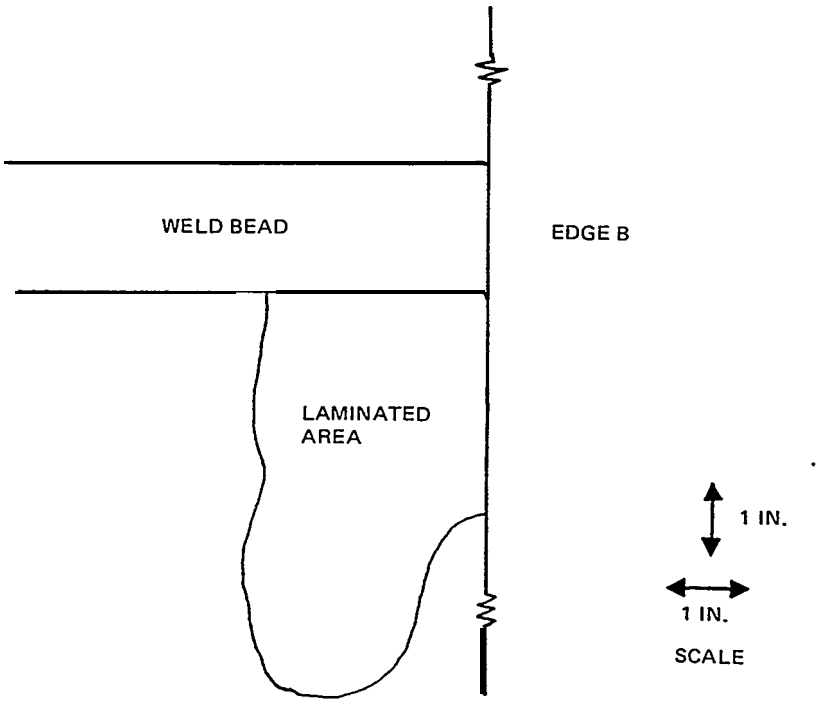


Figure E-1. Laminations in Panel 12

due to the different velocities for each type of wave motion. The sweet - speed and sweep-delay controls were then adjusted so that the first, second, and third reflections, etc. , occurred at the 2, 4, 6, etc. oscilloscope scale-division marks. Next, the proper angle transducer was exchanged with the longitudinal-wave transducer and placed on the IIW block so as to receive a reflection from the 4-in. -radius circle. The sweep-speed and sweep-delay controls were then finally adjusted to show a reflection at the four-scale-division lmark and a much smaller reflection at the eight-scale-division mark.

These adjustments compensated for the sound path through the plastic wedge of the angle transducer and provided a convenient time scale by which to analyze the received signals. For example, signals reflected from a defect 2 in. along the sound path from the point of incidence would then appear at the two-scale-division )mark. The received signal at the eight-scale-division mark occurred from the groove machined at the center of the 4-in. -radius circle after a total sound-beam path of 16 in. in the steel.

With the angle transducer positioned for a maximum reflection from the 4-in. arc, the point of incidence was marked on the transducer at the place where the center groove intersected the transducer. All subsequent measurements of transducer position relative to the weldment being inspected were taken from this point. This point was also used to check the angle of the transducer. This was done by positioning the transducer for a maximum reflection from the 2-in. - diameter lucite cylinder. The 45 - deg transducer was checked on one edge, the 60 - deg transducer could be checked on either of two edges, and the 70 - deg transducer was checked on the edge opposite that used for the 45 - deg transducer. The actual angles measured for the transducers were 45 deg, 62 deg, and 72 deg. The measured angles were used in subsequent calculations of sound-beam paths.

Once the sweep adjustments had been made on the pulser - receiver, the only additional adjustments required were for calibration. The through-hole sensitivity calibration standard was used for this purpose. The transducer was positioned for a maximum reflection from a given hole, and the sensitivity or gain and distance-amplitude correction controls were set to peak the signal at a minimum of 80 percent of full- screen height. This procedure was repeated for several such holes that spanned the range of potential flaw locations for the material thickness being inspected. The adjustments were made so as to have the reflections from each of these holes peak at 80 percent of the full-scale reading.

Some difficulty was experienced in adjusting the distance-amplitude control on the Model 725 Immerscope. The distance-amplitude correction control on this pulser-receiver was called the sensitivity-time control (STC). This control did not function when the instrument was used in the delayed-sync mode. (The delayed-sync mode is the one normally used to provide the desired delay in the display. ) The STC control functioned only in the video-sync mode. In this mode, the sweep is started by the first video pulse occurring after the end of the sweep delay time, rather than immediately at the end of the delay time itself. This mode is normally used for immersion ultrasonic testing, where variations in the water path would cause the received signals to move if the delayed- sync mode were used. For contact shear-wave inspection, however, the only signal that could be relied upon to

trigger the video- sync was the "main-bang." Thus, it was not possible to adjust the sweep delay to position the reflected signals at specific scale division marks. Instead, the positions of the reflected signals from the through holes were marked directly on the oscilloscope screen.

The STC functioned by attenuating the earlier signals relative to the later signals. The earliest signal was attenuated the most, followed by the next earliest signal and so on, out to) a certain maximum time. Beyond the range of this correction, the reflected signals from equivalent-sized through holes decreased with increasing depth. An internal range adjustment setting of three out of a total of five provided the best range for inspection of the steel thiclinesses considered. For the thicker sections of steel, the range was not quite large enough to handle the range of flaws used for calibration. In these cases, a maximum occurred for one of the calibration signals relative to the others.

An alternate calibration method was examined that alleviated the re atively difficult procedure required when using the STC adjustment. In the alternate procedure, the sensitivity or gain was adjusted to give a peak value for the earliest received calibration signal at 80 percent of full-screen height. For this gain setting, the height of the remaining calibration signals was then marked directly on the oscillcscope screen. These points fell upon a very nicely defined exponential decay curve. This curve corresponded to the amplitude rejection level (ARL). Any signals occurring above this curve corresponded to) the signals that would have occurred above 80 percent of full-screen height when using the STC adjustment. The disregard level (DRL) curve was established by dividing the previously determined curve by two and drawing the corresponding curve on the oscilloscope screen.

When the STC adjustment was not used, full use of the delayed-sync capabilities for positioning the reflected signals was made. In many respects, this method of calibration was simpler to set up and use in practice. This method eliminated a somewhat tedious iteration procedure required to set up the STC adjustment properly. The established curves were very repeatable and were obtained through adjustment of a single control, the sensitivity or gain. Once established, the correct gain setting could be determined easily through

a one-point check for a specific through hole, adjusting the gain for the appropriate signal height for that hole.

The weld inspection was performed for longitudinal and transverse discontinuities as described in the specification. The inspections were performed on both sides of the weld from the same surface. As none of the welds had been ground flush, inspection for transverse discontinuities was performed with the transducer angled about 15 deg from the weld axis and moved parallel to the weld length. When discontinuities were detected, records were made of the transducer position and signal amplitude. The transducer position was measured from the point of incidence of the sound beam to the center of the weld bead, and from the centerline of the transducer wedge to the end of the weld.

Position measurements were made at the ends of discontinuities. The discontinuity length could be determined from the difference between these measurements. The maximum signal height for each defect was also recorded, as well as its position on the oscilloscope screen. Thus, information was available about the position, length, depth, and ultrasonic reflected signal amplitude for each defect detected.

## E. 3 LIQUID- FILLED WHEEL SHEAR WAVE

A shop Handy Hoist was used to manipulate the wheel. The wheel was clamped to the underside of a beam extending to one side of the hoist platform. The hoist was used to raise, lower, and roll the wheel in a straight line relative to the test panel.

The calibration of the wheel presented some unique problems. First, the internal angle of the wheel had to be adjusted for the desired internal angle in the steel. The internal angle adjustment knob is calibrated with a range from O to 25, with each division corresponding to 2 deg. The correct angle setting can be calculated using Snell's Law and the velocity of sound in the wheel and in steel. The velocity of sound in the wheel is 0. 654 x $10^5$ in. /sec. The velocity of shear waves in steel is 1.268 x $10^5$ in. /sec. The internal angle settings for shear-wave inspection of steel are presented in Table E-2.

Table E-2

ANGLE SETTINGS FOR WHEEL

| Angle in Steel (deg) | Internal Angle (deg) | Wheel Settings |
|---|---|---|
| 45 | 21.4 | 10.70 |
| 60 | 26.5 | 13.25 |
| 70 | 29.0 | 14.50 |

These are the calculated settings that should be used, assuming that the wheel is correctly oriented with respect to the material being inspected. The" settings should be changed if the wheel is not exactly perpendicular to the material. The wheel orientation is determined by adjusting the internal angle for a maximum in the multiple internal reflections for longitudinal waves in the material. The setting obtained under these conditions can then be used as a zero-reading adjustment to the calculated settings. Using this method, however, does not result in an accurate setting. When checked using the IIW block, the angles were off approximately 4 deg. The IIW block could be used to set the proper angle but was somewhat awkward for this purpose. Instead, special calibration wedge blocks were machined as described previously. These blocks were placed on top of the material being inspected. The wheel was then positioned on top of the block, and the internal angle was adjusted for a maximum reflected signal from the face of the wedge. In this way, the internal angle could be very accurately set to compensate for the orientation of the wheel and allow for backlash in the angle adjustments.

The setting of the internal angle is quite simple but could be incorrectly set if the wrong signal is maximized. The possible types of signals that are obtained during this adjustment are shown in the following series of photographs.

The wheel was positioned on the 70-deg wedge block with the centerline of the wheel approximately 2-1/8 in. from the edge. The internal angle was adjusted for a very large angle and was then reduced until the signal was maximized. The signals occurring for an angle setting of 22. IO are shown in Figure E-2. These signals correspond to surface-wave reflections. The

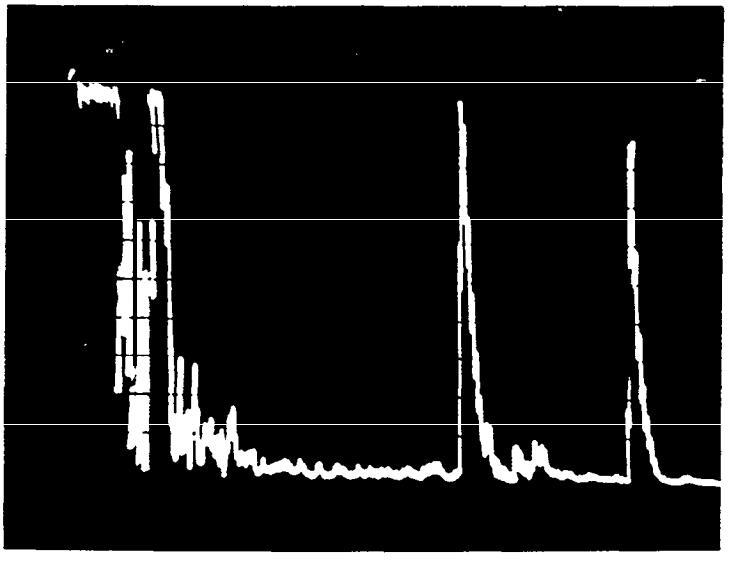

Figure E-2. Two Surface-Wave Reflections

first, and the stronger of the two, corresponds to a reflection from the 70-deg-angle edge. The second reflection corresponds to a reflection from the bottom angle after passing around the 70-deg angle. This fact could be verified by dampening the received signals. By placing a finger on the top of the wedge block along the sound path between the wheel and the 70-deg edge, the reflection from both edges was reduced, as shown in Figure E-3. If a finger was placed on the face of the wedge between the two angles, only the second signal was dampened, as shown in Figure E-4.

If the internal angle was reduced further, these two signals disappeared, and a new signal appeared. This signal was a maximum at the angle setting of 20-35 and corresponded to a 70-deg shear wave, as shown in Figure E-5. This signal could not be dampened as were the surface wave signals, and was generally stronger. The photograph shown was taken with 28 dB attenuation inserted in the line, as compared to the first three figures.

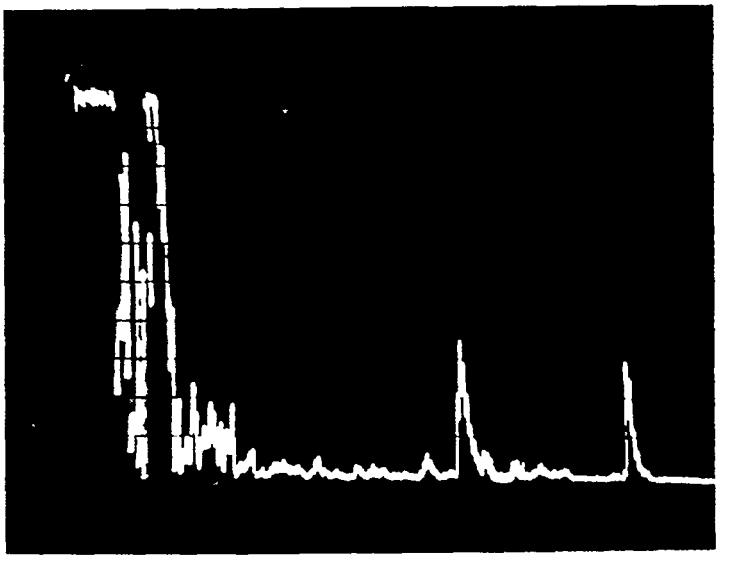

Figure E-3. Both Surface-Wave Reflections Damped



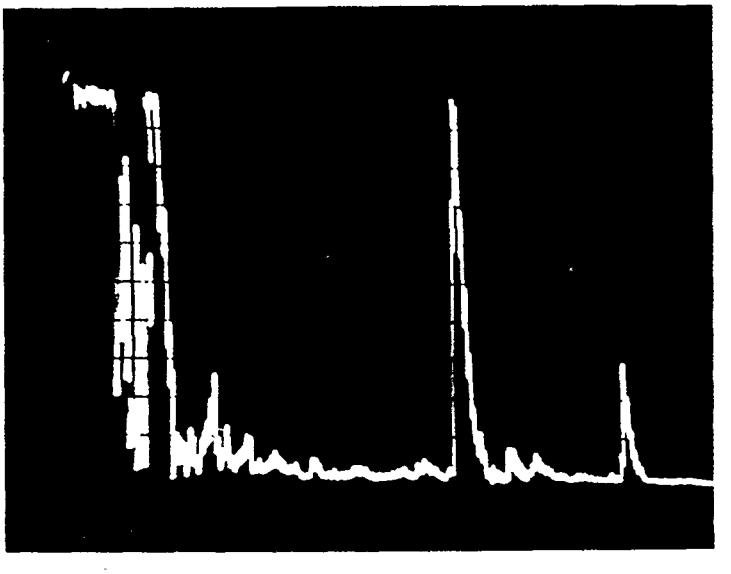

Figure E-4. Second Surface-Wave Reflection Damped

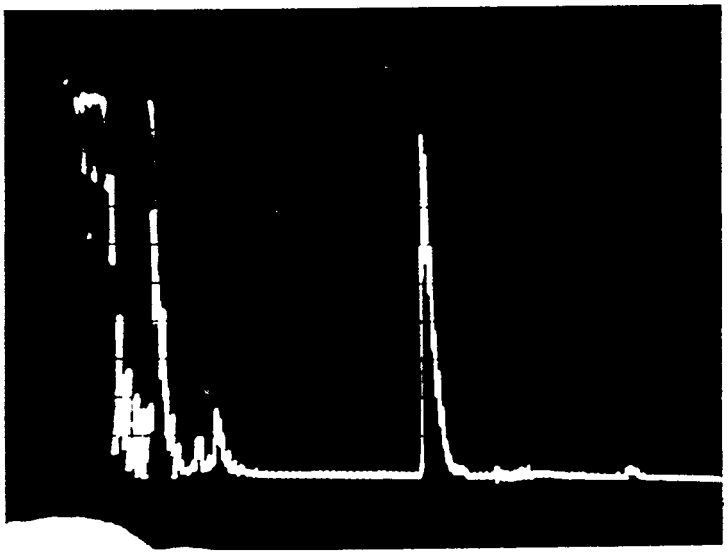

Figure E-5. 70-Deg Shear Wave, 28-dB Attenuation

If the angle was reduced still further, the 70-deg shear wave disappeared, and a new signal appeared as shown in Figure E-6. This signal became a maximum for an angle setting of 16. 65 and corresponded to a reflection from the bottom angle at an internal angle in the steel of approximately 50 deg from the normal. This signal was also quite strong. This figure was taken with 34 dB attenuation.

Finally, as the angle setting was reduced still further, multiple internal reflections of longitudinal waves were set up in the wedge block. This occurred for an angle setting of 5.00, which corresponded to the zero correction.

The operation of the wheel was hindered by the presence of internal reflections within the wheel. Internal reflections would not be a problem if they did not occur within the time range of interest. As received, however, a ghost or unwanted reflection occurred within the range of interest for inspection of 1/2-in. - thick material at 70 deg. This signal occurred at the

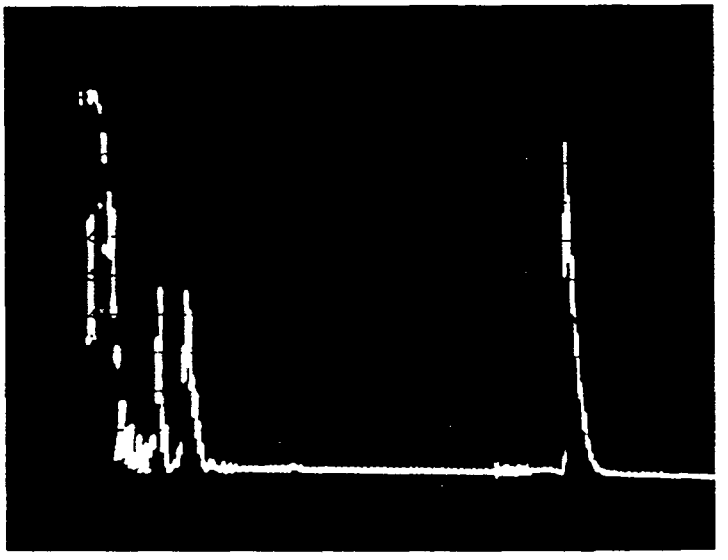

Figure E-6. Reflection From Bottom Angle, 34-dB Attenuation

equivalent flaw depth of slightly less than 1 in. This reflection seriously interfered with the inspection. The position of this reflection changed somewhat with angle settings. For a 60- deg shear wave, the reflection occurred just outside the position of a 1- in. - deep hole; thus, inspection of 1/2-in. - thick material could be done at 60 deg. This reflection had several peculiar features. First, the reflection was not present at all angles but was present for the range of 45 deg to 70 deg. When present, the reflection would not vary in time for a given angle setting but would change in amplitude with wheel rotation. The reflection did not correspond to any of the liquid/tire or tire/steel interface echoes.

The wheel was disassembled to examine the source of this reflection more closely. The tire was removed, and the remainder of the device was immersed in a tank of water to check its function. It was determined that the piezoelectric element was not properly backed or dampened and was "looking" in the backward direction. Thus, the element was detecting reflections from the internal transducer holding mechanism. The problem was

rectified by adhesively bonding a piece of closed-cell sponge to the back of the piezoelectric element. The ghost reflection then disappeared. The wheel was reassembled and further evaluated.

Another unwanted internal reflection was identified when performing the sensitivity calibration for 1 - in. - thick specimens. With an angle setting of 70 deg and a through-hole depth of 2 in. , it was found that internal reflections interfered with the detection of reflections from the 2 - in. - deep hole. At an angle setting of 70 deg, the internal angle of the wheel transducer was 29 deg. While the internal holding mechanism geometry was not known exactly, the approximate timing of the internal reflections indicated that they occurred after a reflection from the liquid-tire interface and an additional reflection somewhere near the axle of the wheel.

It was found that inspection of 1 - in. - thick material could be accomplished without interference using an angle setting of 60 deg. For l - 1/2-in. - and 2 - in. - thick material, to avoid the interference of this unwanted signal, the inspections were performed using two angles, 45 deg and 60 deg. The 60 - deg angle was used to perform an inspection without a bounce from the bottom surface. The 45 - deg angle was used to perform an inspection after a bounce from the bottom surface. In this way, the entire weld volume could be inspected, even though the internal reflection was present but not in the range of interest.

It was not possible to completely avoid the presence of this internal reflection for the 2- in. - thick material when using an angle setting of 45 deg. The reflection occurred at a position equivalent to a hole depth of approximately 3 - 1/2 in. This means that approximately the top 1/2 in. of a 2 - in. - thick weld is not inspectable with the wheel as currently designed. It should be possible to dampen and eliminate this reflection in a manner similar to that employed for the other internal reflection. It would be necessary to disassemble the wheel and determine the actual sound path. Then it would be necessary to place an absorbing material in the sound-beam path.

It was desired to calibrate and use the liquid-filled wheel in a manner as close to that of manual contact inspection as possible. The wheel was

calibrated using the same through-hole sensitivity calibration standard as for manual-contact inspection. An initial problem in this respect was that the wheel does not easily slide perpendicular to its rolling direction. This, however, is the direction that the calibration standard should be moved to perform the sensitivity calibration adjustments. It was found that the use of oil as a couplant considerably simplified this procedure in allowing the wheel to slide relative to the standard.

The procedure used to operate the wheel was somewhat involved and cumbersome. The test panel was placed on a small flat. The wheels of this flat were blocked to prevent it from rolling. The surface of the specimen was checked for any conditions that might lead to poor coupling. Any such conditions found were removed through disk sanding, filing, or other methods. Oil couplant was applied to the material adjacent to either side of the weld. The Handy Hoist was positioned alongside the flat, the wheel was lowered until it was just in contact with the test specimen, and then the hoist was aligned such that the wheel would roll along a line evenly spaced from the weldment. The wheel would then be slid along its support beam perpendicular to the rolling direction until the wheel was over the area to be inspected for laminations.

The wheel was attached to the pulser - receiver and was lowered until the contact patch was just flat on the specimen. Then the wheel angle was adjusted for maximum multiple internal - reflection response for longitudinal waves. There are two such adjustments, one for the primary angle of the internal transducer and another for the other axis to keep the transducer normal to the panel surface. The wheel was then rolled for the length of the weld while observing the oscilloscope screen for evidence of laminations.

Next, the wheel was raised, and an appropriate wedge-angle block for the material thickness being inspected was placed under the wheel. The wheel was then lowered onto the top of the wedge block. The wheel was positioned along its support beam length such that the desired angle would intercept the wedge face at its center. The wedge itself was placed relative to the weld such that the edge of the wedge was parallel to the direction of the weld. The angle adjustment for the wheel was made for the maximum reflected

signal for the angle desired, as described earlier. Both angle axes were adjusted for the maximum in this signal. The wheel was raised, and the through-hole sensitivity calibration standard was placed on top of the wedge block. The wheel was then lowered until the contact patch was just flat on the calibration standard. The calibration standard was moved back and forth underneath the wheel while calibrating the pulse r-receiver for the necessary distance and amplitude - sensitivity corrections. Finally, the calibration blocks were removed from underneath the wheel, and the wheel was lowered until it was properly in contact with the test specimen.

The wheel was then positioned at the desired distance from the weld for the given angle. Marks spaced by the amount that the wheel fixture was to be moved between passes were placed on the wheel fixture. The corresponding index or start mark was marked on the beam for the first pass. With each successive pass, the wheel would be moved along the beam length to line up the appropriate index marks for the next pass.

For the first few panels inspected in this manner, the angle and sensitivity adjustments were checked for each pass. It became evident that once set up, the wheel maintained these adjustments very well. Subsequently, later panels were. inspected after an initial setup without checking each pass. For the 1-1/2 - in. - and 2 - in. - thick panels, the internal angle was readjusted halfway through the inspection, and the corresponding sensitivity adjustments were made. The remainder of the passes were then made for this new angle setting.

As each defect was found, records were made of the beginning and ending locations, the signal amplitude, and the signal position. This was done for each defect and each pass. The results of the various passes were then superimposed to provide a complete picture of the defects detected.

### E. 4 DELTA SCAN

A discussion of delta- scan theory is given in References 47 through 49. Optimum parameters for the delta - scan setup are given in Reference 47 for various thicknesses of steel.

## E. 5 ACOUSTIC HOLOGRAPHY

The technical report on the evaluation of acoustic holography by Holosonics is presented in Ref. 57. The specimen numbers used by Holosonics differ from those in the rest of the report, as shown in Table E-3.

Table E-3
NUMBERING SCHEMES

| Specimen No. | Holosonics No. |
|---|---|
| 3 | 8 |
| 4 | 9 |
| 5 | 10 |
| 6 | 7 |
| 7 | 5 |
| 8 | 6 |
| 9 | 3 |
| 10 | 4 |

Acoustic holography is a form of ultrasonic inspection in which information about the amplitude and phase of the sound is used to generate an optical Pres - entation of the defects. The holographic information is obtained by electronitally combining the received pulse-echo signal with the reference-source oscillator. A hologram is generated by photographing a light source that moves with the scanning transducer in a raster scan and is modulated in intensity by the holographic information. The optical presentation of the defects is then made by illuminating the hologram using a laser.

A Model 200 HolScan scanner was used to generate a hologram of the inspection results. The hologram may be thought of as a window through which the observer views the defect condition in the metal. The terms "focused - image holograms and "intensity scans" used in the Holosonics report refer to methods of viewing. The reference beam may be thought of as being equivalent to a light source. Focused-image holograms are generated with this light source within the window area but uniform over the whole area. Both phase

and amplitude information are recorded. Reconstruction of this type of hologram is required to obtain the necessary resolution for thick metal sections.

For thin metal sections, reconstruction of the hologram may not be required for the necessary resolution. In this case, it may be possible to obtain the necessary resolution from the simpler intensity scans. The intensity scan is essentially the absolute square of the signal obtained from the holographic recording and is presented much the same as a C-scan.

The transducer used was about 1 in. in diameter with a focal length of 4 in. The transducer was oriented such that the focal point was near the surface of the material being inspected. The half-beam angle was approximately 7 deg in water. This angle was refracted in the steel. For longitudinal inspection, the half-angle increased to 28 deg. For shear-wave inspection, the beam spread was from 22 deg to 62 deg in steel. This orientation was used for shear-wave inspection of all material thicknesses.

The scanning velocity was 3 in. /see with an increment step of 0. 018 in. Due to the limited scan aperture, usually six or more scans were made per specimen. Two were longitudinal scans, two were shear-wave from one side of the weld, and two were shear-wave from the other side of the weld. Between longitudinal and shear-wave types of scans, the specimens had to be moved and leveled the appropriate distance from the transducer. For the thicker specimens, it was estimated that at least 30 min of scanning time were required. These inspection rates could probably be increased through the use of a specially designed scanning fixture for weld inspection.

The transducer frequency was 3 MHz. Experience with other thick steel samples has indicated that this frequency provides adequate resolution. The system could be operated at frequencies from 500 kHz to 10 MHz if less or greater resolution were required.

In the Holosonics report, the hologram interpreter attempted to identify flaw type from the nature of the hologram. The identification was correct about

one-third of the time. Accuracy in defect identification might improve with experience.

## E. 6 ACOUSTIC EMISSION

Acoustic emissions are the transient elastic waves generated by the rapid release of energy within a material. Acoustic emission monitoring has been applied to in-process weld inspection by several researchers (References 50 through 56).

The method used by these researchers was to detect the emissions from crack formation as the weld cooled, using an acoustic emission transducer coupled to the plate. These signals were then amplified, counted, and displayed as counts received versus time. The weld was then inspected by other means, and the defects found were related to the plot of counts versus time to determine how long after welding the emissions occurred. Since the time delay for crack formation and the proper threshold gain depended upon the welding parameters, a tape recorder was often used to record the emissions for the later analysis.

In this program, a different approach was used for crack detection and location. A Dunegan-Endevco Model 902 flaw locator was used. This instrumentation determined the difference in the arrival time of an acoustic emission event at two separate transducers. Each transducer was placed at one end of the weld being monitored. Prior to the in-process monitoring, background noise and attenuation measurements were taken to help establish the correct transducer frequency to be used, and the threshold gain.

Background noise and attenuation measurements were made on a 1/2 - in. - thick steel panel at the Todd Shipyard Corporation panel line in San Pedro. The Dunegan - Endevco Model 902 flaw locator was used in combination with two Model 801P preamplifiers and S - 140B transducers. A general-purpose oscilloscope and Spencer Kennedy Laboratories Model 364 wide-range solid-state variable electronic filter were also used. By monitoring the background noise detected on the panel line during normal operations, it was determined that a high level of background noise was present. The transducers were

sensitive to many extraneous noise sources at large distances from the receiving transducer. For example, the sensors were able to detect people walking on the panel, sweeping of flux particles, and other noises. These sources were detectable over distances as large as 40 ft.

Attenuation measurements were taken in the following manner. One transducer was used as a test pulser using the Dunegan-Endevco Model 908 pulser. The pulser periodically generated a simulated acoustic emission signal. This signal was then detected by another transducer, which was placed at various distances from the pulsing transducer. The transducer separations used were 2 in. , 5 ft, 10 ft, 15 ft, 20 ft, and 25 ft. For each of these separations, the signal from the receiving transducer was filtered and then observed on the oscilloscope. Three different frequency ranges were investigated. The ranges were 50 to 250 kHz, 400 to 600 kHz, and 900 to 1, 100 kHz. The peak-to-peak voltage of the received signal was determined for each of these frequency ranges and transducer spacings, as shown in Figure E-7.

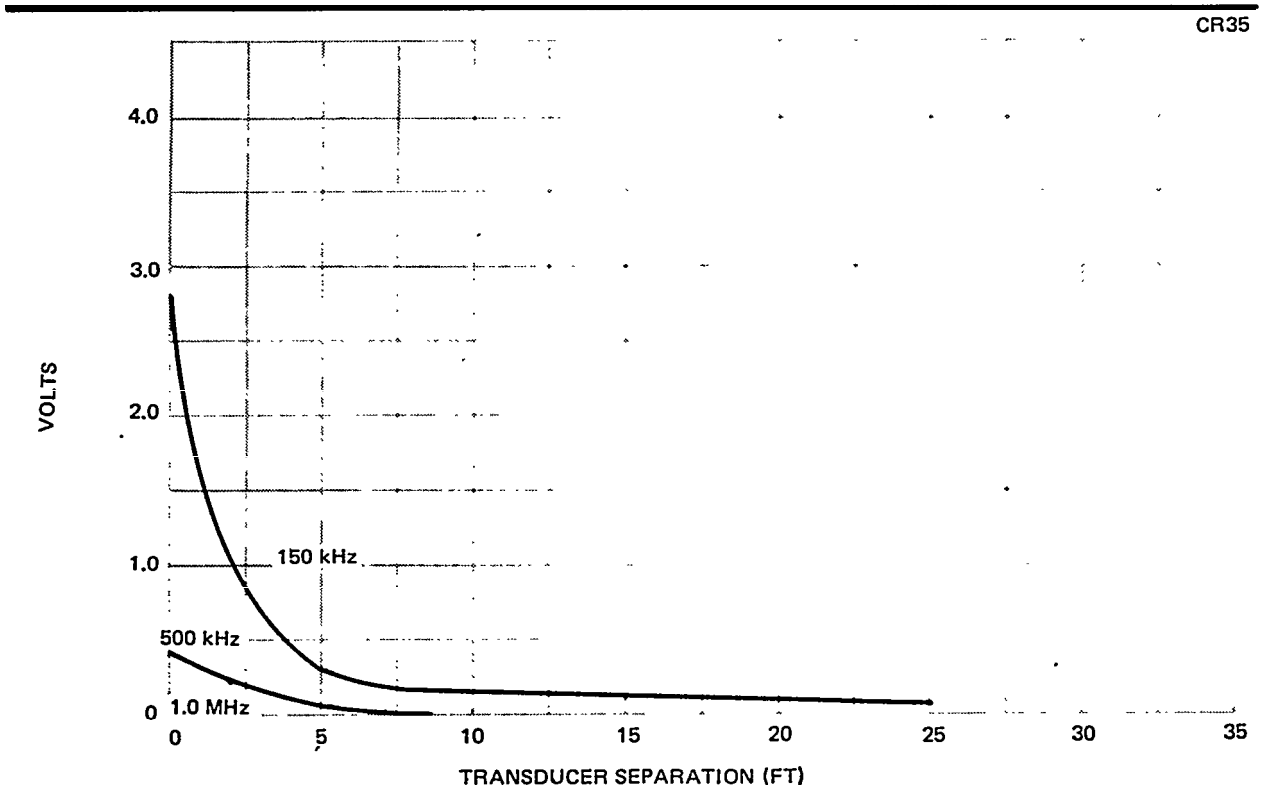


Figure E-7. Acoustic Emission Attenuation

Figure E-7 was generated using a Model S-140B sensor, whose resonant frequency is approximately 150 kHz. The curves of this figure dramatically indicate the fact that very low-level noise sources can be detected at large distances when a 150-kHz sensor is used. By selecting only the frequencies around 500 kHz, the signals were detectable over a much shorter range. From the results of these measurements, it was decided to use Model S-750B transducers with a resonant frequency of approximately 750 kHz. These transducers would still be sensitive to acoustic emission events but would be less sensitive to extraneous noise sources, especially from long distances. Model 802PC preamplifiers were used in combination with these transducers. These preamplifiers provided a gain of 60 dB.

Acoustic emission monitoring during welding was conducted for two test panels. One panel, No. 19, was 1/2 in. thick. The other panel, No. 20, was 2 in. thick. The panels were both 1 ft wide by 4 ft long. After Welding, the panels were trimmed to a 3-ft length. The panels were made 4 ft long since the Dunegan-Endevco Model 902 flaw locator required transducer separations greater than 30 in.

As the acoustic emission monitoring during welding tests was to be conducted without tape recording for later analysis, the appropriate gain and other adjustments had to be decided prior to the tests. A 2- ft-long test panel was welded prior to the 4- ft-long panel to help establish these adjustments. The transducers were coupled, one at each end of the weld, to the panel approximately 5-3/4 in. from the weld and 3/4 in. from the ends using Dunegan-Endevco AC-V9 acoustic couplant. Based on the experience of others, it was decided to run this test using 60 dB gain. This amount of gain was provided by the preamplifiers alone, so that no additional gain was required from the Model 902 flaw locator. Thus, the gain plot settings on the flaw locator were set at 1. 0 for a gain of 1.

The trim potentiometer was then adjusted to give the best linear indication using the test transducer. The instrumentation was placed in the test mode using the Model 908 pulser. By placing the pulser : t some position between the two sensors, the calculated position of the simu ated event was shown on a digital readout. The trim potentiometer was then adjusted until the digital

readout corresponded to the location of the test transducer. With the test transducer located halfway between the two sensors, the potentiometer was adjusted for a reading of 500. With the sensor at 75 percent of the length between the transducers, the reading was 750.

The weld was contaminated using cast- iron filings. Two sections of the weld were contaminated, one section approximately 5 in. long and another section approximately 3 in. long. The weld groove was filled flush with the contaminated filings.

The weld was made while the acoustic emissions were monitored. The instrumentation gave very little indication of flaw location, although the cast iron generated surface cracks that were visible. It was decided that perhaps the gain setting was too low, as there was a very small number of indications.

The same experimental setup was used to monitor the full-size, 2-in. -thick panel. Contaminant was placed in the weld groove as shown in Figure E-8.

CR3S

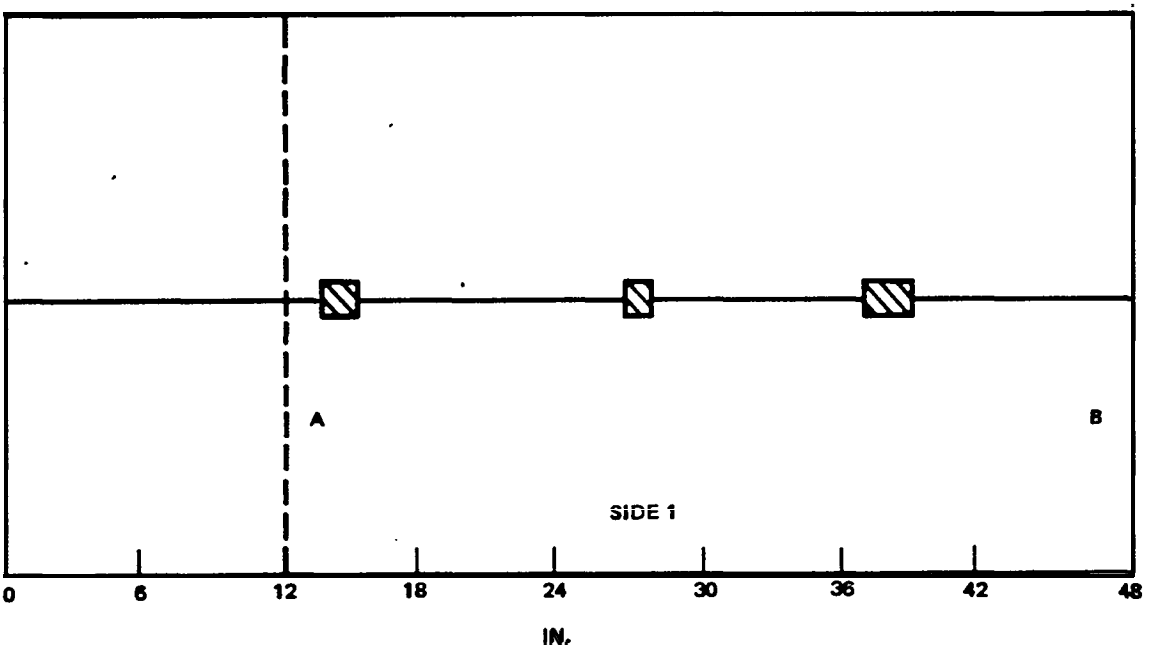


Figure E-8. Contaminant Locations for 2-in.-Thick Panel

For these tests, the Model 902 gain potentiometer was set at 3.16 for a total system gain of 80 dB.

Prior to welding, several background noise tests were made. First, the submerged arc-welding machine was run over the panel with and without flux but without welding. The instrumentation detected very little indication of extraneous noise sources for either case.

The first pass of the weld was made and monitored using the acoustic emission instrumentation. After the weld was completed, an x-y plotter was used to display the total number of calculated events versus their calculated locations. This plot showed a large spike at the 50 - percent mark. This condition was a sign that the gain was too high and was detecting primarily extraneous noise. This occurred because the internal digital counter started at 500 and then either counted up or down, depending upon which transducer was triggered first. The counting process was stopped by the next signal detected by the other transducer. If there was a large amount of random noise present, this counter would be turned on and off quickly, resulting primarily in calculated locations at the 50 - percent mark.

The weld was also monitored during cooldown for 15 min after the weld was completed. These plots did not indicate any significant emissions. After the weld had cooled and extra flux was vacuumed up, the instrumentation was used to generate spikes at the indications of slag cracks. The positions of these spikes did not correlate with any of the small indications on the previous plots. Thus, it did not appear that the emission locations being plotted corresponded to specific slag cracks.

Monitoring was continued for many additional passes in case any cracks should grow during further welding. None of the plots indicated the detection of any crack locations, although in several cases very loud audible pings were heard, probably due to crack extension.

After the passes for Side 1 had been completed, it was decided to monitor the passes for Side 2 using both the flaw location technique and the signal-count-rate-versus-time technique. Additional instrumentation was assembled for

this purpose. A Dunegan-Endevco Model 301 totalizer was used with a Model 402 reset clock, Model 502 ramp generator, and Model 702 audio monitor.

The reset clock was used to periodically reset to zero the total number of counts summed by the totalizer. The ramp generator was used to create a count - rate-versus - time plot. The ramp generator created a voltage proportional to the time to drive the x-axis of an x-y plotter. The audio monitor provided an audio indication of the signals being detected by the instrumentation.

The 2 - in. - thick panel was turned over, and contaminant was added at the corresponding locations of Side 1. The weld was monitored, and a count-rate-versus-time plot was made in addition to the flaw locator plots. No flaws were detected. Actual flaws were seen at six locations at the conclusion of the first pass. The flaw detector plot still showed a spike at the 50-percent mark due to noise. The remaining passes were also monitored without detecting any further crack growth.

Thirteen weld passes were made for the 2 - in. - thick panel. The first three passes were made on Side 1 using 3/16 - in. - diameter L61 wire. The next seven passes were made on Side 2 using 7/32 - in. - diameter L60 wire. The final three passes were made on Side 1 using L60 wire. All passes were made using 760 flux. Depending upon the pass, the welding parameters varied from 700 to 900 amp, 35 to 37 v, and 15 to 18 in. /min travel speed.

Different procedures were used for the monitoring of the 1/2 - in. - thick panel to try to avoid the unwanted spike at 50 percent. Additional extraneous noise sources were investigated as well. The new procedure for setting the gain was to place the transducers the desired distance apart and then place the test transducer adjacent to one of these transducers. In the test mode, the gain was adjusted for the other transducer until the flaw locator indicated that the instrument was detecting the pulse. The procedure was repeated in a similar manner for the other transducer. Next, the trim potentiometer was adjusted to obtain readings of 000 and 999 with the test transducer adjacent to one or the other of the transducers. This procedure resulted in less than 80 dB total gain.

A preliminary 1 /2- in. - thick plate weld 24 in. long was monitored with the transducers adjacent to but not coupled to the panel to determine if any electromagnetic radiation was the source of the noise. This did not appear to be a problem for the welding process itself, although several times during the preliminary test setup, extraneous noise signals were detected, as indicated by the audio monitor. One source of noise was an overhead crane that would normally be used in the area where the tests were being conducted. During the actual welding procedure, this and all other electrical activity was terminated in the immediate area.

Again, cast-iron contaminant was added to the weld groove as shown in Figure E-9. The welding was monitored using both techniques. The 1/2-in-thick panel was welded in two passes. The weld joint was prepared with an 11/16-in. - deep, 90 - deg-included - angle groove on Side 1. Minnesota Mining and Manufacturing backing tape was applied to Side 2 to eliminate burnthrough. Both passes were made using 3/16-in. - diameter L61 wire and 760 flux. The

CR35

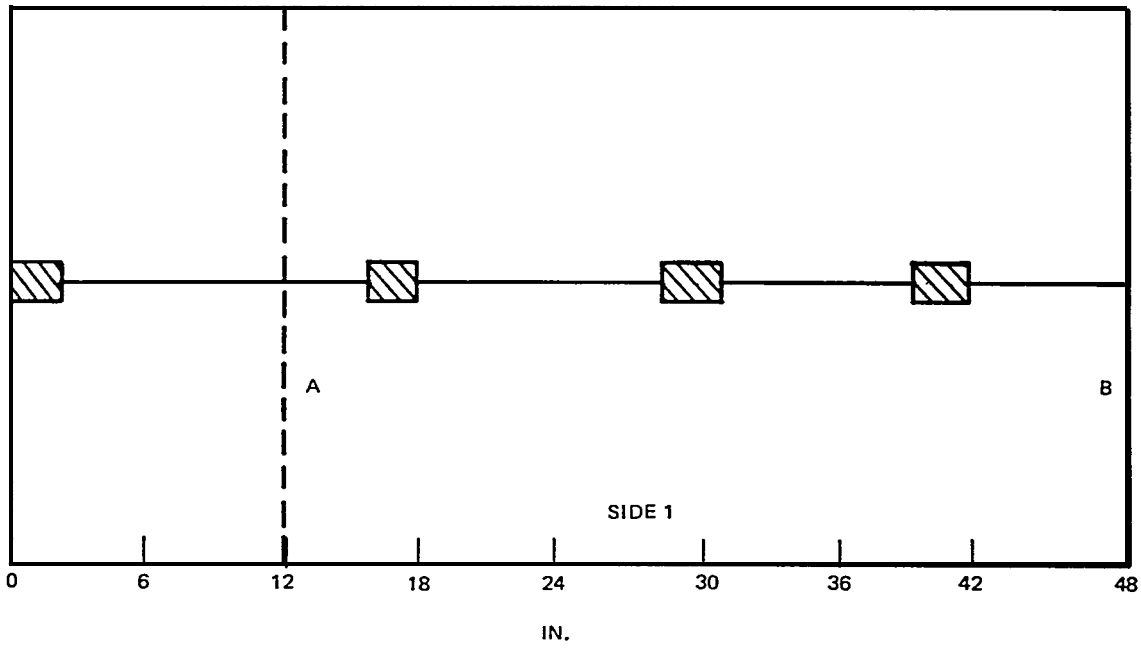


Figure E-9. Contaminant Locations for 1/2-In.-Thick Panel

welding parameters were 475 amp, 34 v, and 14 in. /min for Side 1 and 700 amp, 36 v, and 20 in. /min for Side 2.

Subsequent x-ray and ultrasonic inspection of these panels revealed very few defect indications. Some indications, however, were present for flaws at either end of a contaminated area.

The results of this evaluation indicate that acoustic-emission monitoring technology for welding is not sufficiently developed for sensitive detection and location of crack formation. Current equipment designs are not suitable for shipyard application in terms of reliable defect detection, rugged construction, and rejection of extraneous noise. For these reasons, acoustic emission monitoring cannot be recommended currently as an alternative to conventional inspection procedures.

This program did not examine acoustic-emission detection capabilities for noncrack defects.

## E. 7 DESTRUCTIVE TESTING

The notched fracture specimens were fractured using three-point bending. The specimens were soaked in liquid nitrogen prior to testing. The specimens were soaked until the liquid stopped boiling. At this point, the specimens were at -320° F. The purpose of the liquid-nitrogen soak was to lower the specimen temperature below the nil-ductility temperature for steel. This temperature is approximately -12° F for low-carbon mild steel. Below this temperature, brittle fracture occurs, and the material becomes more sensitive to notch-type defects. A combination of notched specimens and liquid-nitrogen coolant was used to help ensure that the fracture surface would pass through the weldment.

The specimens were loaded in a Baldwin testing machine with a capacity of 60, 000 lb. A special fixture was used that would accommodate specimens up to 3 in. wide by 2 ft long. This fixture is shown in Figure E-10. The fixture consists of two steel plates and two steel pins. The pins have their centers 9 in. apart. The pins were 2-1 /4 in. in diameter. The cold specimen was placed in the fixture with the notch down. A center load was

CR35

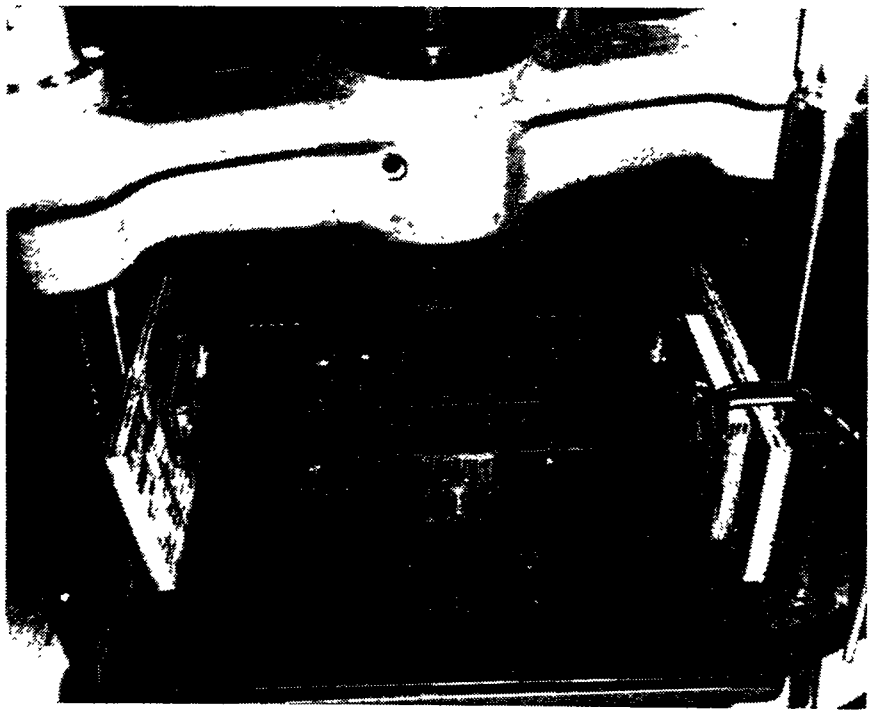

Figure E-1 O. Three-Point Bending Fixture

applied opposite the notch. A steel-and-wood restraining fixture was used to contain the two halves of the specimen as it fractured. The center load was applied to a flat area machined in the weld bead opposite the notch. The specimen was quickly transferred to the fixture, centered, and loaded to ensure that the specimen temperature was below the nil-ductility temperature. The specimens were loaded to failure at a high strain rate.

Several criteria were used for the selection of destructive testing specimens to be fractured. First, it was felt that film radiography provided a realistic determination of the position, size, and type of defect for porosity and slag inclusions. In the case of porosity, the fracture surface probably would not reveal all pores present unless they all happened to lie in the fracture plane. It was felt that the majority of the fracture specimens should have incomplete penetration and crack defects to determine how accurately these defects were detected by film radiography, and to provide a standard of comparison for the other techniques. Thus, a few samples were taken that contained porosity

and slag defects, with the majority of the specimens being taken to bracket suspected incomplete penetration and crack defects to determine their true location and size.

Some attempt was also made to select specimens in which one or another of the techniques provided strong indications of a defect that were not obtained by other techniques to determine which, if any, of the techniques were accurately detecting defects. A total of 22 specimens was selected and fractured in this manner.

The specimens were fractured, and the failure loads were recorded. A list of the failure loads for each of the specimens is shown in Table E-4.

The failure loads did not correlate well with the size of defect. The welds failed in a brittle manner and seemed to bear little relationship to the size of the flaw. In some cases, specimens with large flaws failed at higher loads than similar specimens with small flaws. Apparently the techniques used to ensure that the weld will fail in the weldment do not allow the determination of failure loads. Such determinations would have to be made above the nil-ductility temperature using other, less desirable methods of ensuring failure in the welds. These methods would be less desirable in terms of the amount of weld material exposed as a result of the fracturing.

## E. 7 INSPECTION RESULTS

The inspection results for the panel specimens are shown in Figures E-11 through E-23. The fracture testing results are shown in Figures E-24 through E-29. The inspection results for the pipe specimens are shown in Figures E-30 and E-31.

The figures show the defects detected by each technique for each of the nondestructive test specimens. The symbols used are P for porosity, S for slag inclusion, LP for incomplete or lack-of-penetration defects, and C for cracks. A line is used to indicate the general length over which porosity defects occurred. The welds are labeled with the letters A through E, corresponding to the specimen labels indicated in Figure 2-16.

Table E-4

FAILURE LOADS FOR FRACTURE TEST SPECIMENS

| Specimen No. | Failure Load (lb) | Specimen Thickness (in.) |
|---|---|---|
| 17-1 | 11,700 | 1 |
| 21-1 | 9,200 | 1 |
| 24-1 | 3,500 | 1/2 |
| 24-2 | 8,150 | 1/2 |
| 25-1 | 14,600 | 1 |
| 25-2 | 14,500 | 1 |
| 25-3 | 15,800 | 1 |
| 25-4 | 6,100 | 1 |
| 25-5 | 14,050 | 1 |
| 26-1 | 13,300 | 1-1/2 |
| 26-2 | 11,450 | 1-1/2 |
| 26-3 | 49,500 | 1-1/2 |
| 28-1 | 5,950 | 1 |
| 28-2 | 12,500 | 1 |
| 28-3 | 9,500 | 1 |
| 28-4 | 11,950 | 1 |
| 28-5 | 14,600 | 1 |
| 29-1 | 21,900 | 1-1/2 |
| 29-2 | 34,200 | 1-1/2 |
| 29-3 | 18,550 | 1-1/2 |
| 29-4 | 24,050 | 1-1/2 |
| 29-5 | 11,000 | 1-1/2 |

Rejectable defects are labeled with an R in parentheses. For the ultrasonic inspection results, indications above the ARL are indicated by the letter A. The location of the selected fracture specimens is indicated by short vertical lines spaced 3 in. apart.

The tabulated results are presented in Tables E-5 and E-6 for the panel specimens, Table E-7 for the fracture specimens, and Table E-8 for the pipe specimens. These tables list for each specimen the total weld length, the total defect indications for each technique, and the total common indications for x-ray (or fracture surface) and each technique.

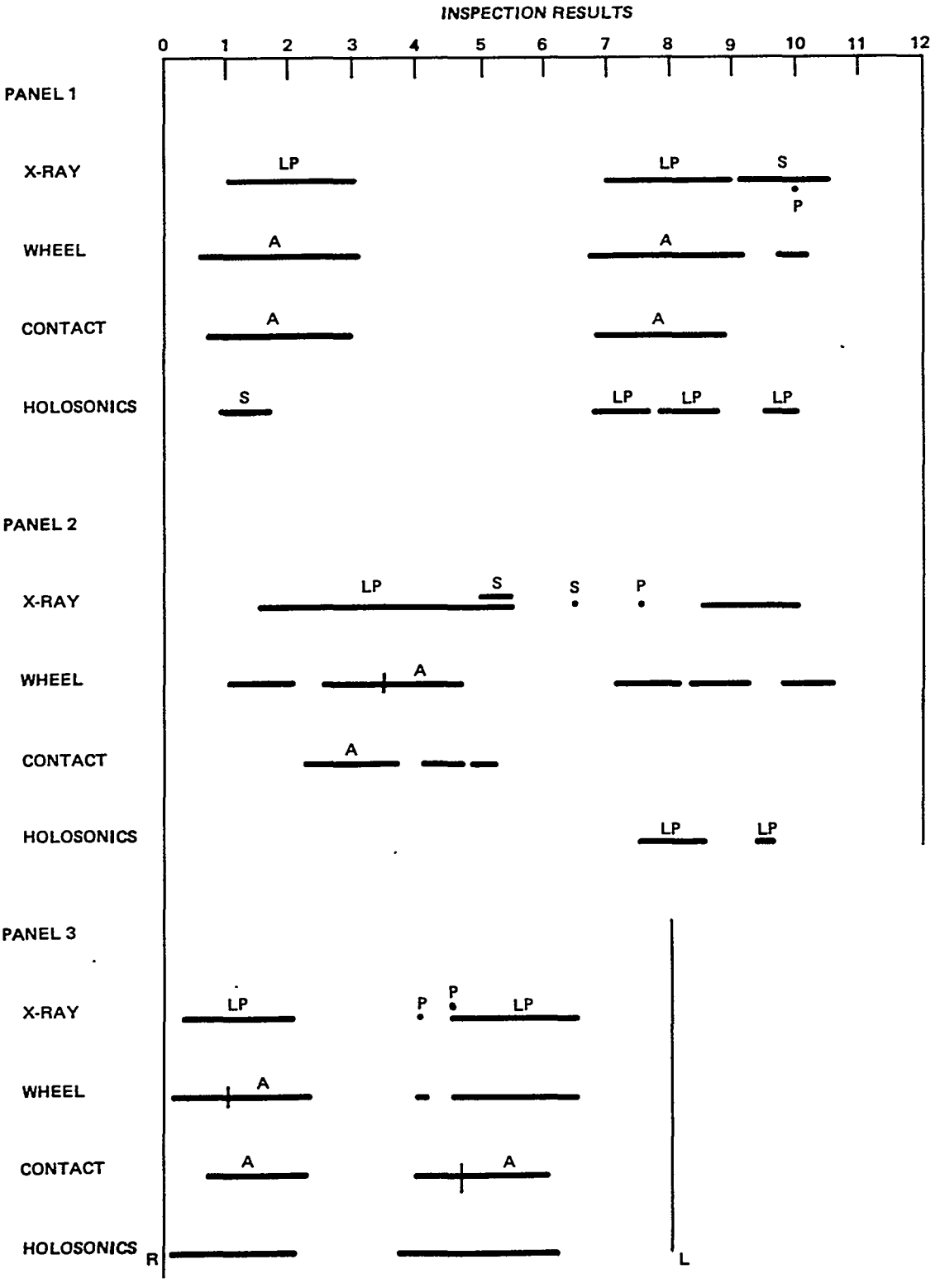


Figure E-11. Inspection Results for Panels 1, 2, and 3

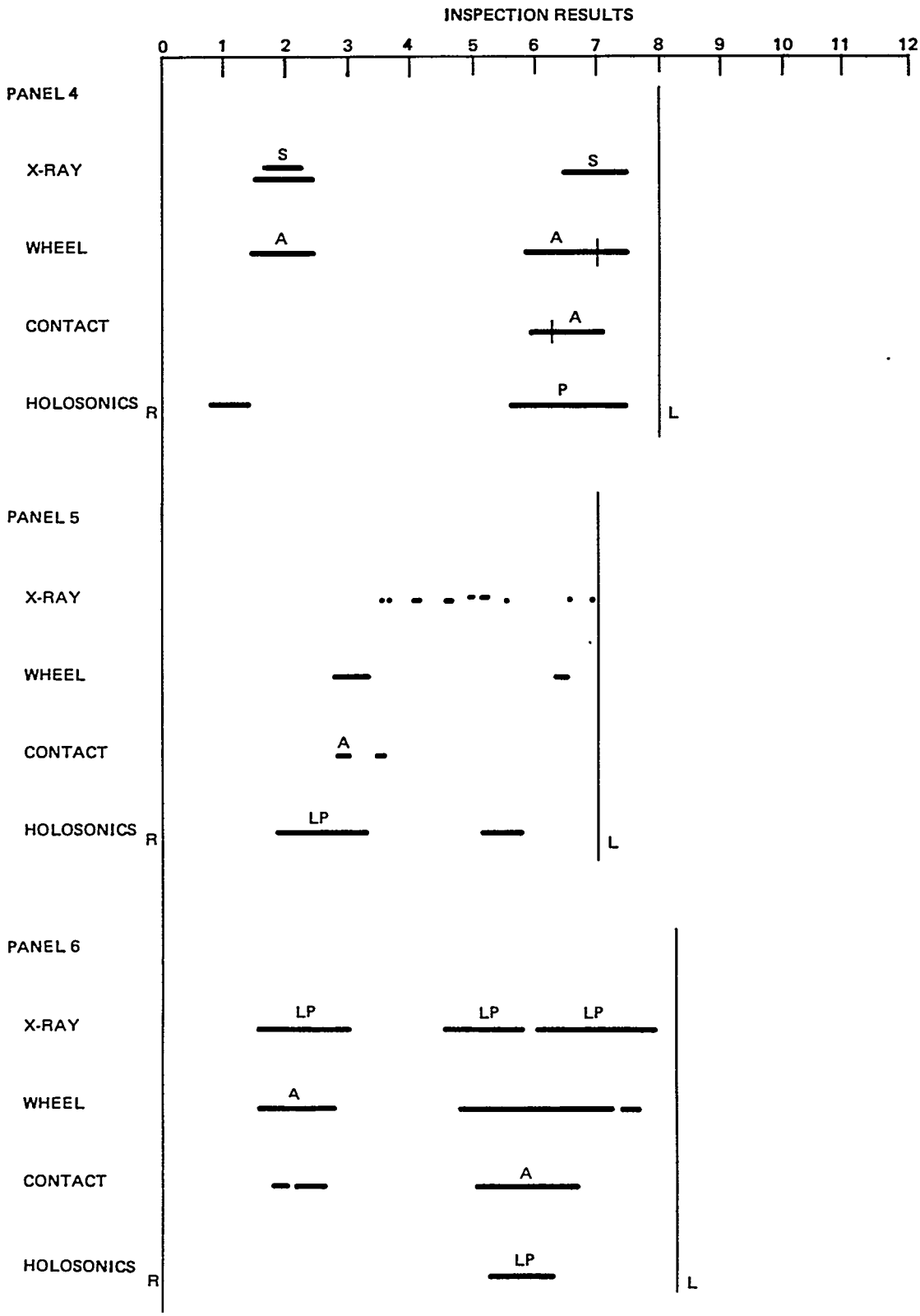


Figure E-12. Inspection Results for Panels 4, 5, and 6

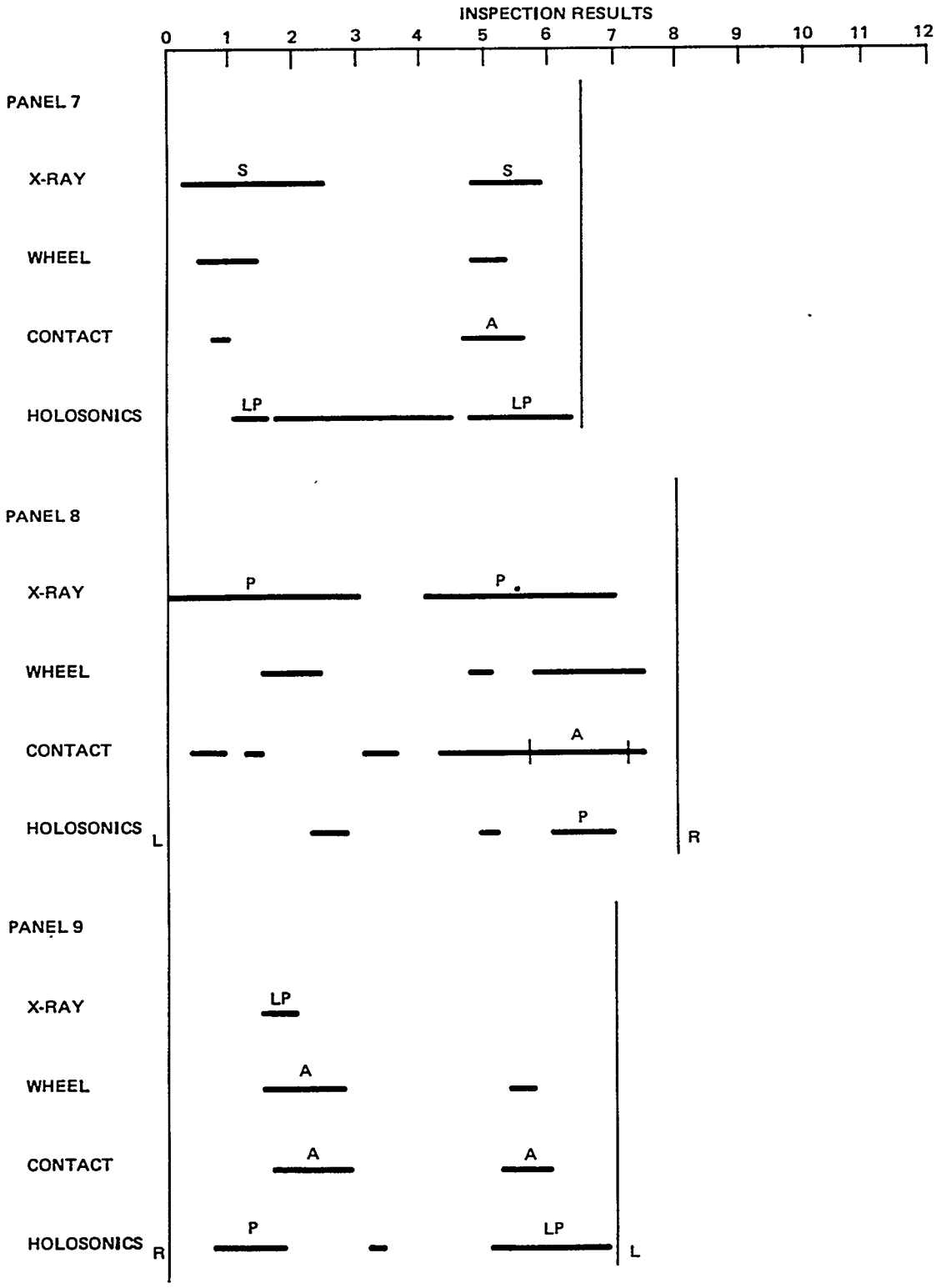


Figure E-13. Inspection Results for Panels 7, 8, and 9

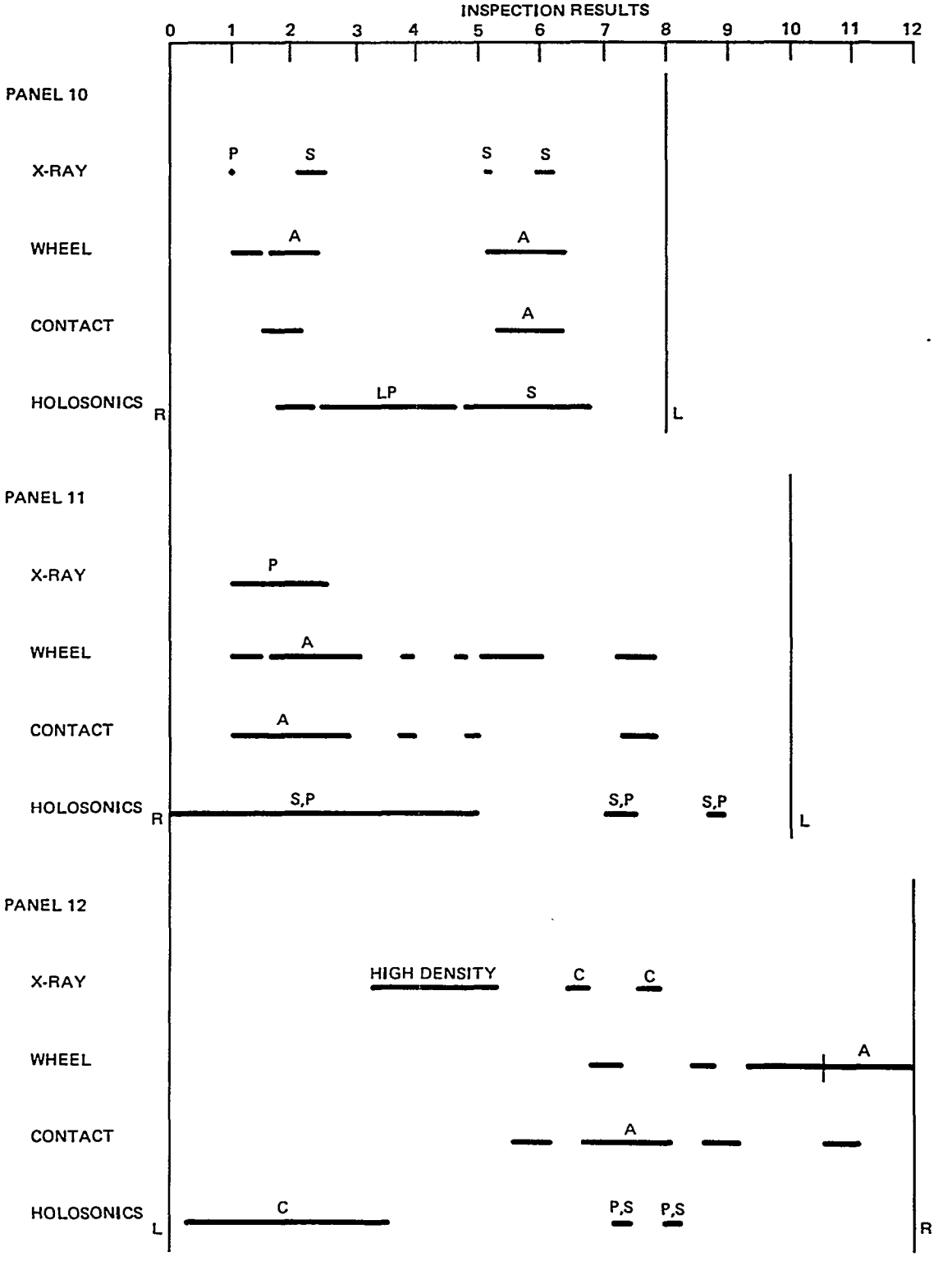


Figure E-14. Inspection Results for Panels 10, 11, and 12

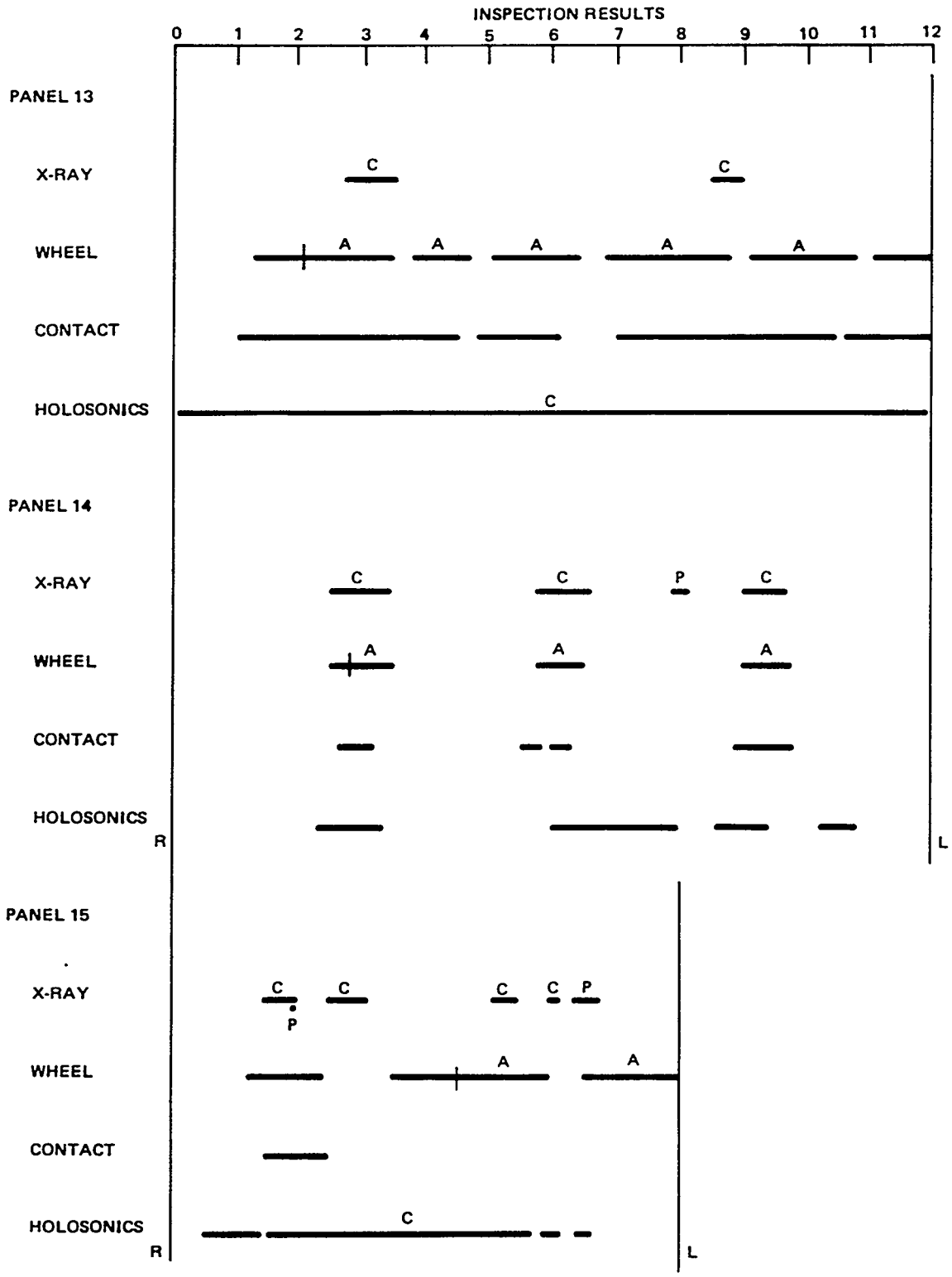


Figure E-15. Inspection Results for Panels 13, 14, and 15

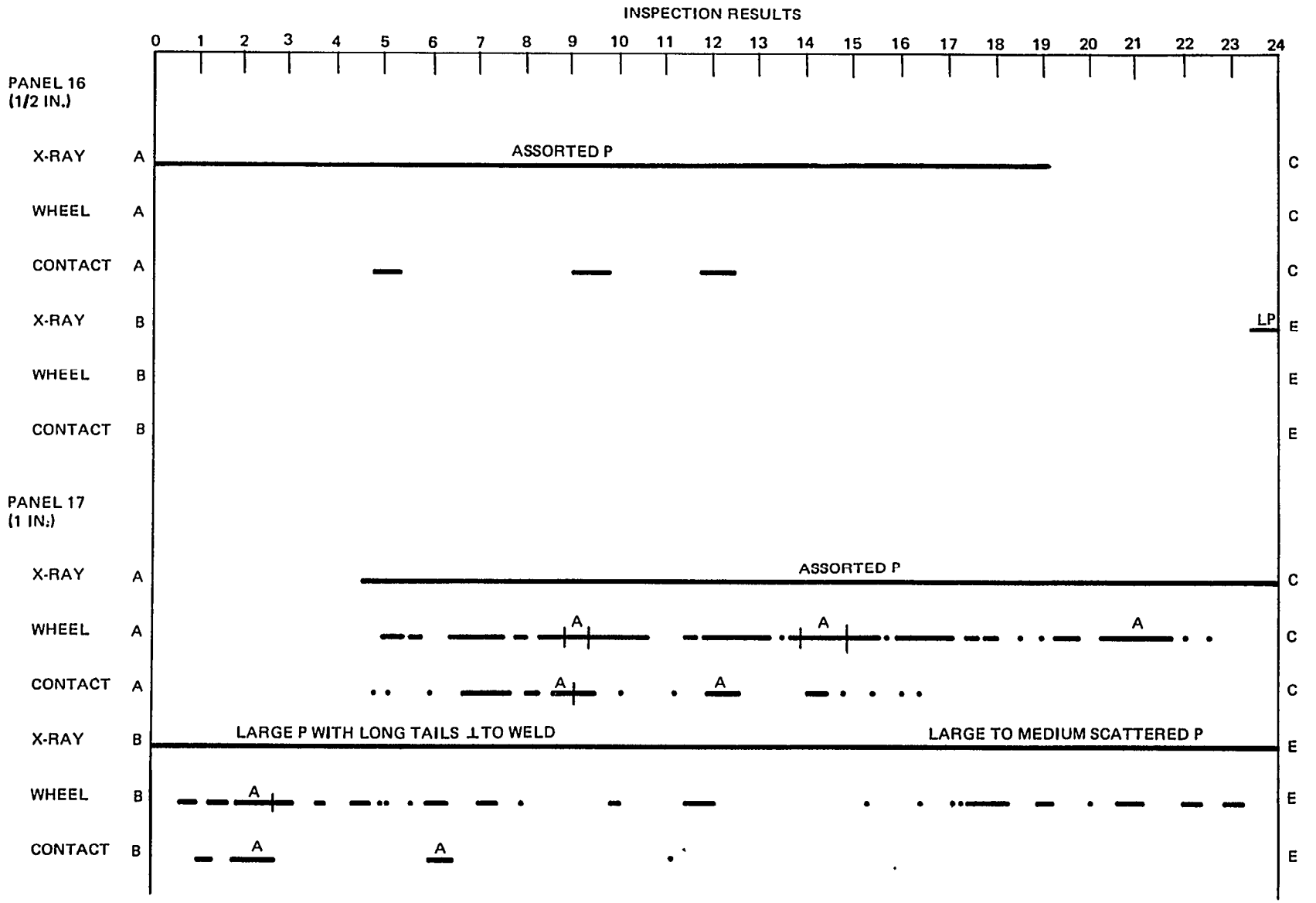


Figure E-16. Inspection Results for Panels 16 and 17

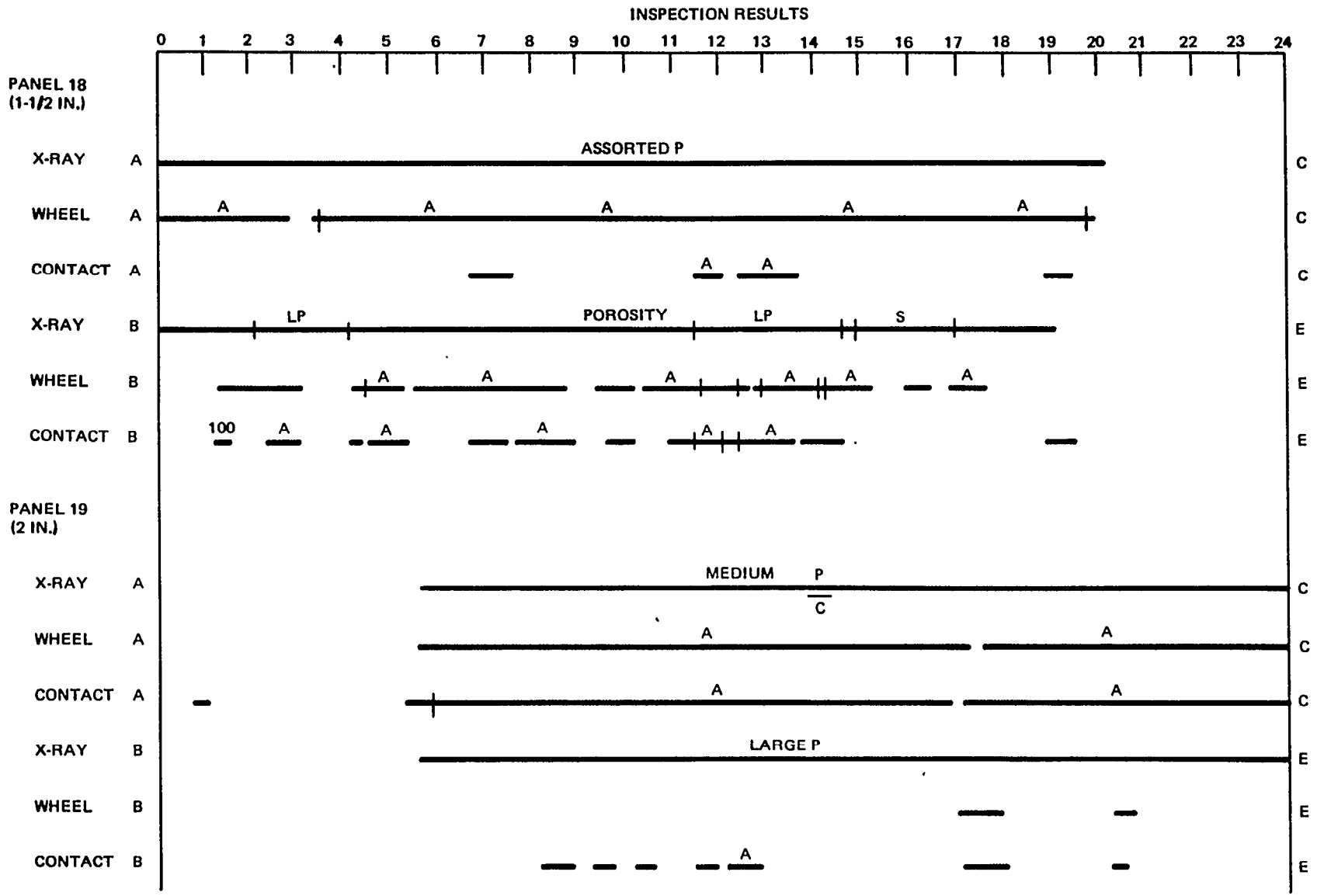


Figure E-17. Inspection Results for Panels 18 and 19

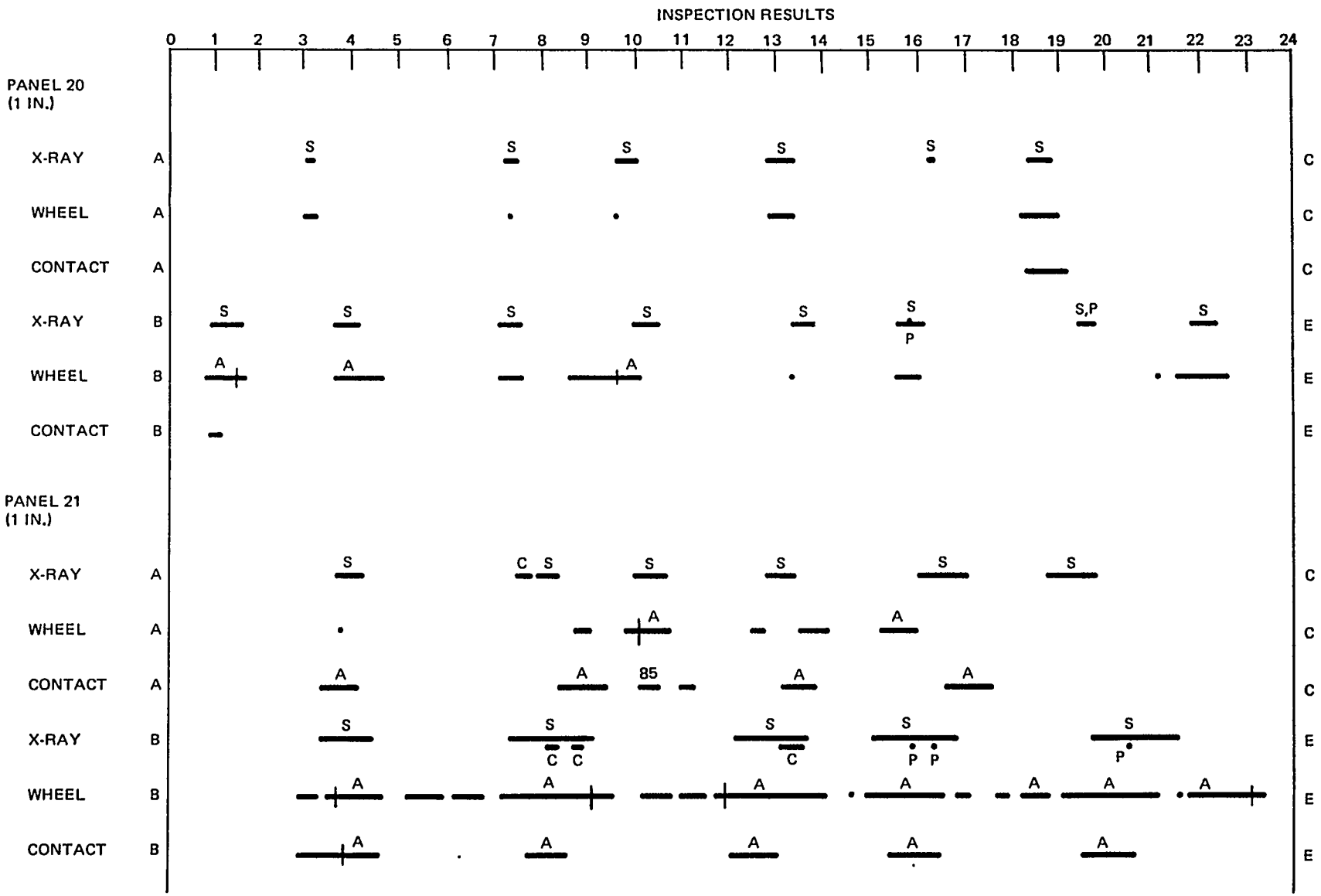


Figure E-18. Inspection Results for Panels 20 and 21

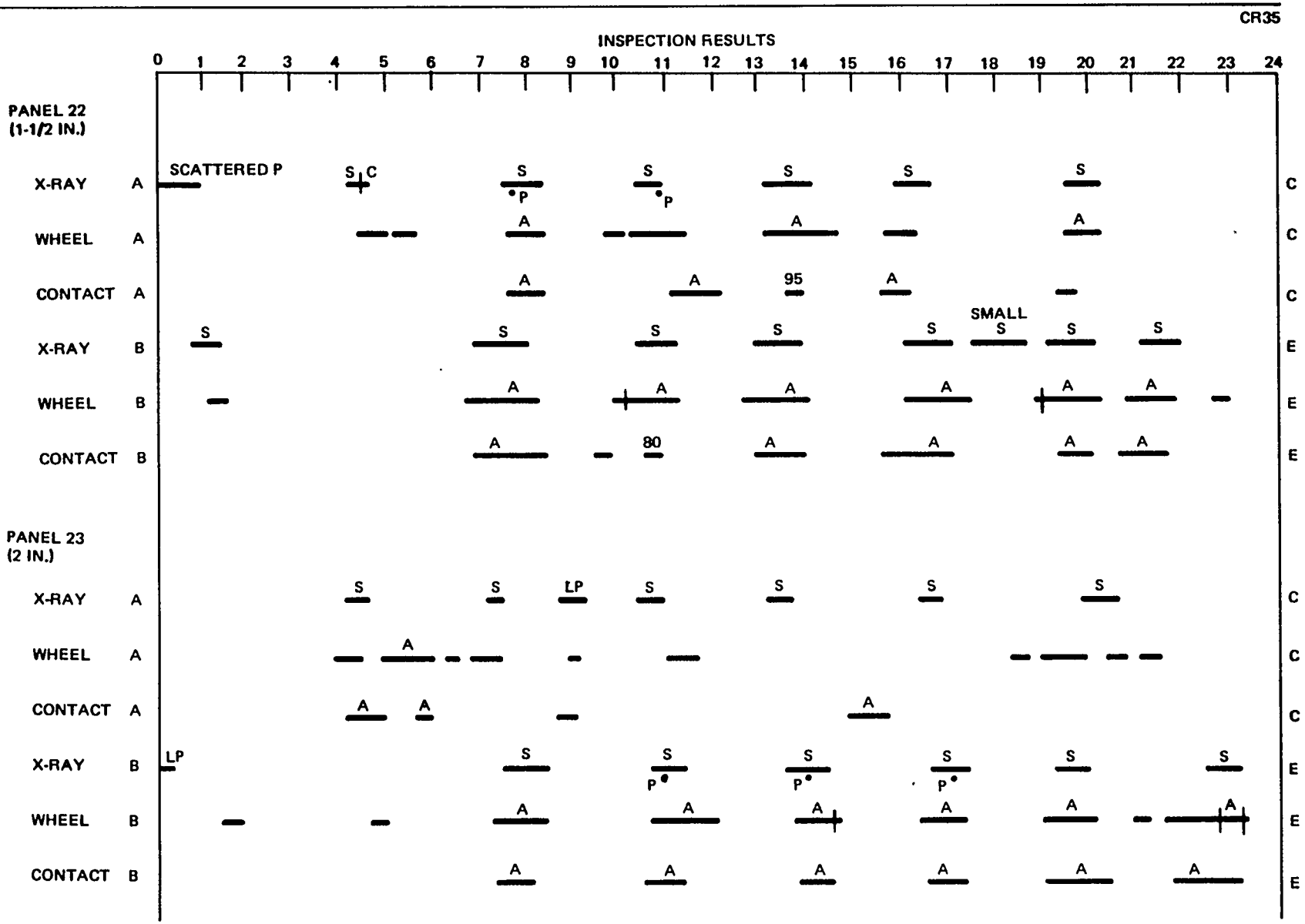


Figure E-19. Inspection Results for Panels 22 and 23

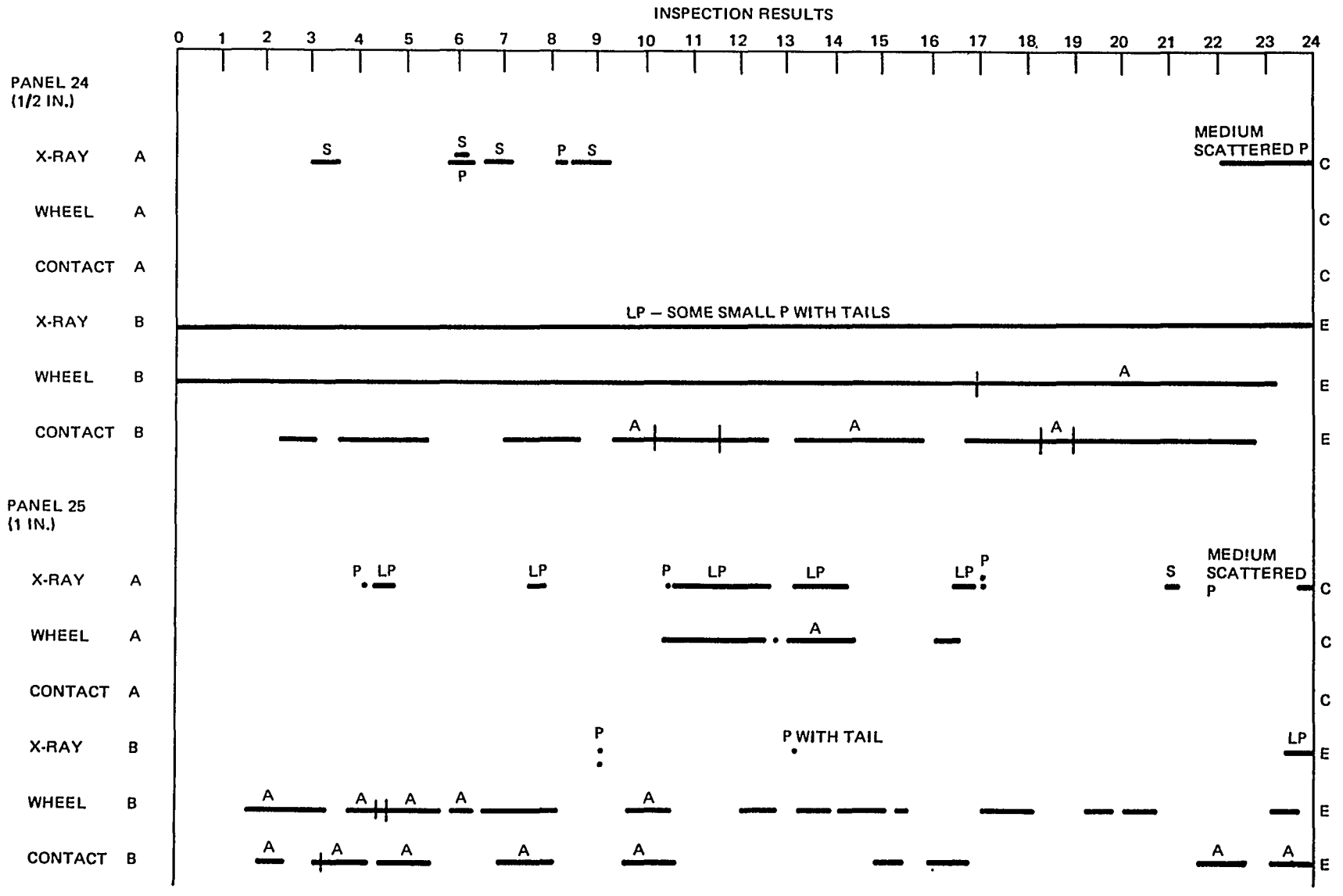


Figure E-20. Inspection Results for Panels 24 and 25

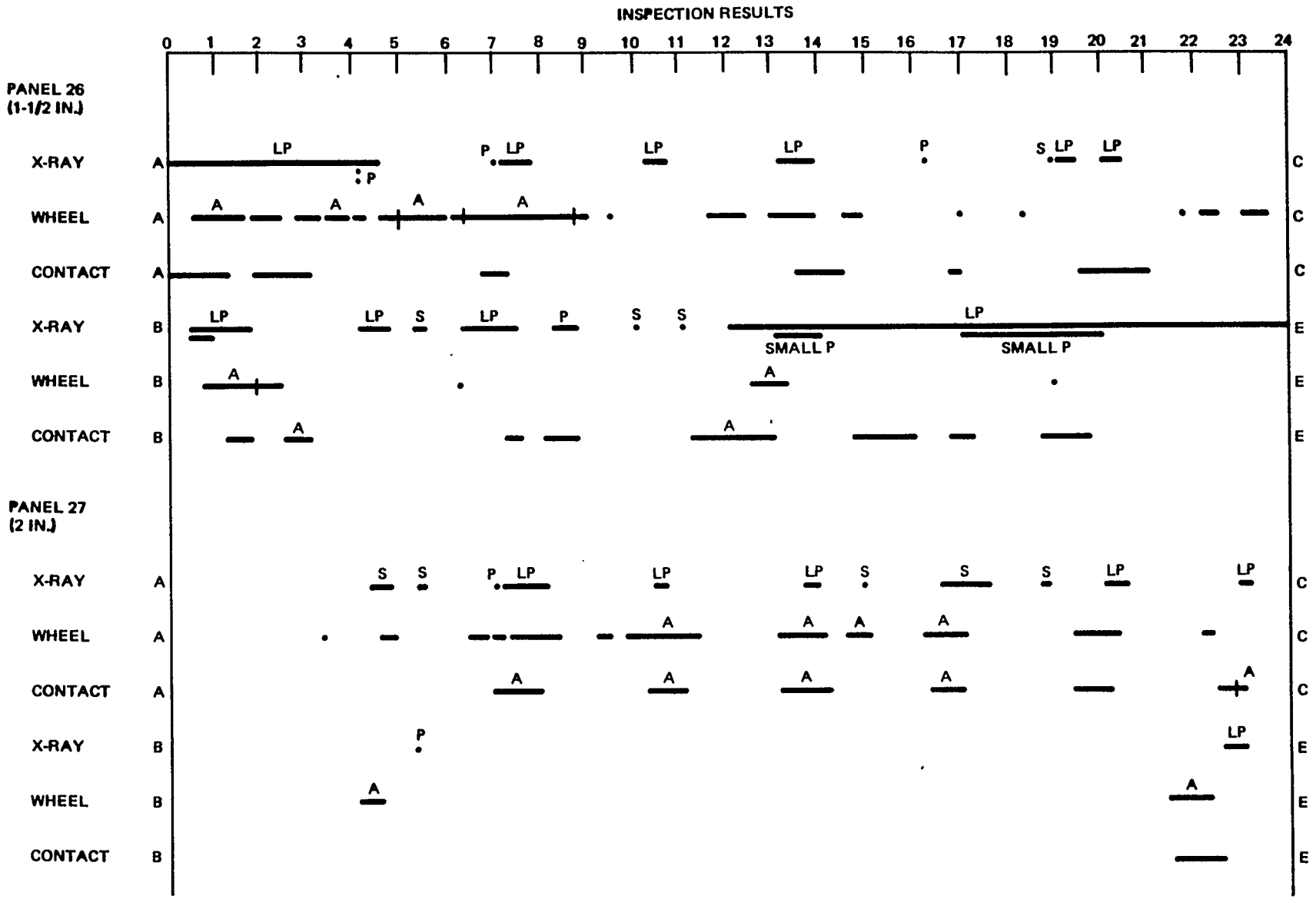


Figure E-21. Inspection Results for Panels 26 and 27

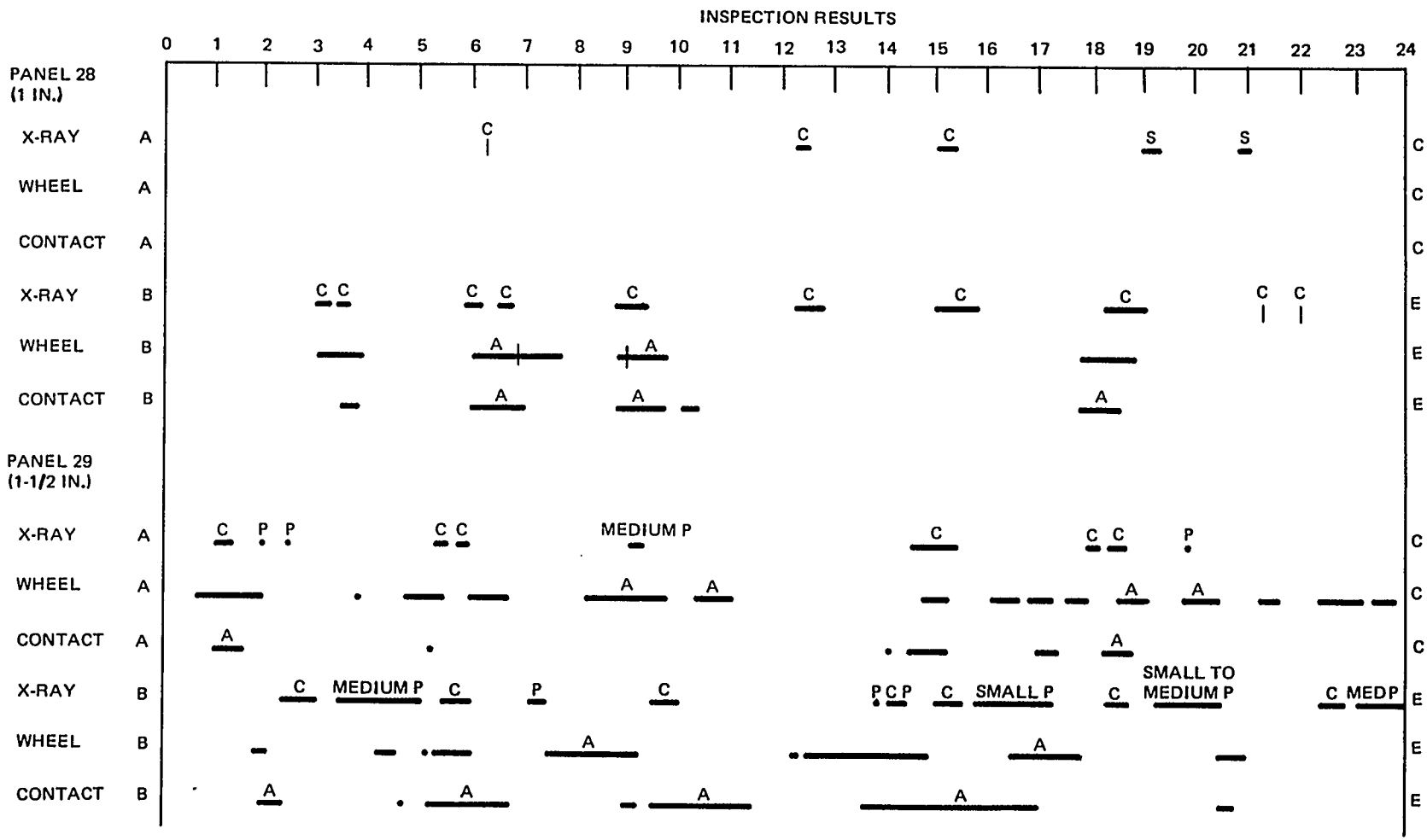


Figure E-22. Inspection Results for Panels 28 and 29

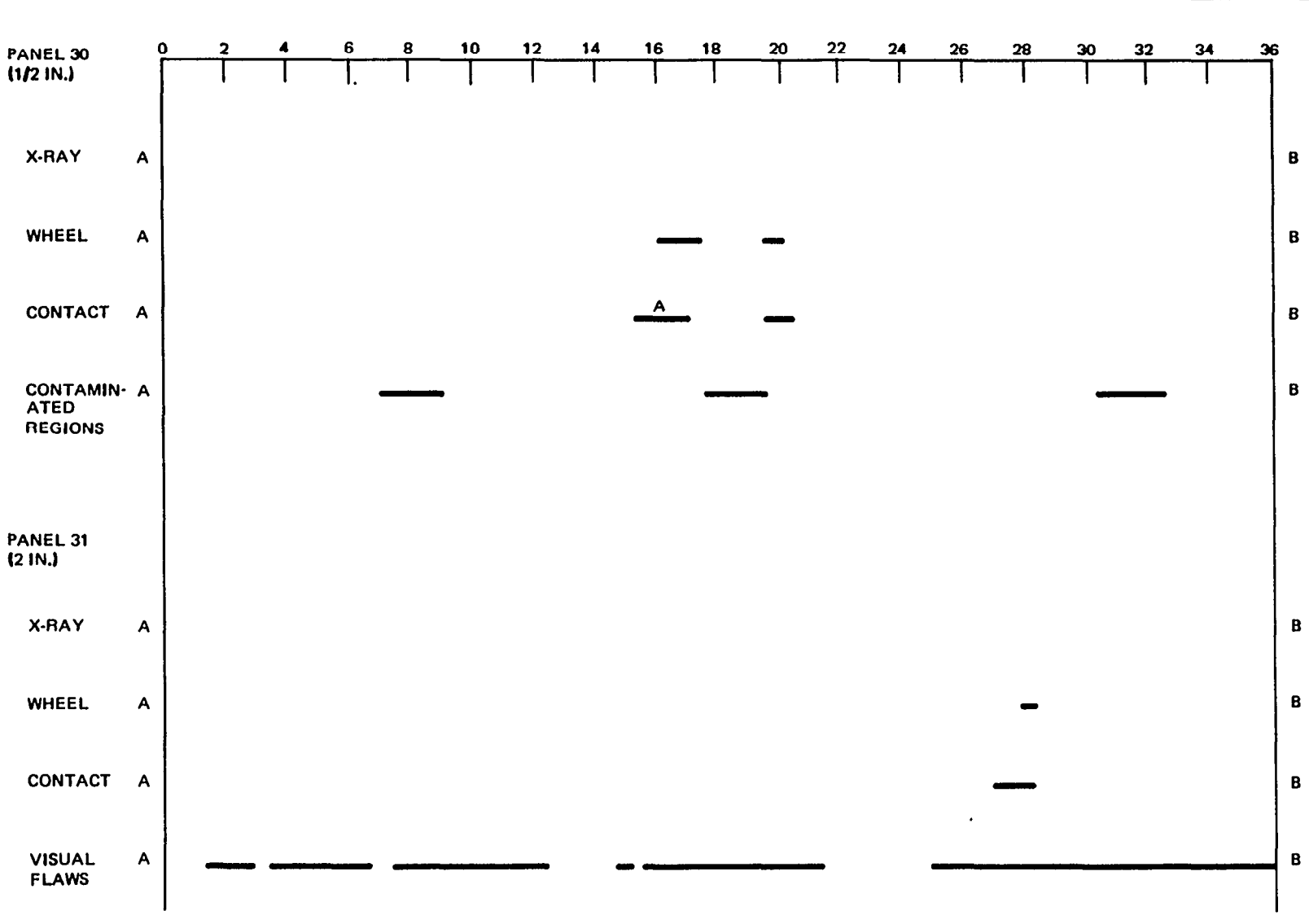


Figure E-23. Inspection Results for Panels 30 and 31

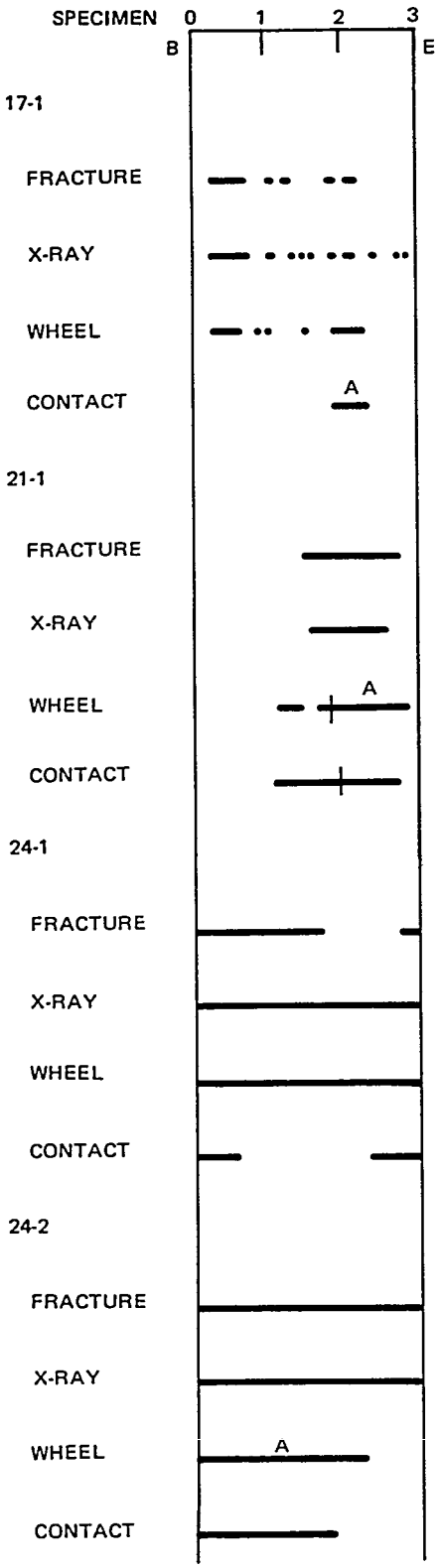


NOTES

1-IN-THICK SPECIMEN

POROSITY 3/4 IN., 1/4 IN., 1/4 IN., 3/4 IN., 3/4 IN. DEEP

POROSITY

3/4 IN., 1/2 IN., 1/4 IN., 5/8 IN., 3/4 IN. DEEP

3/4 IN. DEEP

1-IN.-THICK SPECIMEN

SLAG 1/2 IN. TO 7/8 IN. DEEP

SLAG

1 IN., 3/4 IN. TO 1 IN. DEEP

7/8 IN. TO 1 IN. DEEP

1/2-IN.-THICK SPECIMEN

INCOMPLETE PENETRATION 1/8 IN. WIDE, 1/4 IN. DEEP. INCOMPLETE PENETRATION PROBABLY OVER ENTIRE LENGTH, ALTHOUGH FRACTURE AVOIDED DEFECT.

INCOMPLETE PENETRATION

1/4 IN. DEEP

1/4 IN. DEEP

1/2-IN.-THICK SPECIMEN

INCOMPLETE PENETRATION 1/16 IN. WIDE, 1/4 IN. DEEP

1/4 IN. DEEP

1/4 IN. DEEP

Figure E-24. Fracture Results, Specimens 17-1, 21-1, 24-1, and 24-2

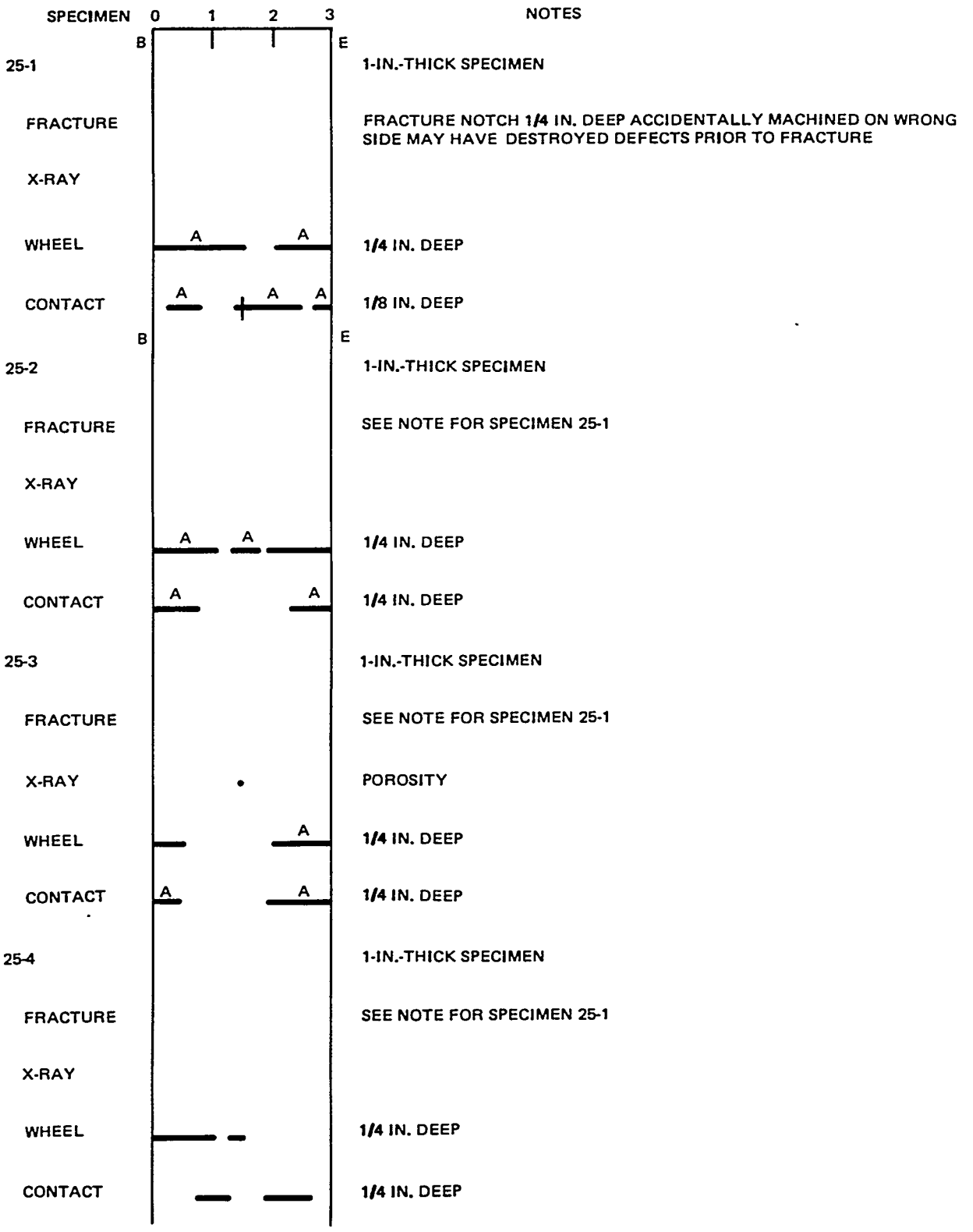


Figure E-25. Fracture Results, Specimens 25-1, 25-2, 25-3, and 25-4

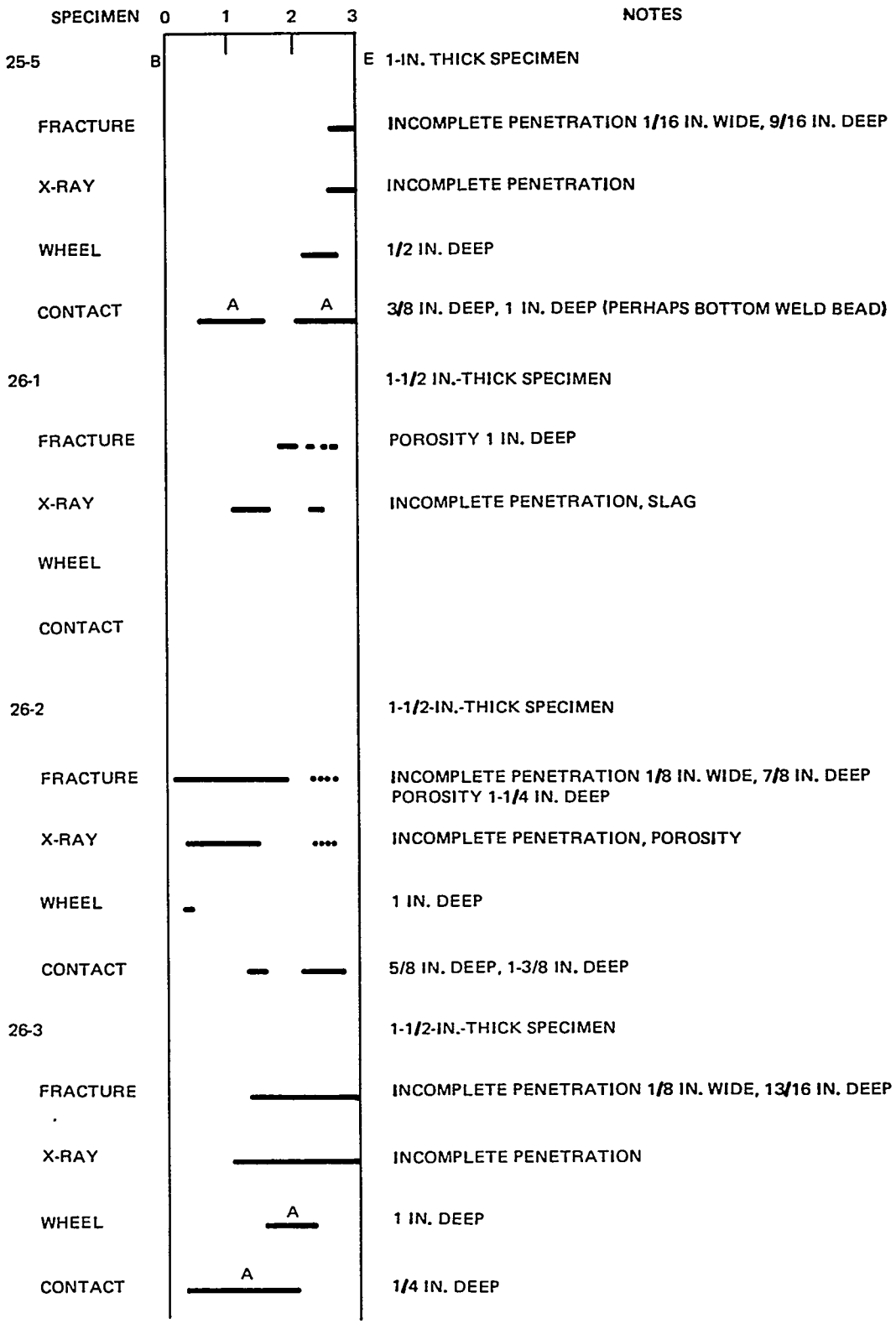


Figure E-26. Fracture Results, Specimens 25-5, 26-1, 26-2, and 26-3

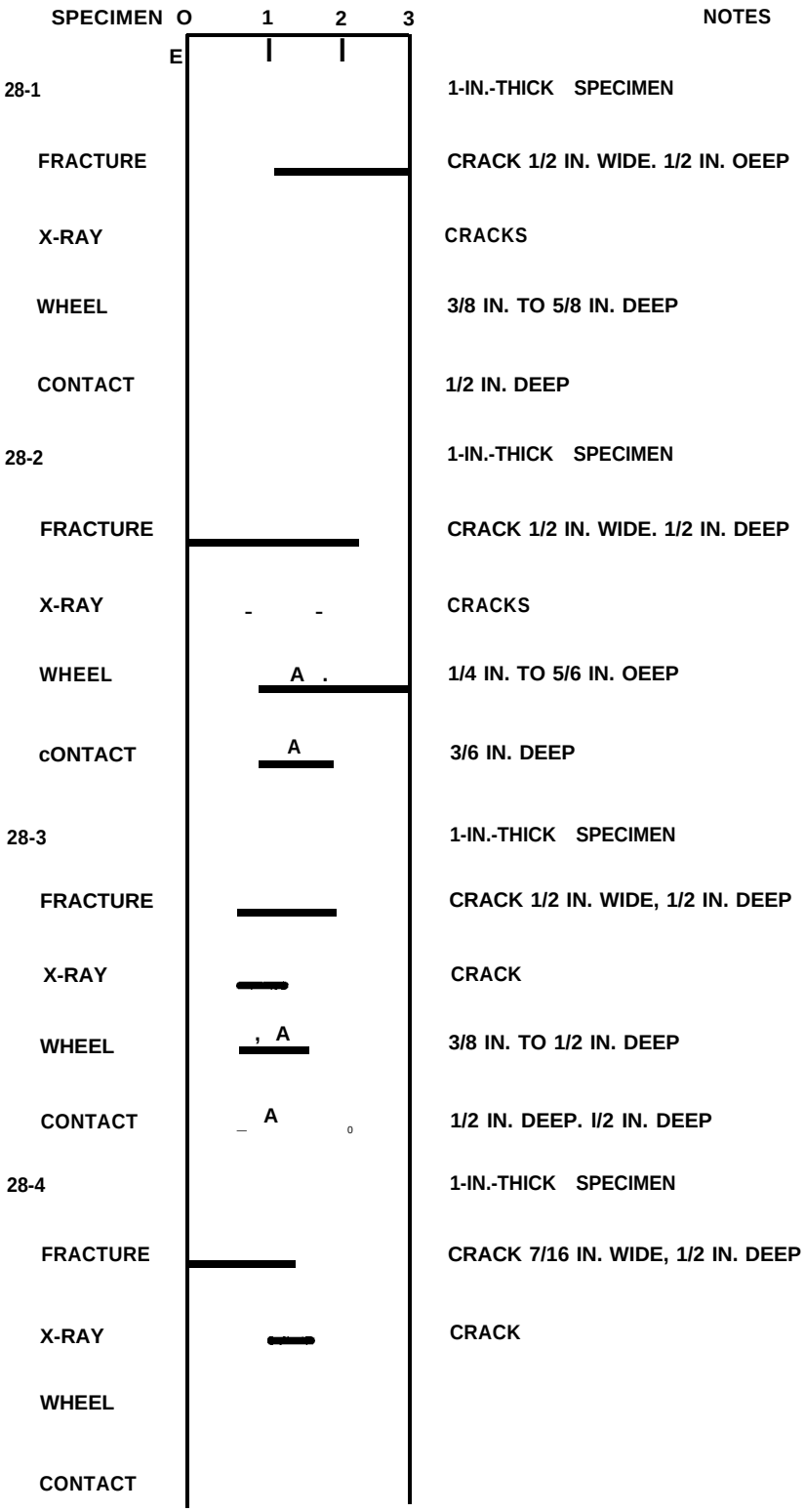


**Figure E-27. Fracture Results. Specimens 28-1.28-2,28-3, and 28-4**

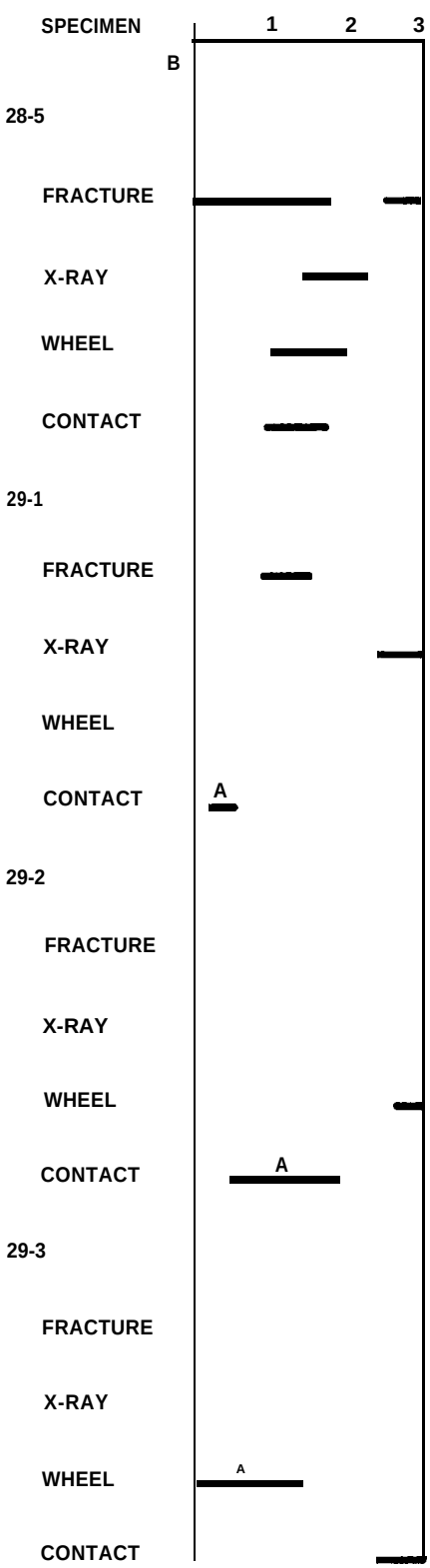


NOTES

1-IN.-THICKSPECIMEN

CRACK 1/2 IN. WIDE, 112 IN. DEERCRACK 1/8 IN. WIDE, 1/2 IN. DEEP

CRACK

112 IN. DEEP

5/8 IN. DEEP

1-1/2 IN.-TH1CK SPECIMEN

CRACK 1/16 IN. WIDE, 3/4 IN. DEEP

CRACK, POROSITY

1/4 IN. DEEP, 1/8 IN. DEEP (REMOVED BY FRACTURE NOTCH)

1/8 IN. DEEP, 1 IN. DEEP

1-1/2 IN.-THICK SPECIMEN

CRACK, POROSITY

1/8 IN. DEEP, 7/8 IN. DEEP

1/8 IN. DEEP (REMOVED BY FRACTURE NOTCH)

1-1/2 IN.-THICK SPECIMEN

CRACK 1/4 IN. WIDE, 1-1/8 IN. DEEP

CRACK

1-1/4 IN. DEEP

1/8 IN. DEEP (REMOVED BY FRACTURE NOTCH)

**Figure E-28. Fracture Results, Specimens 28-5,29-1,29-2, and 29-3**

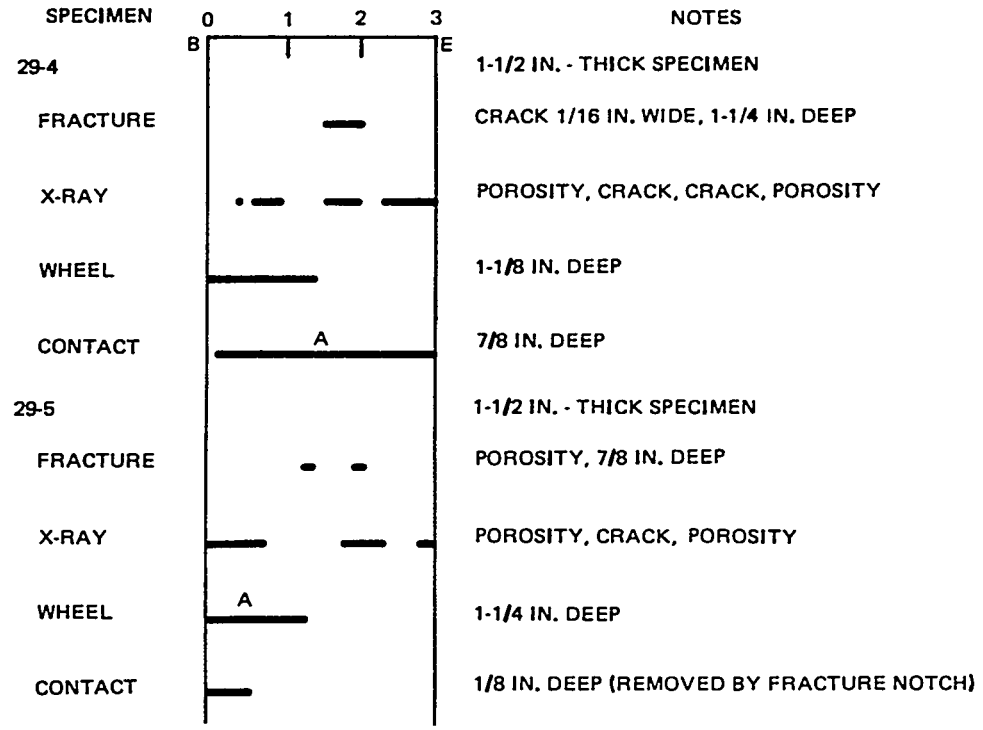


Figure E-29. Fracture Results, Specimens 29-4 and 29-5



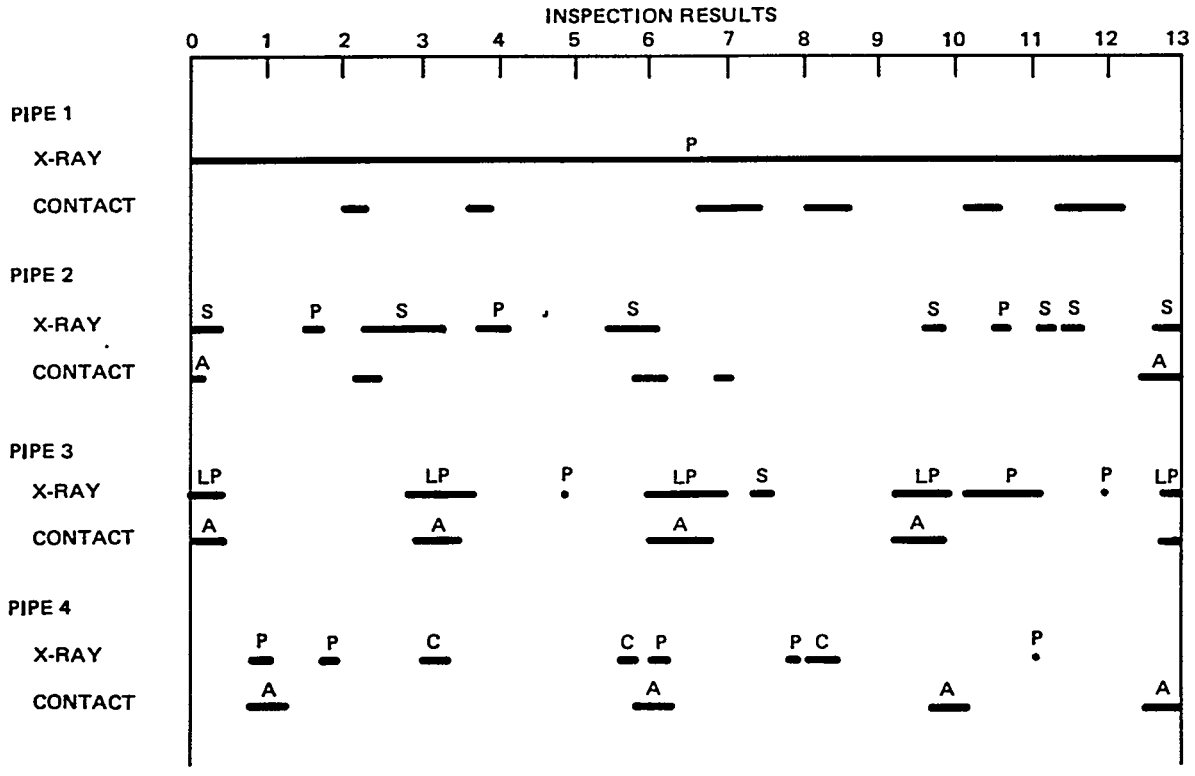


Figure E-30. Inspection Results, Pipes 1 Through 4

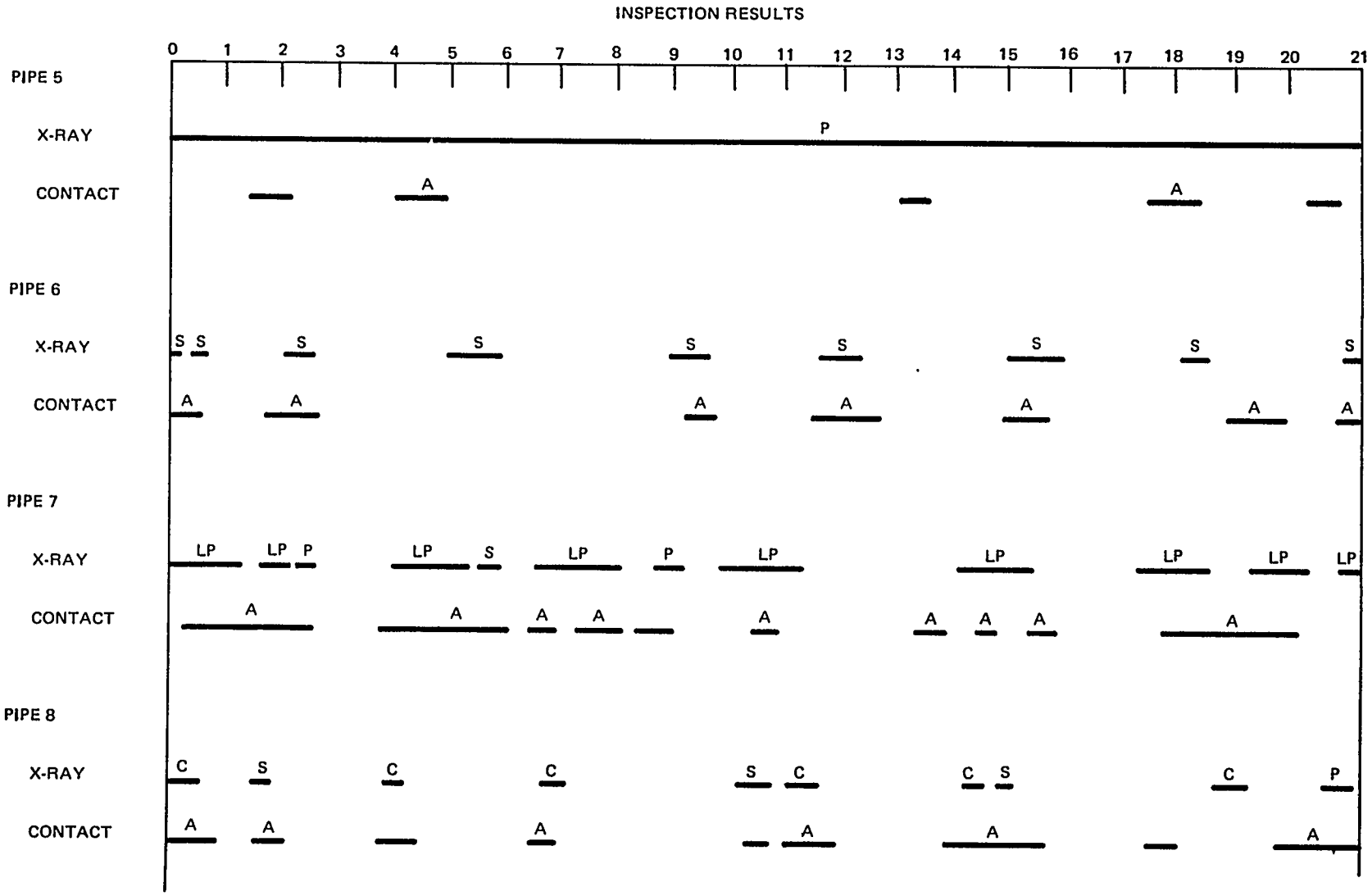


Figure E-31. Inspection Results, Pipes 5 Through 8

Table E-5

REJECTED DEFECTS BY TECHNIQUE FOR SPECIMENS 1 THROUGH 15

| Specimen No. | Total Length (in.) | X-Ray Reiected (in.) | Wheel Rejected (in.) | Contact Rejected (in.) | Holosonics Reiected (in,) | X-Ray and Wheel (in.) | X-Ray and Contact (in.) | X-Ray and Holosonics (in.) |
|---|---|---|---|---|---|---|---|---|
| 1 | 12 | 5-1/2 | 5-1/2 | 4-1/4 | 3 | 4-5/8 | 3-7/8 | 2-5/8 |
| 2 | 12 | 5-3/4 | 5-7/8 | 2-5/8 | 1-3/8 | 3-7/8 | 2-5/8 | 3/8 |
| 3 | 8 | 4 | 4-3/8 | 3-3/8 | 4-5/8 | 3-7/8 | 3 | 3-5/8 |
| 4 | 8 | 2 | 2-5/8 | 1-1/8 | 2-1/2 | 2 | 1/2 | 7/8 |
| 5 | 7 | 3/4 | 0 | 0 | 2-1/4 | 0 | 0 | l/8 |
| 6 | 8-1/4 | 4-5/8 | 4-1)8 | 2-3/4 | 1-3/8 | 3-7/8 | 2-1/2 | 1-1/8 |
| 7 | 6-1/2 | 3-1/8 | 0 | 1-1/8 | 4-3/4 | 0 | 7/8 | 2-1/8 |
| 8 | 8 | 6 | 3-1/8 | 4-5/8 | 1-3/4 | 2-5/8 | 3-5/8 | 1-3/4 |
| 9 | 7 | 0 | 1-3/8 | 2-1/8 | 3-1/4 | 0 | 0 | 0 |
| 10 | 8 | 1-1/8 | 2-1/2 | 1 | 3 | 1 | 3/8 | 1 |
| 11 | 10 | 1-1/2 | 3-7/8 | 2-7/8 | 5-3/4 | 1-3/8 | 1-1/2 | 1-1/2 |
| 12 | 12 | 7/8 | 3-5/8 | 3-1/4 | 3-7/8 | 0 | 3/8 | 0 |
| 13 | 12 | 1-3/8 | 9 | 9-3/4 | 11-3/4 | 1 | 1-3/8 | 1-3/8 |
| 14 | 12 | 2-1/2 | 2-1/2 | 0 | 4-1/4 | 2-3/8 | 0 | 1-3/4 |
| 15 | 8 | 2-1/8 | 5-1/4 | 0 | 3-5/8 | 1-1/4 | 0 | 1-7/8 |
| Total | 138-3/4 | 41-1/4 | 53-3/4 | 39-1/8 | 60-3/4 | 27-7/8 | 20-7/8 | 20-1/8 |

Table E-6

REJECTED DEFECTS BY TECHNIQUE FOR SPECIMENS 16 THROUGH 31

| Specimen No. | Total Length (in.) | X-Ray Rejected (in.) | Wheel Rejected (in.) | Contact Rejected | X-Ray and Wheel (in.) | X-Ray and Contact (in.) |
|---|---|---|---|---|---|---|
| 16AC | 24 | 19 | 0 | 2 | 0 | 2 |
| 16BE | 24 | 1/2 | 0 | 0 | 0 | 0 |
| 17AC | 24 | 19-1/2 | 12-1/2 | 3-1/2 | 12-1/2 | 3-1/2 |
| 17BE | 24 | 24 | 6-3/4 | 1 - 3 / 4 | 6-3/4 | 1-3/4 |
| 18AC | 24 | 20 | 19-1/2 | 1-7/8 | 19-1/2 | 1-7/8 |
| 18BE | 24 | 19 | 12-7/8 | 8-1/4 | 12-7/8 | 8-1/4 |
| 19AC | 24 | 18-1/2 | 18-1/8 | 18-3/8 | 18-1/8 | 18-1/8 |
| 19BE | 24 | 18-1/2 | 0 | 2-1/2 | 0 | 2-1/2 |
| 20AC | 24 | 2-1/8 | 1-5/8 | 0 | 1-1/8 | 0 |
| 20BE | 24 | 4 | 5 | 0 | 2-3/8 | 0 |
| 21AC | 24 | 5 | 2-7/8 | 4-1/4 | 3/4 | 1.3/4 |
| 21BE | 24 | 8-1/8 | 16-1/8 | 5-3/4 | 7-1/2 | 4-3/4 |
| 22AC | 24 | 5-1/4 | 6-1/2 | 2-1/2 | 4 | 1-1/8 |
| 22BE | 24 | 7-1/8 | 8-5/8 | 6-1/8 | 6 | 4-5/8 |
| 23AC | 24 | 9-1/2 | 2-3/4 | 1-5/8 | 2-1/4 | 1/2 |
| 23BE | 24 | 5-1/8 | 8 | 5-7/8 | 4-1/2 | 3-3/4 |
| 24AC | 24 | 4-5/8 | 0 | 0 | 0 | 0 |
| 24 BE | 24 | 24 | 23-3/4 | 16 | 23-3/4 | 16 |
| 25AC | 24 | 4-5/8 | 4-1/8 | 0 | 3-3/8 | 0 |
| 2513E | 24 | 1/2 | 12 | 6-7/8 | 1/4 | 1/2 |
| 26AC | 24 | 7-5/8 | 8-5/8 | 2-1/2 | 4-1/2 | 2-1/2 |
| 26BE | 24 | 17 | 2-1/2 | 6-3/8 | 1-7/8 | 4-1/2 |
| 27AC | 24 | 3-1/2 | 6-7/8 | 2-1/2 | 2-1/4 | 1 |
| 27BE | 24 | 1/2 | 1-1/2 | 0 | 0 | 0 |
| 28AC | 24 | 1/2 | 0 | 0 | 0 | 0 |
| 28BE | 24 | 8-3/4 | 3-3/4 | 3-1/4 | 3-1/4 | 2-5/8 |
| 29AC | 24 | 2-1/2 | 9-3/4 | 1-1/8 | 1-5/8 | 5/8 |
| 29BE | 24 | 9-5/8 | 6-5/8 | 8 | 2-1/8 | 3-1/4 |
| 30AB | 36 | 0 | 0 | 1-3/8 | 0 | 0 |
| 31AB | 36 | 0 | 0 | 0 | 0 | 0 |
| Total | 744 | 269 | 200-3/4 | 112-3/8 | 141-1/4 | 85-1/2 |

Table E-7

DETECTED DEFECTS FOR FRACTURE SPECIMENS

| Specimen NO. | Fracture (in.) | X-Ray (in.) | Wheel (in.) | Contact (in.) | Fracture and X-Ray (in.) | Fracture and Wheel (in.) | Fracture and Contact (in.) |
|---|---|---|---|---|---|---|---|
| 17-1 | 1 | 1-3/8 | 1-1/8 | 1/2 | 7/8 | 7/8 | 3/8 |
| 21-1 | 1-1/4 | 1 | 1-5/8 | 1-5/8 | 1 | 1-1/8 | 1-1/4 |
| 24-1 | 3 | 3 | 3 | 1-1/4 | 3 | 3 | 1-1/4 |
| 24-2 | 3 | 3 | 2-1/4 | 1-7/8 | 3 | 2-1/4 | 1-7/8 |
| 25-5 | 3/8 | 1/2 | 5/8 | 2 | 3/8 | 1/8 | 3/8 |
| 26-1 | 1/2 | 3/4 | 0 | 0 | 0 | 0 | 0 |
| 26-2 | 2-1/8 | 1-3/8 | 1/8 | 1 | 1-3/8 | 1/8 | 1/2 |
| 26-3 | 1-3/4 | 2 | 3/4 | 1-3/4 | 1-3/4 | 3/4 | 3/4 |
| 28-1 | 1-3/8 | 1/2 | 7/8 | 1/4 | 3/8 | 3/4 | 1/4 |
| 28-2 | 2-1/4 | 5/8 | 1-3/4 | 1 | 5/8 | 1-3/8 | 1 |
| 28-3 | 1-3/8 | 5/8 | 1 | 1-1/4 | 5/8 | 1 | 1 |
| 28-4 | 1-1/2 | 1/2 | 0 | 0 | 3/8 | 0 | 0 |
| 28-5 | 2-1/8 | 3/4 | 1 | 3/4 | 1/4 | 5/8 | 3/4 |
| 29-1 | 1/2 | 2 | 0 | 1/4 | 1/4 | 0 | 0 |
| 29-3 | 5/8 | 1/2 | 1-3/8 | 0 | 3/8 | 0 | 0 |
| 29-4 | 1/2 | 1-3/4 | 1-3/8 | 2-7/8 | 1/2 | 0 | 1/2 |
| 29-5 | 1/4 | 1-1/2 | 1-1/4 | 5/8 | 1/8 | 1/8 | 0 |
| Total | 23-1/2 | 21-3/4 | 18-1/8 | 17 | 14-7/8 | 12-1/8 | 9-7/8 |

**Table E-8**

**REJECTED DEFECTS BY TECHNIQUE FOR PIPE SPECIMENS**

| Specimen No. | Total Length (in.) | X-Ray Detected (in.) | Contact Detected (in.) | X-Ray and Contact (in.) |
|---|---|---|---|---|
| 1 | 13 | 13 | 3-1/2 | 3-1/2 |
| 2 | 13 | 4-1/4 | 1-7/8 | 1-1/4 |
| 3 | 13 | 4-3/4 | 3 | 2-7/8 |
| 4 | 13 | 2 | 2 | 1/2 |
| 5 | 21-1/4 | 21-1/4 | 3-3/4 | 3-3/4 |
| 6 | 21-1/4 | 5-5/8 | 5-3/8 | 3-1/4 |
| 7 | 21-1/4 | 11-3/8 | 10-5/8 | 3-5/8 |
| 8 | 21-1/4 | 4-5/8 | 7-1/2 | 3-5/8 |
| Total | 137 | 66-7/8 | 37-5/8 | 22-3/8 |

## Appendix F
## AUTOMATED ULTRASONIC INSPECTION SYSTEM

As a result of this program, it was recommended that an automated inspection system employing the liquid-filled wheel be developed. This appendix describes the features and advantages of such a system.

The ABS currently recognizes contact ultrasonic inspection, but film radiography is often favored by the shipyards because it is well understood and furnishes a permanent record. Current manual ultrasonic procedures require a highly skilled operator performing visual data interpretation and manual recording while conducting the inspection. Subsequently, accept-reject decisions are made according to established ABS specifications. This rather complex procedure could be considerably simplified by employing the liquid - filled wheel as part of an automated inspection system that would:

A. Eliminate the need for a skilled operator.
B. Automatically interpret the received signal.
c. Determine position and length of flaw.
D. Apply accept-reject criteria.
E. Provide a permanent inspection report.
F. Significantly increase inspection speed.

The proposed prototype automated shear-wave inspection system would include the liquid - filled wheel, a fixture to adapt the wheel for shipyard inspection, signal-processing electronics, and associated software. A conceptual drawing of the system being applied in shipyard inspection is shown in Figure G-1.

The wheel fixture would ensure proper alignment of the wheel with respect to the panel and weld being inspected. The fixture would be portable and easily operated by unskilled labor. It could either be used manually, requiring human interpretation of the ultrasonic signals, or as part of an automated inspection system.

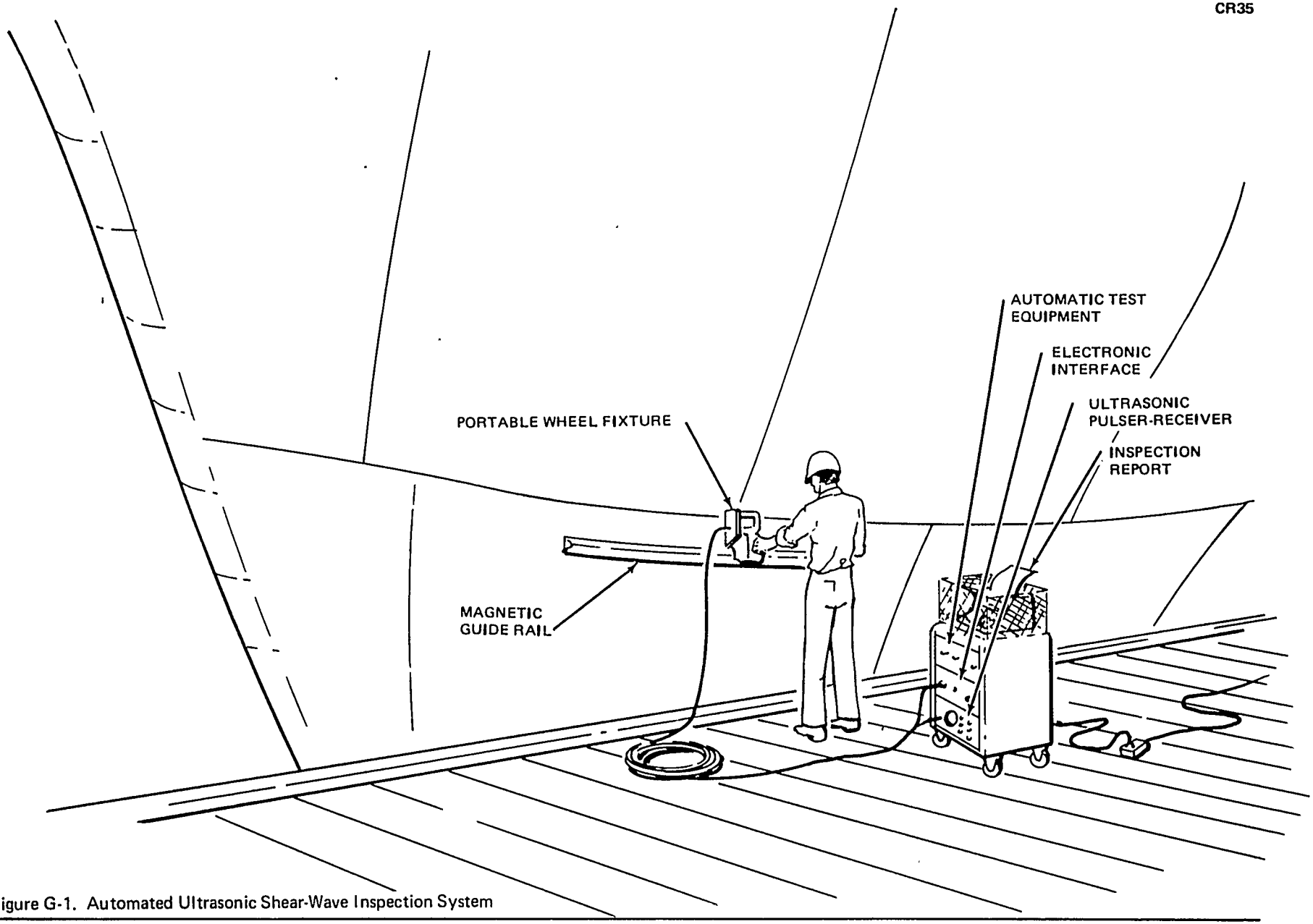


Figure G-1. Automated Ultrasonic Shear-Wave Inspection System

The hardware interface would convert analog wheel position and ultrasonic received - signal-versus - time information to digital values that could be processed by the minicomputer. The system would perform data acquisition, signal processing, analysis, and permanent recording. The system would eliminate the time required for human interpretation, and ins pection would be accomplished at about 1 ft of weld per minute. This rate would require that the operator roll the wheel at about 1 ft/ sec once the fixture has been properly positioned. The higher rate would be for longer lengths of weld, which would require proportionately less setup time for the length of weld being inspected. The system should be capable of even greater inspection rates with high-speed fixturing, which might be employed for inspection of panel line welds. The system should also be adaptable to application with other types of transducer fixturing, such as the use of water columns for coupling.

The system would provide a permanent record of results —either a typed inspection report listing the position and lengths of rejectable defects, or an indication of rejectable defects that could be marked directly on the weld being inspected. Due to the rapid inspection time and the use of unskilled personnel, it is estimated that the total inspection cost would be approximately 1/10 of that required for radiography.

Once a prototype system is developed and reliability of its operation is verified through field testing, considerable refinement could be made. For example, the pulse r-receiver and signal-processing electronics could be combined into a compact, portable instrument without an oscilloscope. Proper functioning of the system would be assured through the use of calibration test standards. The operational sensitivity, accept-reject criteria, and types of inspection could be modified. Once developed, the system could easily be modified for new applications such as fillet weld inspection.

## Appendix G: Addition of Height and Depth to UT Criteria

This appendix extends the reasoning presented in Section 2.2.4, "Fatigue Growth of Weld Defects" to a tentative conclusion on the usefulness of height and depth as UT criteria. In the report, an approximate fatigue-growth analysis yielded the formula

$$\frac{1}{a_0} - \frac{1}{a_f} = 0.163\ Y$$

which is based on the "fourth power law" and on reasonable assumptions for cyclic stress amplitudes experienced by ship butt welds. tt a It and "a" are original and final dimensions measured from a reference line in the flaw to one growing edge. Y is the time for growth from "$a_o$" to "aft".

Two possible definitions of a flaw's fatigue life were suggested in the report:

A. time for growth of the flaw to full penetration

B. time for growth of the flaw to full penetration and then to a length of 61".

"The upper limit of 6 in. was selected because it seems large enough to be detected in routine surveys and yet appears conservatively under the 8 to 12 inch length that would be critical with respect to brittle fracture if an unusually high stress (in the vicinity of yield strength) occurred when the hull experienced low temperatures." (p. 23)

This analysis begins by assigning a rninirnm fatigue life to each definition to arrive at:

Case (A): an "acceptable" flaw must have a fatigue life of 20 years or more to full penetration.

Case (B): an "acceptable" flaw must have a fatigue life of 30 years or more for growth to a length of 8".*

---

* 8" is the low end of the range for potential brittle fracture. Reducing the maximum flaw length by 2" adds a safety margin of only 6 months to the fatigue life. Therefore 8" is used in this analysis rather than the 6" suggested in the report. The safety factor is more logically included in the minimum fatigue life.

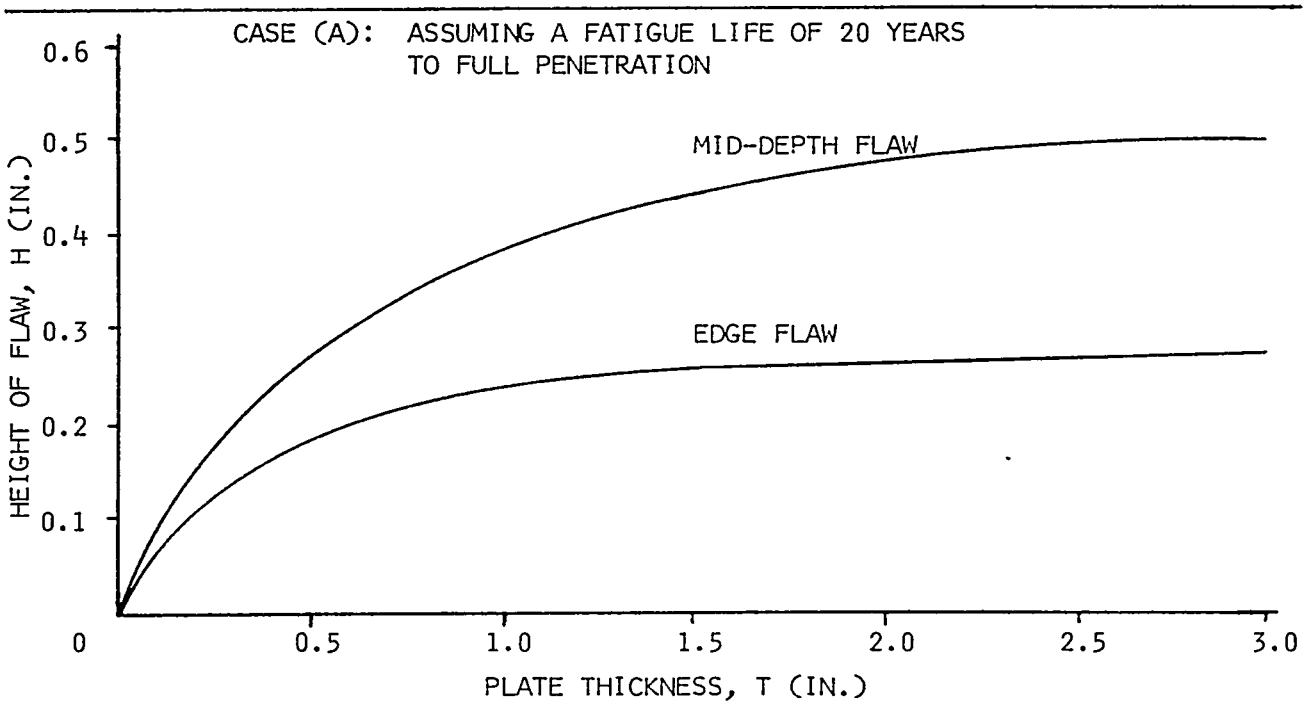


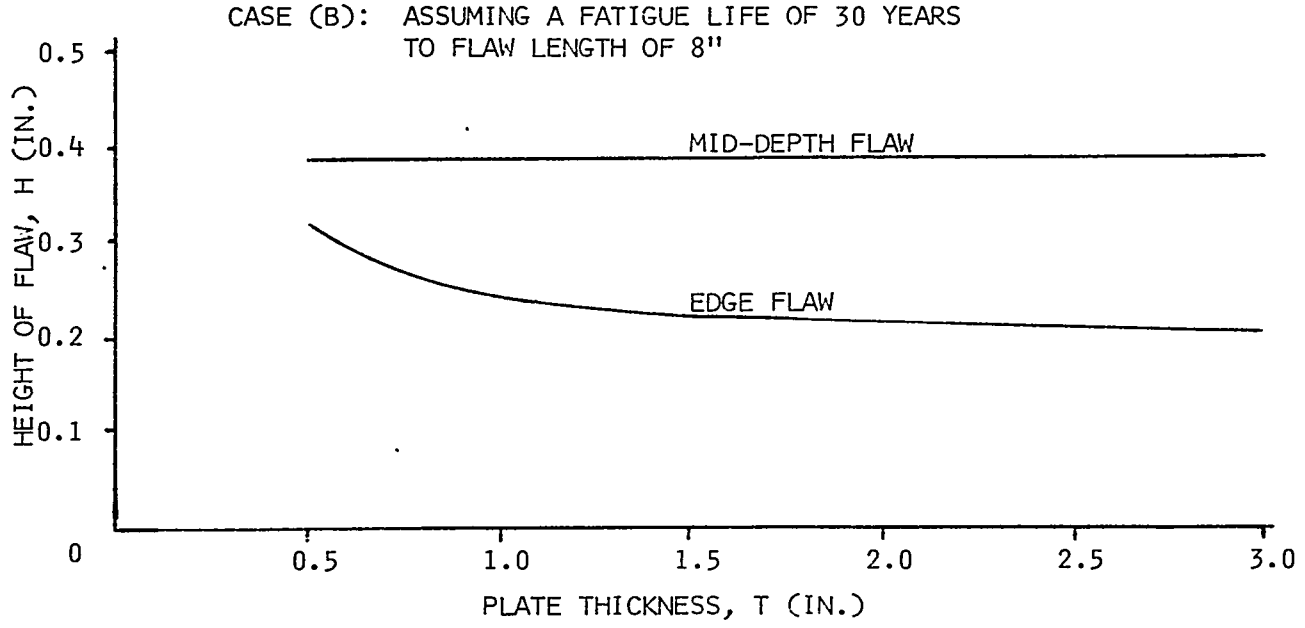


FIGURE G-1: HEIGHT OF FLAW VERSUS PLATE THICKNESS BY DEPTH

Given the minimum fatigue life, curves showing the maximum flaw height for two depth conditions and all plate sizes can be drawn as shown in Figure G-1. The formulas for the curves are derived in Figure G-3. The derivation of the formulas is straightforward except for an assumption made in order to confine the analysis to height and depth criteria:

> When a flaw achieves full penetration, its length is approximately equal to its height - "a consequence of the tendency for irregular defects to grow toward a circular shape" (p. 24).

The assumption that at full penetration the flaw has grown. to circular shape is weak. But it does allow direct comparison of the Case (A) and Case (B) fatigue life definitions. Figure G-2 shows that the two definitions lead to similar values for acceptable flaw height.

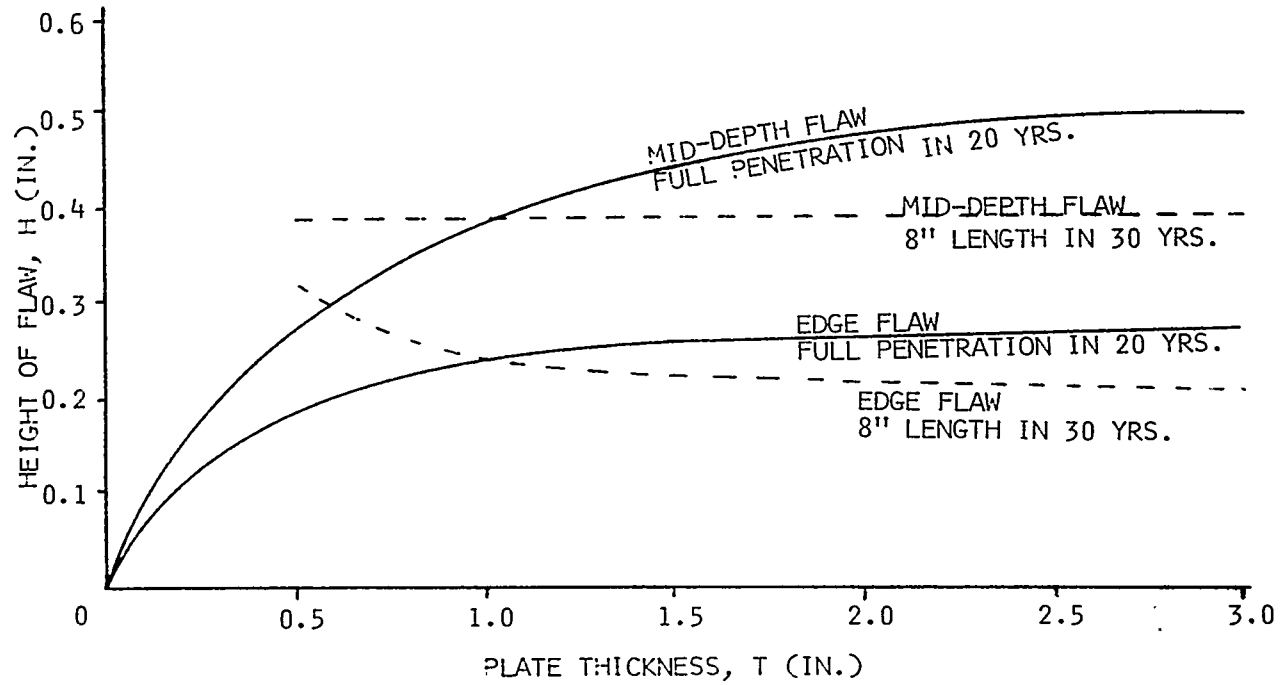


FIGURE G-2: COMPARISON OF FLAW HEIGHTS FOR TWO DEFINITIONS OF MINIMUM FATIGUE LIFE,
FULL PENETRATION IN 20 YEARS (——)
8" FLAW LENGTH IN 30 YEARS (- - -)

Case (A): Y = 20 years to full penetration.

$$\left[ \frac{1}{a_o} - \frac{1}{a_f} \right] = 0.163 \ (\ 20) = 3.25$$

Condition 1, edge flaw: $a_o = H$, $a_f = T$

$$\left[ \frac{1}{H} - \frac{1}{T} \right] = 3.25$$

$$H_1 = \frac{1}{3.25 + 1/T}$$

Condition 2, mid-depth flaw: $a_o = H/2$, $a_f = T/2$

$$\left[ \frac{1}{H/2} - \frac{1}{T/2} \right] = 3.25$$

$$H_2 = \frac{1}{1.63 + 1/T}$$

---

Note, the depth of the flaw affects the fatigue life by at most a factor of 2:

for an edge flaw: $Y_1 = \frac{1}{0.163} \left[ \frac{1}{H} - \frac{1}{T} \right]$

for a mid-depth flaw: $Y_2 = \frac{1}{0.163} \left[ \frac{1}{H/2} - \frac{1}{T/2} \right] = 2\ Y_1$

---

Case (B): Y = 30 years to full penetration and growth to 8" length.

$$\underbrace{\left[ \frac{1}{a_o} - \frac{1}{a_f} \right]}_{\text{to full penetration}} + \underbrace{\left[ \frac{1}{a_o} - \frac{1}{a_f} \right]}_{\text{\& to 8" length}} = 0.163\ (30) = 4.88$$

Condition 1, edge flaw: $a_o = H$, $a_f = T$ to full penetration

plus $a_o = T/2$, $a_f = 8/2$ to 8" length

$$\left[ \frac{1}{H} - \frac{1}{T} \right] + \left[ \frac{1}{T/2} - \frac{1}{8/2} \right] = 4.88$$

$$\left[ \frac{1}{H} - \frac{1}{T} \right] = 5.13$$

$$H_1 = \frac{1}{5.13 - 1/T}$$

Condition 2, mid-depth flaw:

$a_o = H/2$, $a_f = T/2$ to full penetration

plus $a_o = T/2$, $a_f = 8/2$ to 8" length

$$\left[ \frac{1}{H/2} - \frac{1}{T/2} \right] = \left[ \frac{1}{T/2} - \frac{1}{8/2} \right] = 4.88$$

$$\left[ \frac{1}{H/2} - \frac{1}{8/2} \right] = 4.88$$

$H_2 = .39$ inches for all thicknesses

FIGURE G-3: DERIVATION OF FLAW HEIGHT VERSUS PLATE THICKNESS FORMULAS

The definition of fatigue life as time to full penetration is more easily defended than a definition which considers only catastrophic failure and allows leaks. Based on time to full penetration, height and depth criteria could be constructed as shown in the following table.

| Plate Thickness: | Maximum Acceptable Height: edge flaw | Maximum Acceptable Height: mid-depth flaw |
|---|---|---|
| 1/2" | .20" | .251" |
| 5/8" to 1" | .20" | .30" |
| 1" to 3" | .25" | .40" |

Table G–1: Maximum Acceptable Flaw Height by Depth for Different Plate Thicknesses

The order-of–magnitude of the dimensions in the above table suggeszs that the current UT accept\reject criteria would not be significantly improved by addition of height and depth. Also, discussions with shipbuilders cast some doubt on whether shipyard-applied UT can achieve accuracy commensurate with the dimensions shown. There is no doubt that measuring the two additional dimensions would be more difficult and costly than current practice.